AFRL-RX-WP-TR-2011-4069

HIGHLY EFFICIENT FLEXIBLE HYBRID PHOTOVOLTAIC CELLS BASED ON LOW-BAND-GAP CONJUGATED POLYMERS SENSITIZED BY NANOPARTICLE-GRAFTED CARBON

Sam-Shajing Sun

Norfolk State University

Liming Dai

University of Dayton

SEPTEMBER 2010
Final Report

STINFO COPY

AIR FORCE RESEARCH LABORATORY
MATERIALS AND MANUFACTURING DIRECTORATE
WRIGHT-PATTERSON AIR FORCE BASE, OH 45433-7750
AIR FORCE MATERIEL COMMAND
UNITED STATES AIR FORCE

NOTICE AND SIGNATURE PAGE

This report was cleared for public release by the USAF 88th Air Base Wing (88 ABW) Public Affairs (AFRL/PA) Office and is available to the general public, including foreign nationals. Copies may be obtained from the Defense Technical Information Center (DTIC) (http://www.dtic.mil).

AFRL-RX-WP-TR-2011-4069 HAS BEEN REVIEWED AND IS APPROVED FOR PUBLICATION IN ACCORDANCE WITH THE ASSIGNED DISTRIBUTION STATEMENT.

*//Signature//

MICHAEL F. DURSTOCK
Senior Research Engineer

//Signature//

RICHARD A. VAIA, Acting Branch Chief
Nanostructured and Biological Materials Branch
Nonmetallic Materials Division

//Signature//

SHASHI K. SHARMA, Deputy Chief
Nonmetallic Materials Division
Materials and Manufacturing Directorate

REPORT DOCUMENTATION PAGE

Form Approved
OMB No. 0704-0188

1. REPORT DATE *(DD-MM-YY)*	2. REPORT TYPE	3. DATES COVERED *(From - To)*
September 2010	Final	10 September 2007 – 11 August 2010

4. TITLE AND SUBTITLE
HIGHLY EFFICIENT FLEXIBLE HYBRID PHOTOVOLTAIC CELLS BASED ON LOW-BAND-GAP CONJUGATED POLYMERS SENSITIZED BY NANOPARTICLE-GRAFTED CARBON

5a. CONTRACT NUMBER
FA8650-07-C-5058

5b. GRANT NUMBER

5c. PROGRAM ELEMENT NUMBER
62102F

6. AUTHOR(S)
Sam-Shajing Sun (Norfolk State University)
Liming Dai (University of Dayton)

5d. PROJECT NUMBER
4347

5e. TASK NUMBER
20

5f. WORK UNIT NUMBER
12100102

7. PERFORMING ORGANIZATION NAME(S) AND ADDRESS(ES)

Norfolk State University
700 Park Avenue
Norfolk, VA 23504

University of Dayton (UD)
Dayton, OH 45469-0240

8. PERFORMING ORGANIZATION REPORT NUMBER

9. SPONSORING/MONITORING AGENCY NAME(S) AND ADDRESS(ES)
Air Force Research Laboratory
Materials and Manufacturing Directorate
Wright-Patterson Air Force Base, OH 45433-7750
Air Force Materiel Command
United States Air Force

10. SPONSORING/MONITORING AGENCY ACRONYM(S)
AFRL/RXBN

11. SPONSORING/MONITORING AGENCY REPORT NUMBER(S)
AFRL-RX-WP-TR-2011-4069

12. DISTRIBUTION/AVAILABILITY STATEMENT
Approved for public release; distribution unlimited.

13. SUPPLEMENTARY NOTES
PAO Case Number: 88ABW-2011-0234; Clearance Date: 20 Jan 2011. Report contains color.

14. ABSTRACT

During the entire project period, significant progress was made on the design, modeling, synthesis, and characterization of several series functional and processable electro-active conjugated polymers with evolving frontier orbital energy levels and energy gaps that are very attractive for optoelectronic applications at VIS-NIR radiation energy ranges. Details of these new functional polymer developments are described. In addition, quantum dot grafted carbon nanotubes for potential optoelectronic applications were studied. All materials developed were fabricated into devices and their performance characteristics were evaluated. These include low-band-gap conjugated polymers such as 55-C12-PTV, SFPTV and P(C6OTV-SFTV), as well as the (-DBAB-)n block copolymer systems, and quantum dot-grafted carbon nanotubes.

15. SUBJECT TERMS

16. SECURITY CLASSIFICATION OF:			17. LIMITATION OF ABSTRACT:	18. NUMBER OF PAGES	19a. NAME OF RESPONSIBLE PERSON *(Monitor)*
a. REPORT Unclassified	**b. ABSTRACT** Unclassified	**c. THIS PAGE** Unclassified	SAR	90	Michael F. Durstock **19b. TELEPHONE NUMBER** *(Include Area Code)* N/A

Standard Form 298 (Rev. 8-98)
Prescribed by ANSI Std. Z39-18

Table of Contents

PROJECT STATEMENT OF WORK (SOW)

The contract project awardee (NSU) and sub-awardee (UD) shall perform the following tasks as a basic obligation of this award:

Task #1. Low Band Gap Polymers
The awardee (Professor Sun's group at NSU) shall design, synthesis, and characterize processable, stable, and functional donor or acceptor type polymer blocks with energy gaps in the range of 0.5-2.0 eV, and also develop donor/acceptor block copolymers for potential photovoltaic functions.

Task #2. Quantum Dots Substituted Carbon Nanotubes
The subawardee (Professor Dai's group at UD) shall develop quantum dots derivatized carbon nanotubes for both sunlight harvesting and charge transport functions as described in the proposal.

Task #3. Thin Film Flexible Solar Cells
The awardee shall collaborate with sub-awardee and/or the Air Force Research Lab to develop and evaluate thin film flexible solar cells or photo detectors fabricated from the developed materials.

Task #4. Other Tasks and Responsibilities
The awardees/subawardees shall report the project generated data and any progress in a timely manner to the awarding agency as required, typically annually. In addition, the awardees shall accomplish other scientific and educational goals/objectives per federal and state general policies or guidelines for such awards. These may include, but are not limited to, student thesis work, research exchanges and collaborations with other organizations or labs, presentations and publications in the scientific communities or public, patenting, marketing or commercialization of research generated intellectual properties where applicable or necessary.

1. NEW POLYMER DEVELOPMENTS (PROJECT TASK #1, NSU)

During the entire project period, significant progresses have been accomplished on the design, modeling, synthesis, and characterizations of several series functional and processable electro-active conjugated polymers with evolving frontier orbital energy levels and energy gaps that appear very promising for optoelectronic applications at VIS-NIR radiation energy ranges. Details of these new functional polymer developments are described below.

1.1 A New Series of S,S-Dioxo-Thienylenevinylene (SF-TV) Based Conjugated Copolymers with Taylored Frontier Orbitals and Energy Gaps

Abstract: A series of evolving frontier energy levels and gaps sulfone-containing thienylenevinylene-based conjugated co-polymers have been synthesized via the Horner-Emmons reactions between 2,5-bis(diethoxyphosphorylmethyl)-3,4-dihexyl-1,1-dioxo thiophene and a series of different donor type dialdehyde co-monomers. The resulting polymers (SF-PTVs) contain alternating donor (benzene or thiophene ring with/without alkoxy substituents) and acceptor (1,1-dioxo thiophene) units. A range of HOMO/LUMO levels and energy gaps (between 1.0 eV to 2.0 eV) were achieved in these new polymers. The use of oxidized thiophene moiety (sulfone unit) brings about 0.3 eV in reduction of energy gap. Computational study on the model oligomers of P(C6OTV-SFTV) and related structures reveals that the reduction is mainly due to the removal of aromaticity of the thiophene. The donor-acceptor interaction is also responsible for about one third or less of the energy gap reduction. Theses polymers have very good thermal stability (dynamically, 258°C or higher), and their decomposition start with loss of mass as in contrast to regular PTVs which decompose initially by cross-linking.

1.1.1 Introduction

Availability of stable, processable, functionalizable, and evolving low energy gap (E_g) n-type of conjugated polymers is critical for developing various types of donor-acceptor (D/A) based polymer electronic and optoelectronic (OE) devices,[1-2] for instances, devices made of all-polymer D/A bulk heterojunctions,[1-3] donor-acceptor block copolymers[4]. The later has been the focus of our studies.[5,6] One of the great challenges in D-A block copolymer OE device development is to develop a series of acceptor polymer blocks having the following features: 1. Absorption spectrum covers a good portion of visible solar spectrum (with energy gaps E_g in the range of 1-2 eV), 2. LUMO level is sufficiently low to enable photo-induced electron transfer from donor polymers and to maintain air stability, 3. End-group functionalities allow covalent coupling with other donor block(s). In general, energy gaps of conjugated polymers may be reduced by incorporating the following structural features: aromatic units with low resonance energy, strongly coupled donor-acceptor substituents, large and coplanar π-systems, high regioregularity of side chains, *etc*.[7] Due to its low resonance energy and good chemical stability, thiophene ring has been widely used for developing low energy gap conjugated polymers. Insertion of a C=C bond between every two thiophene rings leads to polythienylenevinylenes (PTVs) with lower E_gs in the range of 1.5-1.8 eV.[8-11] Our goal is

to develop new PTV-like polymers having not only low E_gs, but also low LUMO levels. A series of novel sulfone (SF)-containing polythienylenetetravinylene repeating unit [P(C6OTV-SFTV) in **Scheme 1.1.1**] has thus been designed and developed. These new polymers can be considered as a PTV with the sulfur in every other thiophene ring being oxidized to sulfone (-SO$_2$-). Oxidation of the sulfur not only cause the thiophene ring to lose its aromaticity but also inserts a strong electron-withdrawing group in the πconjugated main chain.[12] Significant reductions in both E_g and LUMO levels have been achieved. By using co-monomers with different aromatic resonance energy and with/without electron donating side groups, a series of sulfone-containing conjugated polymers with a wide range of energy gaps have been obtained. Furthermore, the terminal functional groups and chemical schemes of these polymers would enable block copolymer supramolecular structure developments.
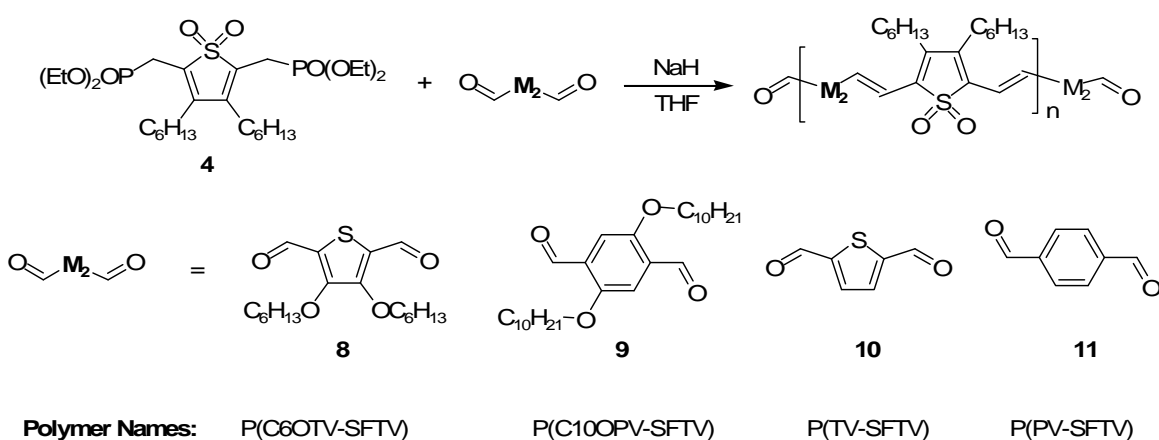
Scheme 1.1.1 Synthetic scheme of SF-PTV derivatives with sulfone embedded in polymer conjugated backbones.

1.1.2 Experimental

Starting Materials and Instrumentation: All starting materials, reagents, and solvents were purchased from commercial sources (Sigma Aldrich and Fisher-Scientific) and used as received unless noted otherwise. NMR spectra were obtained from a Bruker Advance 300 MHz spectrometer with TMS as the internal reference. Elemental analysis was performed by Atlantic Microlab Inc. UV-vis data were collected on a Perkin Elmer Lambda 900 Spectrophotometer. Photoluminescence experiments were performed on an ISA Fluoromax-3 luminescence spectrofluorometer. Differential scanning calorimeter (DSC) and thermal gravimetric analyzer (TGA) data were collected by Perkin Elmer DSC-6 and TGA-6. Measurements of polymer molecular weights were done on a Viscotek GPC system with a UV-Vis absorption detector at ambient temperature using tetrahydrafuran as the solvent. Polystyrene standards were used for conventional calibration.

Cyclovoltammetry. Electrochemical studies were performed on a Bioanalytical (BAS) Epsilon-100w tri-electrode cell system. Three electrodes are a Pt working electrode, an ancillary Pt electrode, and a silver reference electrode (in a CH$_3$CN solution of 0.01 M AgNO$_3$ and 0.1 M tetrabutylammonium hexafluorophosphonate, TBA-HFP). The polymer samples were dissolved in hot solvents (such as o-dichlorobenzene) and then coated onto Pt working electrode. The measurements were performed in 0.1 M

TBA-HFP/acetonitrile solution purged with nitrogen gas. Between the experiments, the surface of the electrodes were cleaned or polished. Scan rate was 100mV/s. Ferrocene (2 mM in 0.10M TBA-HFP/CH_3CN solution) was used as an internal reference standard and its HOMO level of -4.8 eV was used in calculations.

2,5-Bis-bromomethyl-3,4-dihexylthiophene (2): To a 125 ml round bottom flask were added 2,5-dihexyl thiophene (2.67 g, 10.6 mmol), paraformaldehyde (0.952 g, 31.7 mmol), acetic acid (25 ml), 4.92 g HBr in 30% acetic acid, and a stirring bar. The mixture was stirred at room temperature for three hours. The mixture was poured into 30 ml of water and 30 ml of hexane in a separation funnel. Saturated aqueous $NaHCO_3$ was added to adjust the water phase to weakly basic. The top organic layer was collected, dried with MgSO4, filtered, and condensed by vacuum rotary evaporation with water bath temperatures controlled near 40°C. Heating was stopped immediately once the solvent was mostly removed to minimize decomposition of the product. The yield was 86% (4g). The product could not be purified, but was sufficiently pure for use in the next step. ^{1}H NMR (CDCl$_3$): δ (ppm) 0.90 (t, 6H, -(CH$_2$)$_4$CH$_3$), 1.33-1.52 (m, 16H), 2.51 (t, J=7.7 Hz, 4H), 4.65 (s, 4H). (The spectrum is given in Supporting Information).

2,5-Di(bisethoxyphosphorylmethyl)-3,4-hexylthiophene (3): In a glove box, a mixture of 2,5-dibromomethyl-3,4-dihexylthiophene (4 g, 9.1 mmol) and triethyl phosphite (6.05 g, 36.4 mmol) was stirred in a 125 ml round bottom flask at 135°C for 6 hours. The remaining P(OEt)$_3$ was removed by vacuum distillation and a light blue oil was obtained: 4.94g, yield 98%. ^{1}H NMR (CDCl$_3$): δ (ppm) 0.90 (t, J=6.6 Hz, 6H), 1.35-1.75 (m, 28H), 2.45 (t, J = 6.8 Hz, 4H), 3.28 (d, J=19.2 Hz, 4H, CH$_2$PO(EtO)$_2$), 4.06 (quadruplet, J=7.3 Hz, 8H). ^{13}C NMR (CDCl$_3$): δ (ppm) 14.10, 16.39, 22.64, 25.6, 27.27, 29.59, 30.65, 31.69, 62.29, 124.15, 139.61. (The spectra are given in Supporting Information).

2,5-Di(bisethoxyphosphorylmethyl)-1,1-dioxo-3,4-hexylthiophene (4): To a 100 ml of round bottom flask were added 2,5-di(bisethoxyphosphorylmethyl)-3,4-dihexylthiophene (2.48 g, 4.5 mmol) and m-chloroperoxybenzoic acid (3.165g, 18 mmol,), CH$_2$Cl$_2$ (20 mL) and a stirring bar. The mixture was stirred at room temperature for about two hours. CH$_2$Cl$_2$ was removed by rotary evaporation at 40 ^{o}C under reduced pressure. The residue was diluted with 30 ml of hexanes and kept in a freezer for two days. The mixture was filtrated to collect the liquid part which was transferred into a separation funnel. aqueous solution of Na$_2$CO$_3$ was added to make the water phase very basic. The hexane phase was collected, dried, condensed. The crude product mixture was purified by column chromatography (125ml silica gel, 1:2 ethyl acetate/hexanes) to give 1.3g product, 49.4% yield. ^{1}H NMR (CDCl$_3$): δ (ppm) 0.90 (t, J=6.6 hz, 6H), 1.32-1.66 (m, 28H), 2.45 (t, J=6.21 Hz, 4H), 3.00 (d, J=20.91 Hz, 4H), 4.15 (quintet, J=7.73 Hz, 8H). ^{13}C NMR (CDCl$_3$): δ (ppm) 14.01, 16.31, 20.60, 22.49, 26.11, 28.28, 29.53, 31.44, 62.82, 127.55, 142.64. (The spectra are given in Supporting Information). Anal. Calc.: C, 53.41; H 8.62; S, 5.48; Found: C, 53.29; H, 8.69; S, 5.62.

3,4-Bishexyloxythiophene (6): To a 2-neck round bottom flask equipped with a thermometer were added 3,4-dimethoxythiophene (12.49g, 86.7 mmol), anhydrous hexanol (35.56g, 0.384 mole), and p-toluenesulfonic acid monohydrate (0.5g, 2.61 mmol). The mixture was stirred at 90-95 ^{o}C for 25 hours with vacuum applied occasionally to remove side product methanol to drive the reaction to completion. The mixture was poured into a 1L separation funnel. Dilute HCl was added to neutralize the mixture, which was then extracted with 100ml of hexanes. The extract was dried with

magnesium sulfate, filtered, condensed by rotary evaporation and vacuum distilled to 21.08g product with a 95% yield. ^{1}H NMR (CDCl$_3$): same as in ref. 18.

2,5-dibromo-3,4-bishexyloxythiophne (7): To a stirred mixture of 3,4-bishexyloxythiophen (7.0 g, 24.6 mmol) and N, N-dimethylformamide (anhydrous, 38 ml) in dark, N-bromosuccinimide (9.63 g, 54.1 mmol) in 100 ml of DMF was added over two hours from an addition funnel. One hour after the addition, the mixture was transferred into a 500ml separation funnel and diluted with 30 ml of water. The mixture was extracted with 100 ml of hexanes. The extract was collected, dried with magnesium sulfate, filtered, and condensed. The residue was purified by a silica gel column using hexanes as the eluent to afford 6.64 g oil with a yield of 61%. ^{1}H NMR (CDCl$_3$): δ (ppm) 0.90 (t, 6H), 1.32 & 1.45 (m, 16H), 1.72 (quintet, J=6.6 Hz, 4H), 4.05 (t, J=6.8 Hz, 4H). ^{13}C NMR (CDCl$_3$): δ (ppm) 14.05, 22.62, 25.53, 29.90, 31.57, 73.94, 95.25, 147.59. The spectra are given in SI.

2,5-dialdehyde-3,4-bishexyloxythiophne (8): To a mixture of n-BuLi (1.6 M in hexane, 26.7 ml, 42.8 mmol) and THF (67 ml) cooled in dry ice/hexane bath, a solution of 2,5-dibromo-3,4-bishexyloxythiophene (6.30 g, 14.3 mmol) in 10.0 ml of THF was added slowly through a syringe. Two minutes later, DMF (anhydrous, 3.33 g, 45.6 mmol) was added and the mixture was warmed to room temperature, and poured into a separation funnel that contained 67 ml of water and 67 ml of hexanes. After usual workup, the crude product was purified by silica gel column chromatography using 1:17 ethyl acetate: hexanes mixture as the eluent to afford 3.90 g pure product with a yield of 80%. ^{1}H NMR (CDCl$_3$): δ (ppm) 0.91 (t, 6H), 1.33&1.46 (m, 16H), 1.80 (quintet, J=6.8 Hz, 4H), 4.27 (t, J=6.6 Hz, 4H), 10.10 (s, 2H). ^{13}C NMR (CDCl$_3$): δ (ppm) 182.19, 154.98, 131.17, 75.67, 31.46, 29.83, 25.44, 22.55, 13.99. The spectra are given in SI. ^{1}H NMR peaks are same as reported (though the literature data[18] was not as detailed as presented here).

Poly(3,4-bishexyloxythienylenevinylene-S,S-dioxide-3',4'-dihexylthienylenevinylene), P(C6OTV-SFTV): In a glove box, NaH (20.1 mg, 0.837 mmol) in 10 ml vial with 4 ml THF was added dropwise to a stirred solution of **4** (213.5 mg, 0.365 mmol) and co-monomer **8** (116.4 mg, 0.342 mmol) in 2 mL of THF in a 20 ml flask at room temperature. Twenty-one hours later, a few drops of acetic acid were added to neutralize the solution. The solution was dropped into stirred methanol. The resulting dark blue polymer solid was collected by filtration, washed with methanol many times, and dried in air a day and in vacuum at 65 ^{o}C for 24 hours. Yield: 0.135 g, 58%. ^{1}H NMR (CDCl$_3$): δ (ppm) 0.93 (m. 12H), 1.36 (m, 28H), 1.79 (m, 4H), 2.45 (t, 4H), 4.12 (s, 4H), 6.69 (d, J=16Hz, 2H), 7.45 (d, J=16 Hz, 2H). ^{13}C NMR (CDCl$_3$): δ (ppm) 14.1, 22.63, 25.62, 29.4, 30.07, 31.56, 74.37, 112.29, 123.40, 125.88, 135.50, 138.39, 149.86. (Some aliphatic carbon peaks are overlapped)

Poly(thienylenevinylene-S,S-dioxo-3',4'-dihexylthienylenevinylene), P(TV-SFTV): To a solution of 2,5-thiophenedicarboxaldehyde (50.3 mg, 0.359 mmol) and **4** (200.0 mg, 0.342 mmol) in THF (2 mL), NaH (18.9 mg, 0.788 mmol) in 3mL THF was added dropwise. No immediate color change upon NaH addition was observed. Twenty-two hours after addition, the blue reaction solution was dropped into MeOH (30 mL, acidified with 60 mg HOAc). The polymer product was collected by filtration, and was dried *in vacuo* at 50 ^{o}C for 10 h to afford 127 mg black powder. Yield: 81.5%. ^{1}H NMR spectrum is in **Figure 1.1.1**.

Poly(1,4-phenylenylenevinylene-S,S-dioxo-3',4'-dihexylthienylenevinylene), P(PV-SFTV): Same procedure as used for P(TV-SFTV) and same amount (in mmol) of monomers were used. Yield: 133mg, 93.3%. ^{1}H NMR spectrum is in **Figure 1.1.1**.

**Poly(2,5-bisdodecyloxy-1,4-phenylenylenevinylene-S,S-dioxo-3',4'-dihexylthienylenevinylene), P(C10OPV-SFTV):** Same procedure as used for P(TV-SFTV) and same amounts (# of mmol) of monomers were used. Yield: 205 mg, 80%. ^{1}H and ^{13}C NMR spectra are in **Figure 1.1.1** and **Figure 1.1.2**. ^{1}H NMR (CDCl$_3$): δ (ppm) 0.92 and 0.88 (terminal CH$_3$ of hexyl and dodecyl respectively, m. 12H), 1.1-1.7 (m, 44H), 1.90 (m, 4H), 2.50 (t, 4H), 4.06 (t, J=6.6Hz, 4H), 7.03 (s, 2H), 7.30 (d, J=16.5 Hz, 2H), 7.50 (d, J=16.2 Hz, 2H), 10.44 (terminal CHO). ^{13}C NMR (CDCl$_3$): δ (ppm) 14.15, 22.91, 26.46, 26.72, 29.60, 29.76, 29.89, 29.93, 31.90, 32.20, 69.94, 114.58, 116.97, 127.51, 131.39, 136.73, 138.88, 152.59. (Several aliphatic carbon peaks overlapped)

1.1.3   Results and Discussions

Synthesis of Monomers and Polymers. The structures of the series of S,S-dioxide-thienylenevinylene-based polymers [P(C6OTV-SFTV), P(C10OPV-SFTV), P(TV-SFTV) and P(PV-SFTV)] and their generic synthetic scheme are shown in **Scheme 1.1.1**. The polymers were prepared from two types of co-monomers: the diphosphonate **4** and aromatic dialdehydes (**8, 9, 10, and 11**) via the Horner-Emmons reaction. The diphosphonate monomer (**4**) was synthesized in four steps from 3,4-dibromothiophene (**Scheme 1.1.2**). Compound **1** was synthesized according to the literature procedure.[13] Compound **2** was obtained from bromomethylation of **1** under reaction condition similar to what was recently reported.[14] Better yield (86% vs 75%) was obtained as a result of more detailed study of the reaction. We found that the reaction was very fast and was completed in less than three hours. However, care must be taken during work up because the product **2** is highly unstable and can decompose during solvent rotary evaporation when the temperature was above 50°C. The crude product was pure enough to give a neat ^{1}H NMR spectrum (**Figure 1.1.10** in Supporting Information or 'SI') showing a characteristic singlet peak at 4.65ppm for two –CH$_2$Br groups. **2** is not stable in silica gel column, so the crude product was used in the next step. Instability of **2** at elevated temperatures did not cause any problems in the next step in the Michaelis–Arbuzov reaction[15] run at 135 ^{o}C. Product **3** has a characteristic doublet at 3.20 ppm in the ^{1}H NMR spectrum. Purification of **3** by silica gel column chromatography was attempted but decomposition happened in the column, as a substantial amount of new substance (not present in crude product) was found in collected fractions.[16] The crude product (95% pure, see ^{1}H NMR in **Figure 1.1.10** in SI) was oxidized at the sulfur atom using a literature procedure[12] to give product **4**, which was stable and was purified by column chromatography to give pure product at 49% overall yield for three steps. The ^{1}H NMR spectrum of **4**, also shown in **Figure 1.1.10** in SI, is characterized by a doublet peak at 2.97 ppm for CH$_2$PO(OCH$_2$CH$_3$)$_2$ which was shifted from 3.20 ppm in **3** due to vanishing of the deshielding effect of the thiophene ring as a result of loss of aromaticity of the thiophene ring.[17]
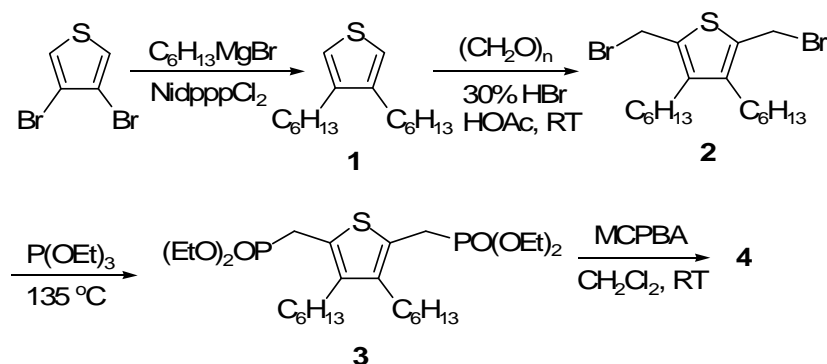
Scheme 1.1.2 Synthesis of the diphosphonate co-monomer **4**.
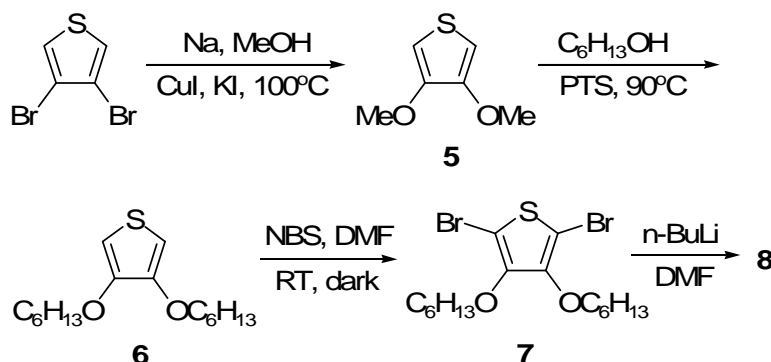
Scheme 1.1.3 Synthesis of the dialdehyde co-monomer **8**.

Synthesis of dialdehyde monomer (**8**) took four steps using a scheme (**Scheme 1.1.3**) different from the one reported in 1999.[18] Compound **5** was synthesized according to a literature procedure.[19] Compound **6** was synthesized from **5** by PTS-catalyzed substitution of methoxy by hexyloxy group at 90 °C. The literature procedure[20] was followed except that the reaction was conducted under a reduced pressure (400-500 mbar) in stead of one atmosphere to constantly remove the side product methanol from the reaction system. With this modification we were able to improve the yield from 54% to 95%. Compound **7** was synthesized from **6** by dibromination and was characterized by the disappearance of the peak at 6.15 ppm in ^{1}H NMR spectrum (**Figure 1.1.12** in SI). Finally, the co-monomer **8** was obtained from **7** by diformylation in 80% yield (^{1}H and ^{13}C NMR spectra in **Figure 1.1.12** and **Figure 1.1.13** in SI). It is noted that errors are found in the literature NMR data.[21]

The polymerization reaction for P(C6OTV-SFTV) was performed inside a glove box. Initially, 1 eq. of potassium t-butoxide base was used, the blue color appeared within one hour, the reaction progress was followed by ^{1}H NMR analysis and >30% of both monomers remained no matter how long the reaction was allowed to run. Clearly, the base was partially consumed by side reactions. When more and more t-BuOK was added, the characteristic blue-green color of formed oligomers/polymer started to fade even before aldehyde and phosphonate were completely consumed. The color change and NMR data suggested that the double bonds formed in the earlier stage of the reaction were destroyed extensively by the base (now acting as a neucleophile) through the

Michael addition reaction (a nucleophilic conjugate addition). The similar side reaction was reported in the synthesis of CN-PPV.[22] We found that the decomposition could be avoided by using sodium hydride of strictly controlled amount. The deep green-colored polymer products could be obtained routinely. For the ^{1}H NMR in **Figure 1.1.1** bottom, 5% excess of aldehyde monomer was used to control the molecular weight. The phosphonate monomer is fully consumed as indicated by the disappearance of the doublet at 2.97 ppm. The residue aldehyde peak is seen in the spectrum as expected. Two clean doublets at 6.69 ppm and 7.45 ppm, due to the two non-identical protons in the newly formed C=C bond, indicate low content of structural defects.
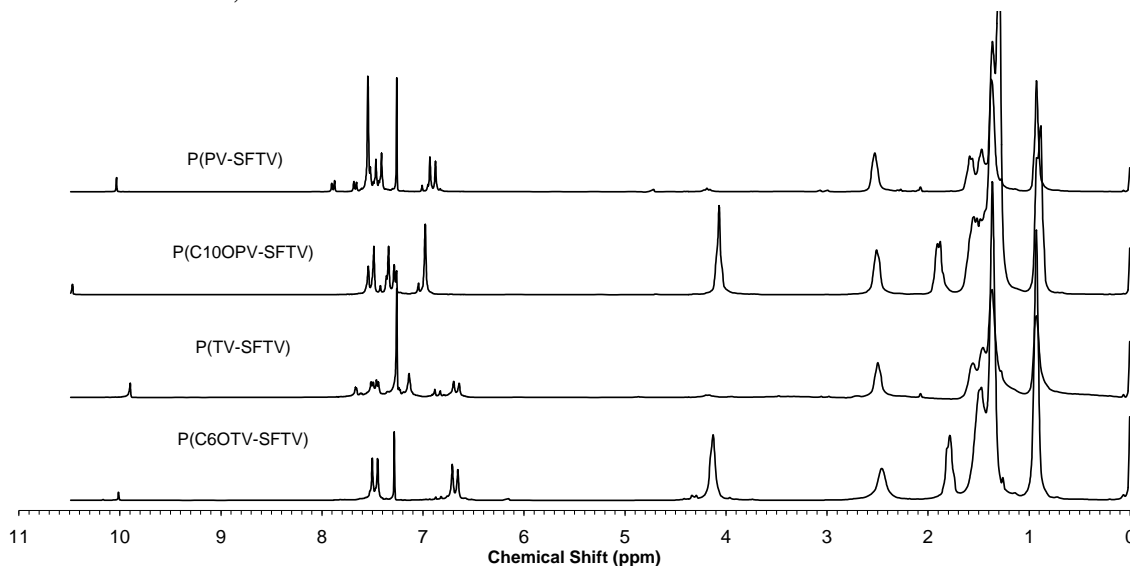

Figure 1.1.1 ^{1}H NMR of P(C10OPV-SFTV), SF-PTV, P(TV-SFTV) and P(PV-SFTV) in CDCl$_3$ at 65°C. The last two polymers are not fully dissolved, thus the solutions have higher content of low MW polymers and higher content of end groups (-CHO).

The other three polymers were synthesized from monomer **4** and dialdehydes **9**,[5] **10**, and **11**, respectively, using similar condition as used for the synthesis of P(C6OTV-SFTV). The ^{1}H NMR spectra of these polymers are shown in **Figure 1.1.1**. In the spectrum of P(C10OPV-SFTV), a singlet at 6.98 ppm (due to two identical phenyl protons) and two doublets at 7.30 ppm and 7.50 ppm (due to the newly formed C=C bond) are as clean as the aromatic peaks in P(C6OTV-SFTV) spectrum. Same combination of aromatic peaks (one single and two doublets) are seen for the other two polymers, P(TV-SFTV) and P(PV-SFTV) with different chemical shifts. However, the peaks due to the terminal aromatic units and aldehyde groups in the spectra of P(TV-SFTV) and P(PV-SFTV) are stronger than the corresponding peaks in the spectra of the other two polymers. This difference is simply due to the fact that P(TV-SFTV) and P(PV-SFTV) have much lower solubility due to less side chains and the dissolved portions in the NMR sample tubes are mostly of low MW and had higher content of terminal units. The solubility of P(C6OTV-SFTV) is good in common organic solvents such as THF (1mg/1mL) and chloroform (2mg/1ml) at room temperature. P(C10OPV-SFTV) is about half as soluble as P(C6OTV-SFTV). Decent ^{13}C NMR spectra were obtained for these

two polymers (**Figure 1.1.2**) and correct counts of aromatic carbon peaks are obtained. The peaks due to terminal units are not observed due to their relatively weak intensities.
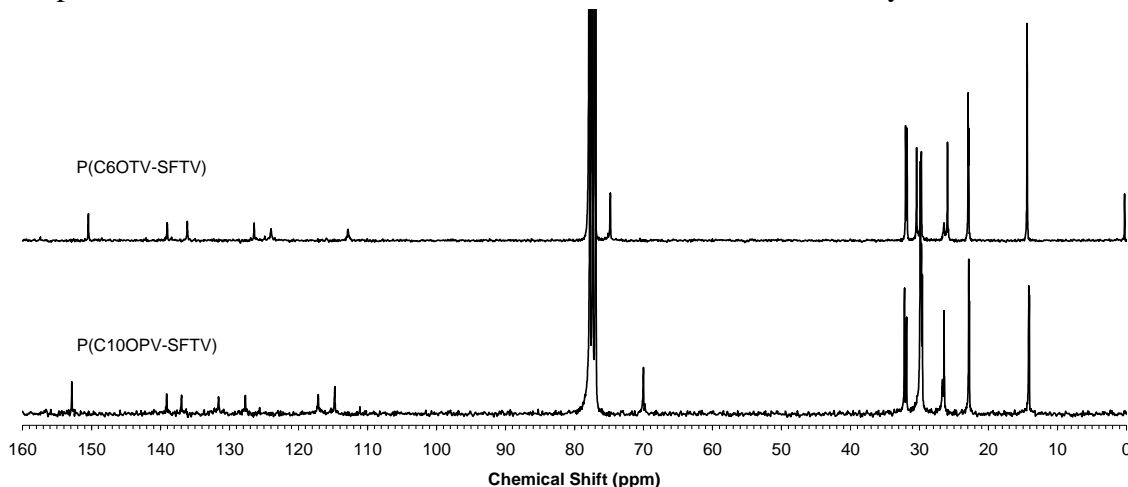

Figure 1.1.2 ^{13}C NMR spectra of P(C10OPV-SFTV) and P(C6OTV-SFTV) in CDCl$_3$ at 65°C. The solubility of the other two polymers are not high enough to obtain good ^{13}C NMR spectra.

Molecular weights of SF-PTVs were measured by GPC. It was found that the refractive index detector signal was severely distorted by the strong absorption of SF-PPVs. An absorption detector was then used in place of the original RI detector. The results are listed in **Table 1.1.1**. Due to the non-stoichiometric use of the two co-monomers and small scale of the reactions, the MWs are not high. In the case of P(PV-SFTV) and P(TV-SFTV), measured MWs were particularly low because only the low MW fractions were dissolved and tested. Reaction scale also affects molecular weight of synthesized polymers, as the amount of NaH is very small for small scale reactions. In a larger scale synthesis of P(C6OTV-SFTV), in which the amount of diphosphonate **4**, was increased from 231 mg to 1.62g, the number average MW (Mn) increased to 16800 (calculated from the proton integration ratio of CHO and OCH$_2$ peaks), which is very close to the value (13590) calculated from the feed ratio of the two monomers (1.05:1 was used) since some of the low MW fraction was lost during the precipitation/filtration process. GPC measurement gave a Mw of 47.7K, a Mn of 21.7K, and a PDI of 2.20. The Mn is higher than the result calculated from ^{1}H NMR integrations as expected.

Table 1.1.1 Molecular weight and thermal properties of the sulfone polymers.

	Mw/Mn/PD	Onset T of endothermic decomposition (DSC)	Onset T of exothermic peaks (DSC)	Onset T for loss of SO_2 (TGA)
P(PV-SFTV)	5350/2880/1.84	280-295	298	292
P(TV-SFTV)	3570/1700/2.10	290	258	258
P(C10OPV-SFTV)	13.6K/5.44K/2.50	290	260	264
P(C6OTV-SFTV)	11.5K/4.34K/2.66	264	-	266

Thermal properties analyzed by DSC, TGA, and NMR. In sulfone-containing polymers, due to the relatively weak C-S bonds, thermally induced chemical decomposition usually begins with the loss of SO_2.[23] DSC, TGA and ^{1}H NMR were used to study the decomposition behaviors of the SF-PTVs. DSC scans of the polymers are shown in **Figure 1.1.3**. In the low temperature range (RT – 250°C), P(C10PV-SFTV) and P(TV-SFTV) undergo a weak exothermic transition at 115°C and 117°C, respectively. They are most likely due to reorganization of side chains. All polymers except P(C6OTV-SFTV) show an endothermic peak above 250°C with onset temperatures listed in **Table 1.1.1**. To determine whether the endothermic process is due to melting or decomposition (loss of SO_2), we selected P(C10OPV-SFTV) for detailed study because its good solubility allows for easy NMR analysis. First, a sample of this polymer was heated quickly in DSC under N_2 atmosphere to 250°C (at a rate of 30 ^{o}C/min) and was held at this temperature for one minute. After cooling to RT, the sample was still in the powder form. ^{1}H NMR of the sample showed no decomposition. Another sample of P(C10OPV-SFTV) was heated to 290°C (the completion temperature of the endothermic peak) and was let cool immediately. The sample was found still in powder form but was only partially soluble in boiling $CDCl_3$. ^{1}H NMR of the soluble part (**Figure 1.1.4**) revealed that the polymer was completely changed (no original aromatic peak seen), however, C10OPV unit and two C_6H_{13} side chains (attached to C=C bond) remained. These observations suggest that the endothermic peak (with an onset at 264°C) is not due to melting, but due to disintegration (most likely loss of SO_2).
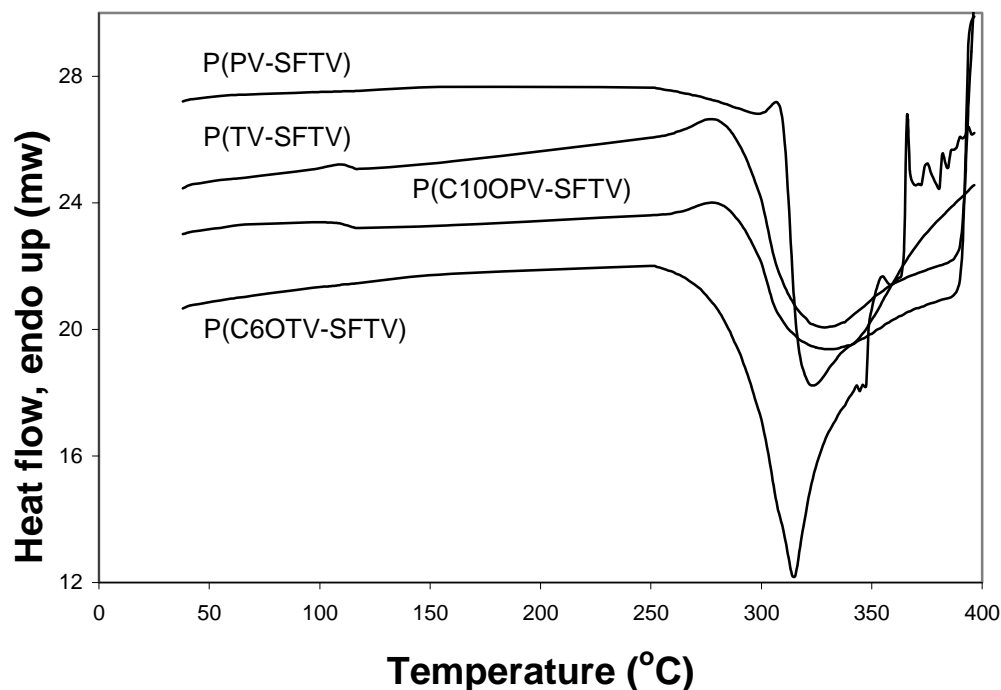
Figure 1.1.3 DSC curves of four sulfone-PTVs.

TGA experiment of P(C10OPV-SFTV) (**Figure 1.1.5**) shows a weight loss onset temperature of 264°C, matching well with the endothermic onset temperature. In the DSC curve of P(C10OPV-SFTV), as well as that of P(TV-SFTV), the endothermic process was overpowered by an exothermic transition (due to reactions involving unsaturated bonds). In the case of P(PV-SFTV) and P(C6OTV-SFTV), the exothermic decomposition processes (by DSC) are coincident with disintegration (weight loss) processes (by TGA), indicating that the heat released from crosslinking reactions of C=C bonds can fully compensate for the heat needed for disintegration reactions (e.g., loss of SO_2) (except for a short temperature range of 300-310°C in the case of P(PV-SFTV)).
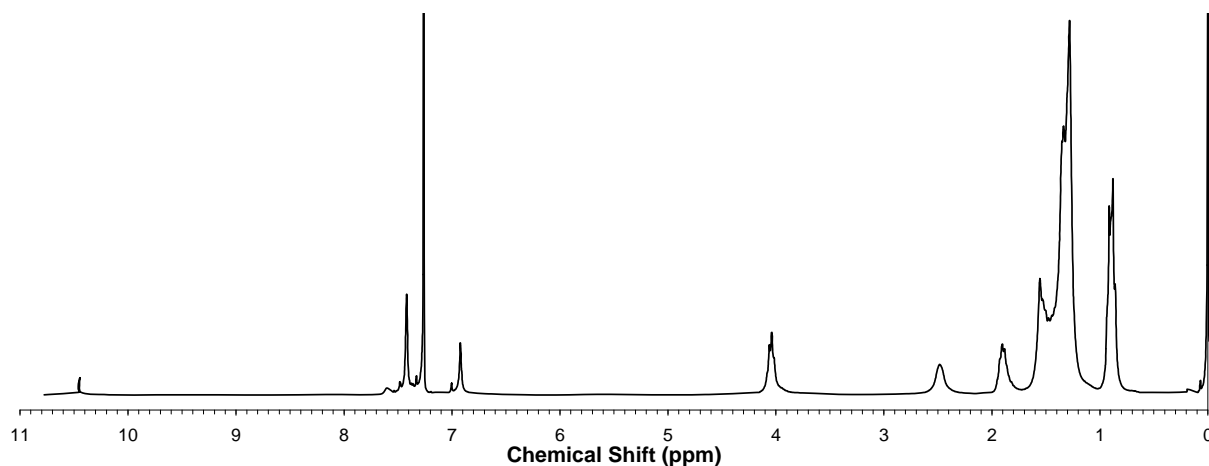

Figure 1.1.4 ^{1}H NMR (CDCl$_3$) spectrum of a P(C10OPV-SFTV) sample heated to 290°C. (DSC, N$_2$, heating rate 10°C/min, no stay at 290°C).
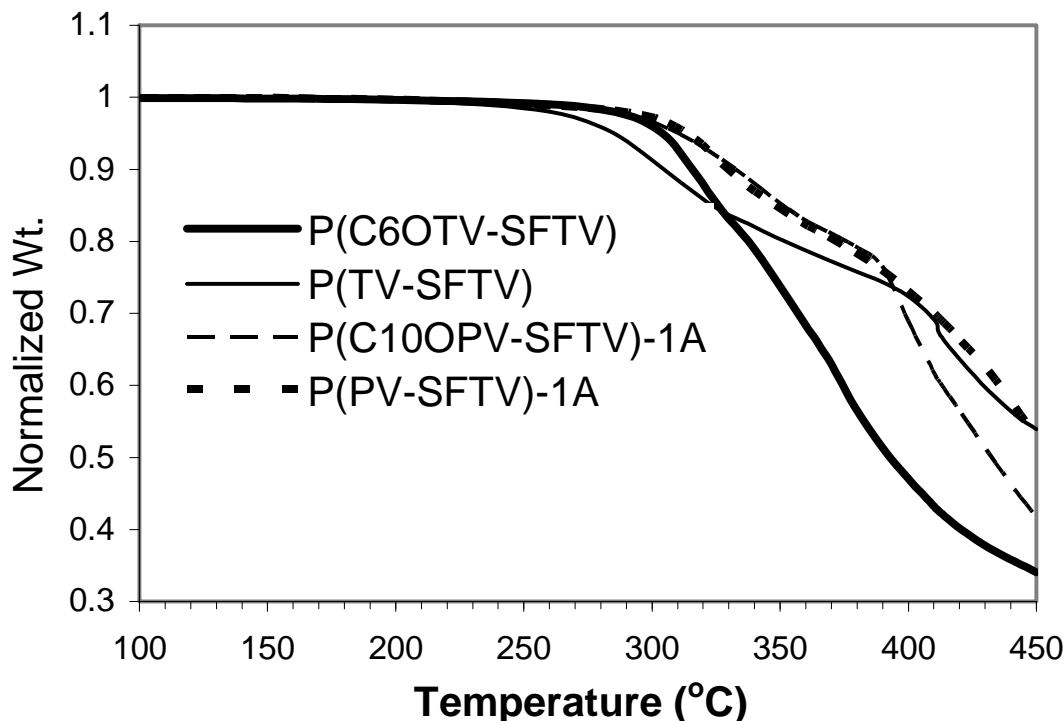
Figure 1.1.5 Thermal Gravity Analysis (TGA) for SF-PTVs.

No melting behaviors of these polymers were observed before their decomposition temperatures. The electron-withdrawing sulfone group should impart good oxidation stability to these polymers. P(C6OTV-SFTV), the most electron-rich among the four, was selected for a static heating test at 160 ^{o}C in air for 30 minutes. The heated sample did not decompose at all as indicated by its ^{1}H NMR spectrum. From the DSC and TGA data presented in **Table 1.1.1**, we conclude that the sulfone-based polymers are dynamically stable to temperatures as high as 258°C.

Optical and electrochemical properties. Figure 1.1.6 top shows the absorption spectra of the SF-PTV solutions of the same nominal concentration (0.1mM in chloroform, boiled, then cooled to RT). The absorption tails of P(C10OPV-SFTV) and P(C6OTV-SFTV) vanishes quickly at the long wavelength side, indicating that the two polymers were fully dissolved. The peak absorbance of the two polymer solutions are 3.11 and 3.27, very close to each other with a difference of ±2.5 % from the average value. In the spectra of the other two polymers, the absorption peaks sit on a slope. The slope, higher at the short wavelength side, is due to light scattering by insoluble polymer particles or precipitate. The two solutions were then filtered with 0.2-µm filters, and absorption spectra of the resulting solutions were obtained. By comparing the peak absorbance (1.10 and 0.753) of the filtered solutions with the average peak absorbance (3.19) of the two fully dissolved polymers, we get estimated solubility of 0.034 mM (15 mg/L) and 0.024 mM (9.7mg/L) for P(TV-SFTV) and P(PV-SFTV) respectively. Normalized absorption spectra of four polymers solutions (fully dissolved or filtered) are shown in **Figure 1.1.6** bottom. The absorption ranges of four polymers span over the full visible range. The absorption λ_{max} and optical energy gaps (E_g^{opt}s, calculated from absorption cutoff wavelengths) are listed in **Table 1.1.2**. The energy gap decreases as the

13

donor unit changes from simple phenylene all the way to 3,4-bishexyloxythienylene, with a good correlation with aromatic resonance energy and electronic richness of the aromatic unit.
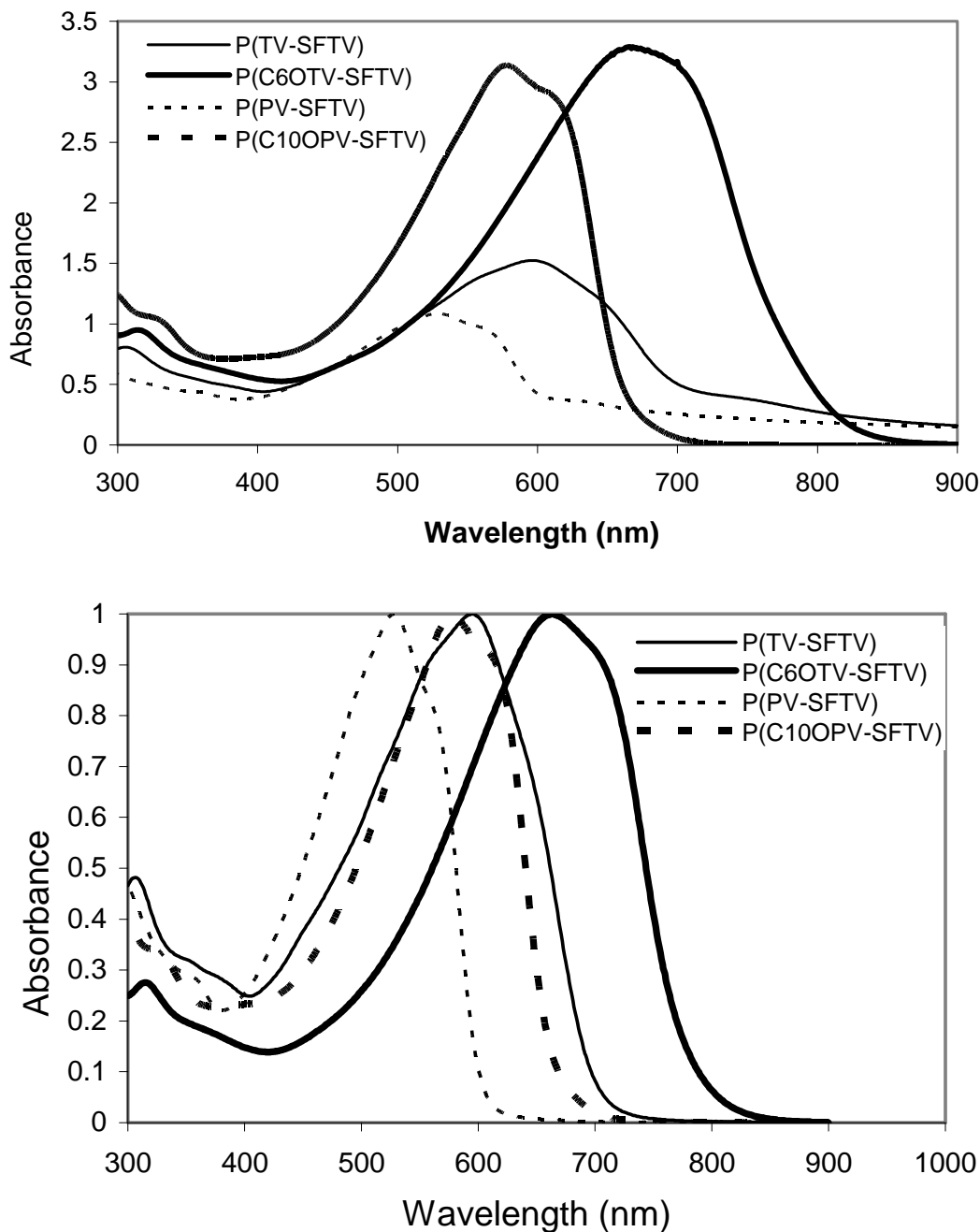

Figure 1.1.6 Top: UV-vis Absorption spectra of SF-PTV chloroform solutions with nominal concentration of 0.1mM without filtration. The later two polymers are not fully dissolved. Scattering of light by the polymer particles is evident in the spectra of these two polymers. Bottom: Normalized UV-vis Absorption spectra of above solutions. P(TV-SFTV) and P(PV-SFTV) solutions were filtered with 0.1 μm filter.

Table 1.1.2 Electronic properties of SF-PTVs

	λ_{max} (nm) (CHCl$_3$/film)	λ_{max} (nm) of PL in CHCl$_3$	λ_{cutoff}/Eg^{opt} (nm/eV)	Onset Redox Potentials (V vs. Ag/Ag+)	LUMO/ HOMO/Eg^{EC} (eV)
P(PV-SFTV)	528/495	550	608/2.04	-1.26/0.80	-3.48/-5.54/2.06
P(C10OPV-SFTV)	578/595	-	684/1.82	--/0.49	--/-5.23/--
P(TV-SFTV)	594/635	-	708/1.75	-1.18/0.62	-3.56/-5.36/1.80
P(C6OTV-SFTV)	663/616	-	806/1.54	-1.20/0.42	-3.54/-5.16/1.62

Photoluminescent measurements were performed for both solutions and films of the polymers; no PL signal was detected for any of the samples. This result is in consistence with non-fluorescent nature of various PTV-based polymers.[9,11,24]

Electrochemical measurements were performed for SF-PPVs in thin films coated on Pt working electrode (**Figure 1.1.7**). LUMO/HOMO levels are estimated from the redox potentials (**Table 1.1.2**) and corresponding electrochemical energy gaps (E$_g^{EC}$s) are also listed in **Table 1.1.2**. The LUMO levels of all SF-PTVs are very close (with differences < 0.1 eV). This is consistent with the fact that the acceptor unit is same for all SF-PTVs and that LUMO level is mostly affected by electron withdrawing group(s) of the π-conjugated systems.[7,25] The SF-PTVs are similar to the well known acceptor polymer CN-PPV[26] in terms of LUMO level, and are likely to function as acceptors when paired with electron-rich π-conjugated polymers. Due to the fact that SF-PTVs have lower E$_g$s and are not luminescent, photoluminescence quenching may not be soly used to confirm the photo induced charge transfer in blend of SF-PTV with commonly used donor polymers. Other types of experiments (such as ESR, PIA, and photo conductivity) should be conducted to confirm the acceptor nature and photovoltaic potentials of these polymers (especially the two soluble polymers).
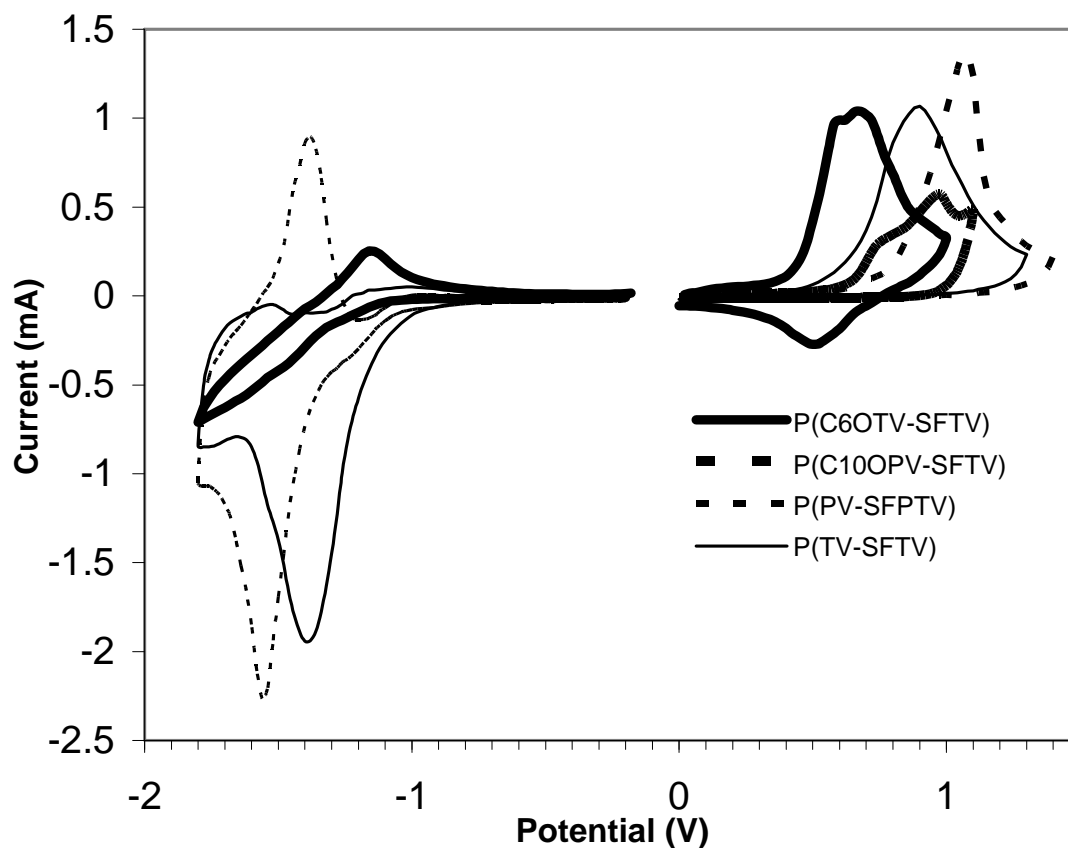
Figure 1.1.7 Cyclic voltamograms of SF-PTV films coated on Pt wire. Reference electrode: Ag in 0.1M AgNO$_3$/MeCN.

Computational Study of HOMO/LUMO Levels and Energy Gaps

Design of model structures. Optical energy gap of P(C6OTV)-SFTV) is 1.54 eV (in chloroform), which is ~0.3 eV lower than the regular monoalkyl-substituted PTV.[10] The reduction in E$_g$ could be attributed to two factors: 1) the loss of aromaticity of the second thiophene unit, and 2) the donor-acceptor interaction between the sulfone acceptor and alkoxy-substituted thiophene donor in the π-conjugated system.[7] To determine which factor is dominant, we conducted computational study on three series of model oligomers (**Figure 1.1.8**): (MeOT-TV)$_n$, (MeOT-4V)$_{n=1-4}$ and (MeOTV-SFTV)$_{n=1-4}$. The later two can be considered as the derivatives of the first structure. (MeOT-4V)$_n$ will allow us to see how much reduction in E$_g$ could be produced by removing aromaticity of the second thiophene ring. (MeOTV-SFTV)$_n$ has the same backbone as P(C6OTV-SFTV). Computation of energy gaps of this series of model oligomers will allow us to find how much additional reduction in energy gap can be obtained by replacing the CH$_2$ unit with a SO$_2$ unit.
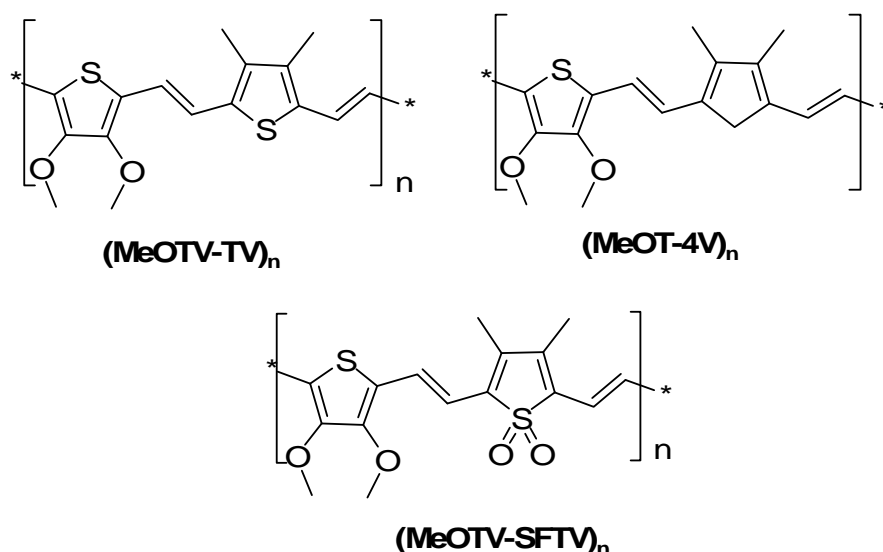
(MeOTV-TV)ₙ **(MeOT-4V)ₙ**

(MeOTV-SFTV)ₙ

Figure 1.1.8 Model structures for DFT computational study.

Computational method. HOMO/LUMO energy levels and E_gs were obtained by quantum mechanical calculation of oligomers with increasing length, and followed by extrapolation of calculated values to infinite chain length.[27] Hybrid exchange-correlation functional B3LYP in the Density Functional Theory (DFT) formalism was used for both geometry optimization and energy calculation, where B3LYP stands for Becke's three parameter hybrid functional using the Lee-Yang-Parr (LYP) correlation functional.[28] As shown by Yang et al,[27] B3LYP (for both geometry optimization and energy level calculation) is one of the best methods for estimating E_gs for PTV polymers under an appropriate computational cost. Considering the computational power available, small basis set 3-21G* was used and implemented in Gaussian 03.[29] The E_gs of polymers were obtained by plotting the E_gs of monomers through tetramers against reciprocal of the number of double bonds on the main chain and extrapolating the fitting line to the infinite number of double bonds, according to the free-electron molecular orbital model (FEMO).[30]

Computational results and discussion. The results of HOMO/LUMO and E_gs for the three series of oligomers are listed in **Table 1.1.3**. The E_g values are plotted in **Figure 1.1.9** as functions of $1/m$, where m is the number of C=C double bonds in the oligomers. Extrapolation of the linear fitting lines results in E_gs of polymers (n=∞) which are also listed in **Table 1.1.3**. The obtained E_g for (MeOTV-SFTV)$_{n=∞}$ is 1.19 eV, smaller than the experimental value of 1.54 eV obtained for P(C6OTV-SFTV) in chloroform solution. The underestimation is consistent with the literature report[27] that the combination of B3LYP/B3LYP at DFT level usually produces E_g lower than experimental results for PTV and other conjugated systems. The E_g of (MeOTV-4V)ₙ is smaller than that of (MeOT-TV)ₙ by 0.2 eV, suggesting that the removal of aromaticity is effective in reducing E_g. But from (MeOTV-4V)ₙ to (MeOTV-SFTV)ₙ, E_g only decreases by 0.097 eV. The results suggest that the low E_g of P(C6OTV-SFTV) is mainly due to the loss of the aromaticity of the thiophene. Since the donor units in other three synthesized polymers are less electron rich, the contributions from D-A interactions should be even less. Although the sulfone group in (MeOTV-SFTV)ₙ is not very effective in reducing E_g, it does bring LUMO down significantly by ~0.7 eV with respect to those of (MeOTV-

17

4V)$_n$, making SF-PTVs potentially useful as electron acceptors in variety of polymer electronic and optoelectronic applications.

Table 1.1.3. Results of DFT calculations.

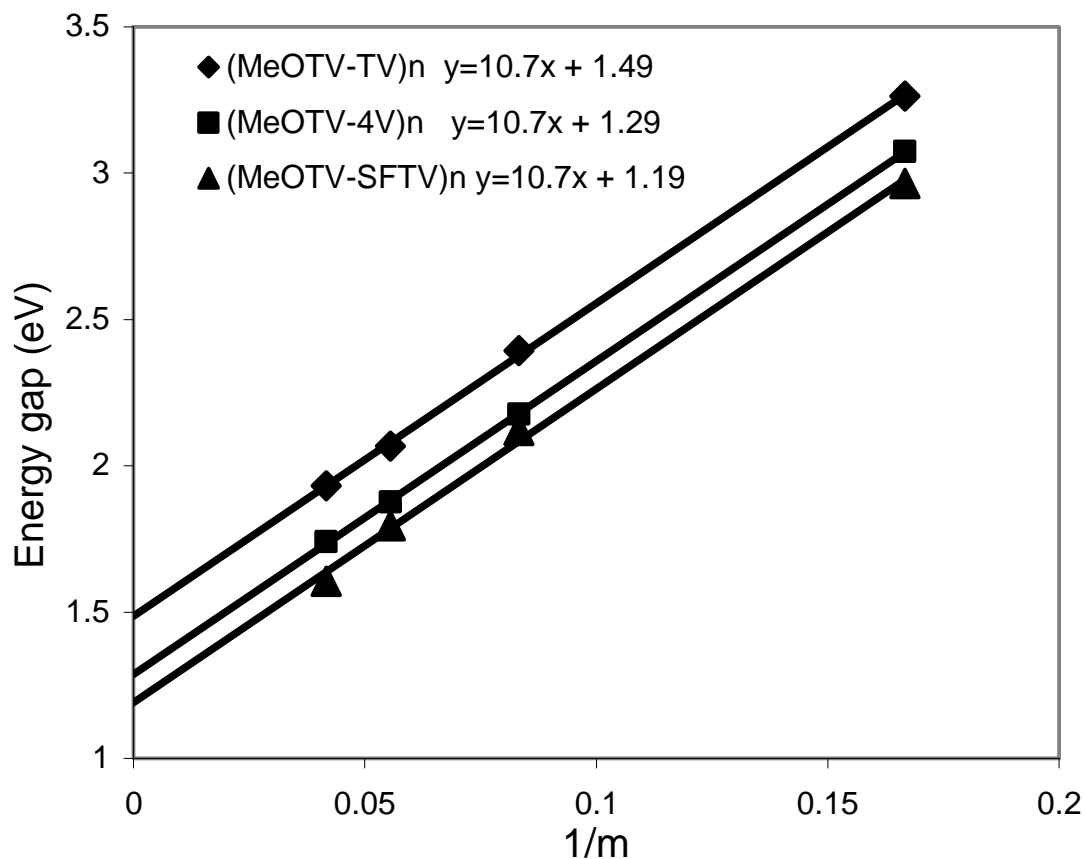|		LUMO (eV)	HOMO (eV)	Eg (eV)
	n=1	-1.496	-4.76	3.264
(MeOT-TV)$_n$	n=2	-1.9856	-4.3792	2.3936
	n=3	-2.176	-4.2432	2.0672
	n=4	-2.2576	-4.1888	1.9312
	n=∞			1.4855
	n=1	-1.4416	-4.5152	3.0736
	n=2	-1.9312	-4.1072	2.176
	n=3	-2.0944	-3.9712	1.8768
	n=4	-2.176	-3.9168	1.7408
(MeOT-4V)$_n$	n=∞			1.2784
	n=1	-2.2848	-5.2496	2.9648
	n=2	-2.8288	-4.9504	2.1216
(MeOTV-SFTV)$_n$	n=3	-2.992	-4.7872	1.7952
	n=4	-2.992	-4.5968	1.6048
	n=∞			1.2313

Figure 1.1.9 Plots of calculated energy gaps versus 1/m where m is the total number of C=C double bonds in each oligomer. Linear fitting of the data points of each series and extrapolation of the fitting lines are also shown.

1.1.4 Conclusions and Summary

A series of conjugated main chain terminal functionalized and evolving energy gap sulfone-containing thienylenevinylene-based co-polymers have been developed and studied. The HOMO/LUMO energy gaps of these polymers were in a range of 1.5-2.0 eV. Oxidation of one of every two thiophene units brings about 0.3 eV in reduction in energy gap. Two thirds or more of the energy gap reduction can be attributed to the removal of aromaticity of the thiophene ring, and the rest is due to the donor-acceptor interaction between the sulfone and RO-substituted thiophene ring. The sulfone group greatly lowers both HOMO/LUMO levels, making these polymers potential electron acceptors (n-type) for polymeric electronic/optoelectronic applications. Lowering HOMO/LUMO levels also improve the air stability of the materials. The sulfone polymers have dynamic stability at 258°C or higher, and the decomposition starts with loss of polymer components in contrast to regular PTVs which decompose initially by cross-linking. The well-defined terminal functional groups (aldehyde or phosphonate) make these polymers potentially ideal acceptor polymer blocks for the development of D-A block copolymer supramolecular nanostructures.[5]

1.1.5 **Supporting Information (SI):** ^1H and ^{13}C NMR spectra of all the precursors to the two monomers are listed here.
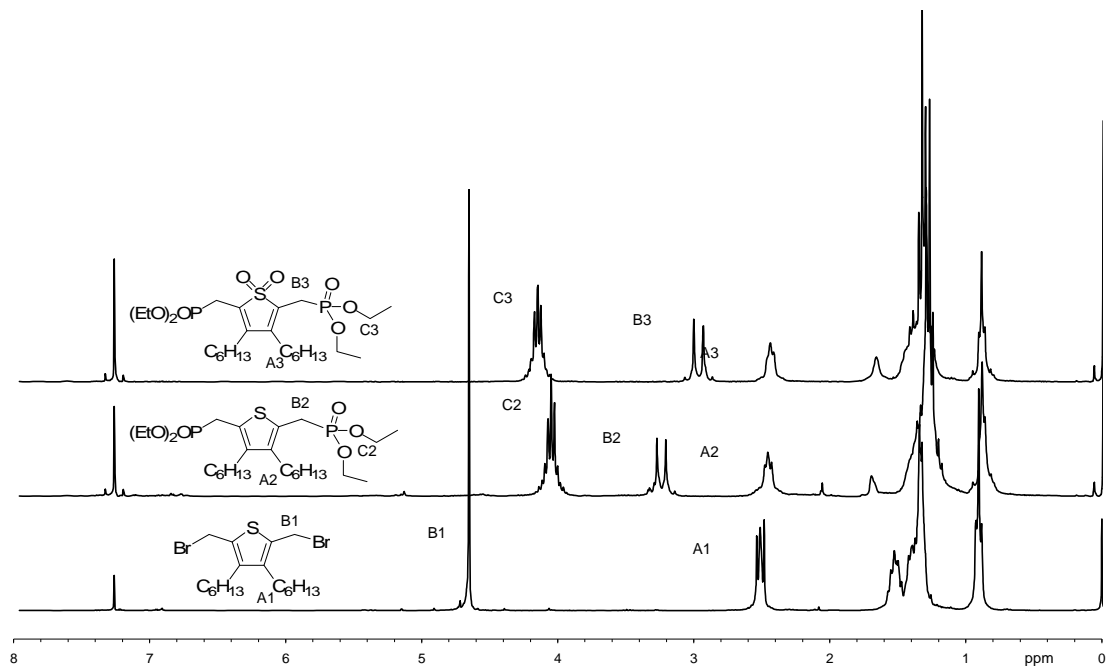

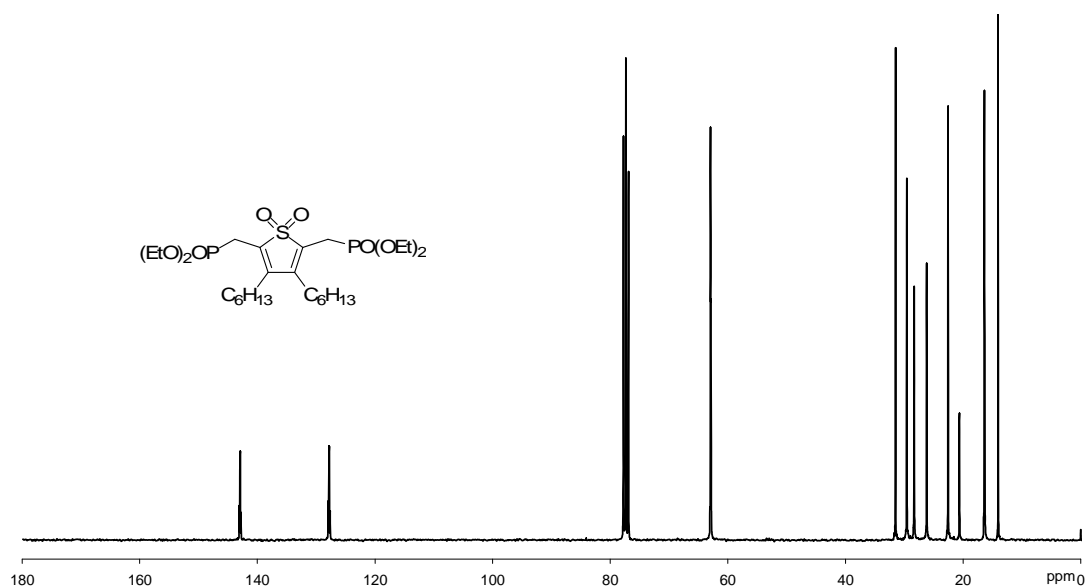**Figure 1.1.10** ^1H NMR spectra of the diphosphonate monomer and its precursors.

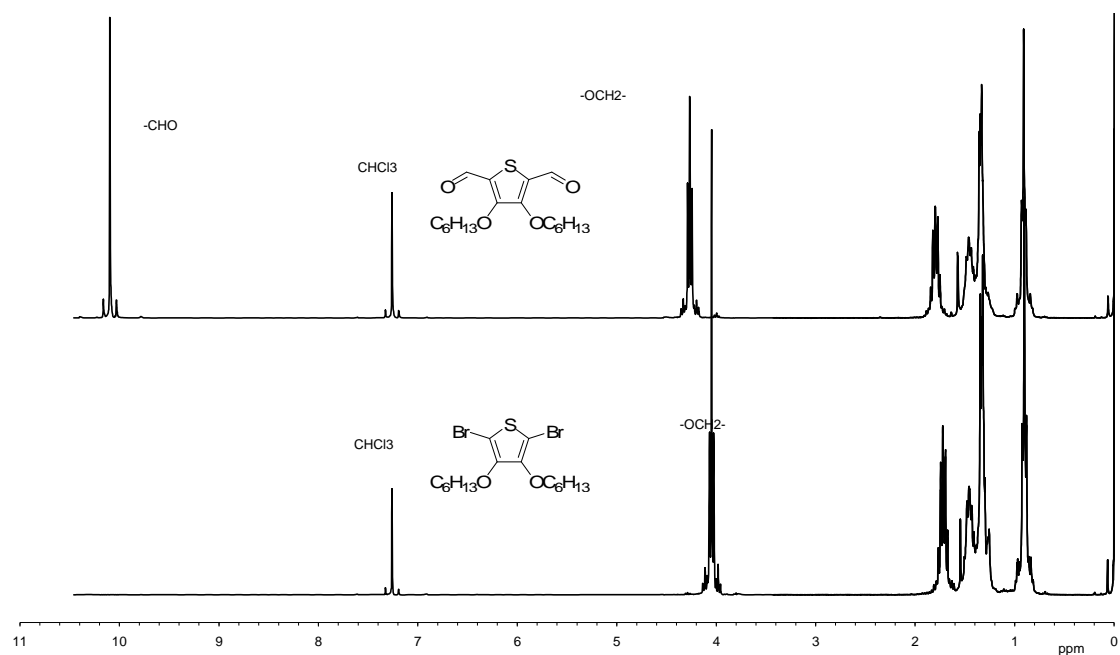**Figure 1.1.11** ^{13}C NMR spectrum of the diphosphonate monomer.

Figure 1.1.12 ¹H NMR spectra of the dialdehyde monomer **8** and its precursor.
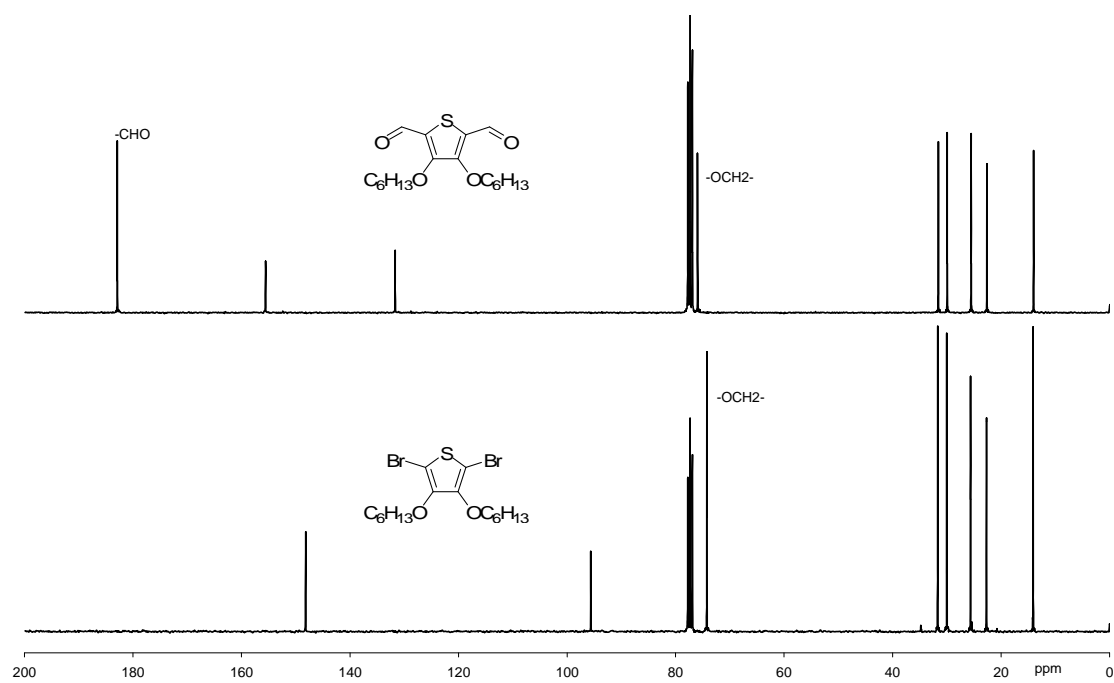

Figure 1.1.13 ¹³C NMR spectra of the dialdehyde monomer **8** and its precursor.

1.1.6   *References and Notes for Part 1.1*

1. Sun, S. and Sariciftci, S., eds., Organic Photovoltaics: Mechanisms, Materials and Devices, CRC Press, Boca Raton, Florida, **2005** (ISBN: 978-0824759636).

2. Zhang, C and Sun, S., "Organic and Polymeric Photovoltaic Materials and Devices", in *Introduction to Organic Electronic and Optoelectronic Materials and Devices*, eds: Sun, S and Dalton, L., CRC Press/Taylor & Francis: Boca Raton, Florida, USA, **2008,** chapter 14, pp 401-420. b) Sun, S. "Organic and Polymeric Solar Cells", in *Handbook of Organic Electronics and Photonics*, edited by S. H. Nalwa, American Scientific Publishers, Los Angeles, California, **2008**, vol. 3, chapter 7, pp 313-350.

3. a) Zhan, X.; Tan, Z.; Domercq, B.; An, Z.; Zhang, X.; Barlow, S.; Li, Y.; Zhu, D.; Kippelen, B. and Marder, S. R. *J. Am. Chem. Soc.* **2007**, 129, 7246-7247. b) Tan, Z.; Zhou, E.; Zhan, X.; Wang, X.; Li, Y.; Barlow, S. and Marder, S. R. *Appl. Phys. Lett.* **2008**, 93, 073309.

4. Scherf, U.; Gutacker, A.; Koenen, N. *Acc. Chem. Res.* July **2008**, ASAP.

5. Zhang C, Choi S, Haliburton J, Cleveland T, Li R, Sun S, Ledbetter A, Bonner C. *Macromolecules***. 2006**, 39, 4317-4326.

6. Sun, S.-S.; Zhang, C.; Ledbetter, A.; Choi, S.; Seo, K.; Bonner, Jr., C. E.; Drees, M. and Sariciftci, N. S. *Appl. Phys. Lett.* **2007**, 90, 043117.

7. Roncali, J. *Chem. Rev.* **1997**, 97, 173-205.

8. Loewe, R. S.; McCullough, R. D. *Chem. Mater.*, **2000**, 12, 3214. And references therein.

9. Hou, J.; Tan, Z.; He, Y.; Yang, C.; Li, Y. *Macromolecules,* **2006**, 39(14), 4657-4662.

10. Gavrilenko, A. V.; Matos, T. D.; Bonner, C. E.; Sun, S.-S.; Zhang, C. and Gavrilenko, V. I. *J. Phys. Chem., C.* **2008**, 112(21), 7908-7912.

11. Synthesis and Characterization of Fully Regioregular Head-to-Tail Poly(3-Dodedyl-2,5-Thienylenevinylene) for Opto-Electronic Applications. Cheng Zhang, Taina Matos, Rui Li, Shahin Maaref, Eric Annih, and Sam-Shajing Sun, Jian Zhang, Xiaomei Jiang. *Submitted to Chemistry of Materials*.

12. Barbarella, G.; Favaretto, L.; Sotgiu, G.; Zambianchi, M.; Arbizzani, C.; Bongini, A. and Mastragostino, M. *Chem Mater.*, **1999**, 11, 2533-41.

13. Diaz-Quijada, G. A.; Weinberg, N.; Holdcroft, S. and Pinto, B. M. *J. Phys. Chem. A* **2002**, 106, 1266-1276.

14. Shahid, M.; Ashraf, R. A.; Klemm, E.; and Sensfuss, S. *Macromolecules*, **2006**, 39, 7844-7853.

15. Bhattacharya, A. K.; Thyagarajan, G. *Chem. Rev.* **1981**, *81*, 415-430.

16. The decomposition of **3** was not mentioned in ref. 14, but is likely the reason for unavailability of elemental analysis data.

17. Günther, H. Chapter 4 in NMR Spectroscopy: Basic principles, concepts, and applications in chemistry. Second Edition English version by John Wiley & Sons **1995**.

18. Akoudad, S.; Frère, P.; Mercier, N.; and Roncali, J. *J. Org. Chem.* **1999**, 64, 4267-4272.

19. Goldoni, F.; Langeveld-Voss, B. M. W.; Meijer, E. W. *Syn. Commun.*, **1998**, 28(12), 2237-2244.

20. Agarwal, N.; Mishra, S. P.; Kumar, A.; Hung, C.-H.; Ravikanth, M. *Chem. Commun.*, **2002**, 22, 2642-2643.
21. In the ^{1}H NMR data of reference 18, two triplets (in stead of one) are listed. Several errors are found in the ^{13}C NMR peak list: 1. Only one thiophenic carbon peak is listed, 2. The 97.2 ppm peak (can not be assigned either to any thiophenic carbon or the aliphatic side chain) is obviously due to impurity, and 3. A few other peaks in the list (147.6, 71.5, 25.7 ppm) also belong to impurities.
22. NC Greeham, SC Moratti, DDC Bradley, RH Friend, AB Holmes, Nature **1993**, 365, 628-630.
23. Samperi, Filippo; Puglisi, Concetto; Ferreri, Tiziana; Messina, Rosario; Cicala, Gianluca; Recca, Antonino; Restuccia, Carmelo Luca; Scamporrino, Andrea. *Polymer Degradation and Stability*, **2007**, 92(7), 1304-1315.
24. A. J. Brassett, N. F. Colaneri, D. D. C. Bradley, R. A. Lawrence, R. H. Friend, H. Murata, S. Tokito, T. Tsutsui and S. Saito, Phys. Rev. B **1990**, 41, 10586.
25. J. Cornil, D. A. dos Santos, D. Beljonne, and J. L. Bredas, *J. Phys. Chem.* **1995**, 99, 5604-5611.
26. Chen, S.-A. and Chang, E.-C. *Macromolecules* **1998**, 31, 4899-4907. And references therein.
27. Yang, S.; Olishevski, P. and Kertesz, M. *Syn. Met.* **2004**, 141, 171.
28. Computational Chemistry: A Practical Guide for Applying Techniques to Real World Problems, 1st ed., Young, D. C. Wiley-Interscience, **2000**.
29. www.gaussian.com
30. Ruedenberg, K.; Scherr, C. W. *J. Chem. Phys.* **1953**, 21, 1565.

1.2 A New Series of Sulfone-Derivatized Phenylenevinylene (SF-PV) Based Conjugated Copolymers with Taylored Frontier Orbitals and Energy Gaps

Abstract: A new series of stable and processable sulfone-derivatized phenylenevinylene based conjugated polymers (SFPVs) containing different donor-type co-monomers have been synthesized and characterized. The polymer main chains are consisted of an electron-accepting unit [2-(decane-1-sulfonyl)-5-(decyloxy)-4-(diethoxyphosphoryl-methyl)bezyl]phosphonic acid diethyl ester, coupled with an electron donating unit which is derived from one of the dialdehyde comonomers based on benzene, thiophene, and pyrrole (with or without alkoxy side chains). The optical energy gaps of the polymers (in solvent) were in a range of 1.9-2.3 eV, with the lowest energy gap obtained from the polymer containing pyrrole as the donor unit. By using a combination of strong donor unit (such as pyrrole) and a relatively weak acceptor unit (sulfone-substituted phenylene), energy gaps of conjugated polymers can be engineered to below 2 eV, while the vinylene bounds are still chemically stable to strong bases as compared to the S,S-dioxo-thiophene based PTV polymers, a property critical for the incorporation of such vinylene-based polymers into block copolymers.

1.2.1 Introduction

Research and development of conjugated electroactive polymers have become intensive in recent years due to their potential applications in a variety of next generation flexible, lightweight, and high speed/capacity optoelectronic (OE) devices such as in organic photovoltaic cells (OPVCs) and photo detectors,[1-5] organic light emitting diodes (OLEDs),[6,7] organic field effect transistors (OFETs),[8] *etc*. The frontier orbital (HOMO/LUMO) levels and excitation energy gaps (E_g) of the conjugated polymers are vital for electronic and optical properties of the polymers and the OE devices made of those polymers. In general, a donor moiety on the conjugated polymer backbone would increase the HOMO and LUMO levels toward the vacuum level, and an acceptor moiety on the conjugated backbone would decrease the HOMO and LUMO levels away from the vacuum level. When both donor and an acceptor moieties were coupled to each other in a conjugated backbone, excitation energy gaps of resulting conjugated polymers could be reduced substantially.[4,9] In an earlier work, we used such strategy and developed several vinylene-based conjugated polymers containing an oxidized thiophene unit (S,S-dioxo-thiophene).[17] However, one disadvantage of S,S-dioxo-thiophene based polymers is that the vinylene bonds in the polymers are relatively reactive and particularly susceptible to the attack of nucleophiles via the Michael addition reaction, making it hard to produce defect-free conjugated polymers, particularly the end-functionalized polymer blocks for further block copolymer synthesis. In another study, we found that when a sulfone acceptor group is attached to a benzene ring, it does not reduce the chemical stability of vinylene unit in PPV copolymers.[16] However, the resulting conjugated polymers (SF-PPVs) have wide energy gaps (> 2.4 eV) as the (substituted) phenylene donor units used are not good donors. In this work, we tune the frontier orbital levels and excitation energy gaps of SF-PV based copolymers via the usage of more electron-rich donor moieties such as thiophenes and particularly a pyrrole unit, which has rarely been used in vinylene-based and DA coupled conjugated copolymers. The synthesized polymers

exhibit better chemical stability than S,S-dioxothiophenevinylene based polymers, and good thermal properties and processability for a variety of potential optoelectronic applications.

1.2.2 Experimental

Starting Materials and Instrumentation: All starting materials, reagents, and solvents were purchased from commercial sources (Sigma Aldrich and Fisher-Scientific) and used without further purification unless noted otherwise. NMR spectra were obtained from a Bruker Advance 300 MHz spectrometer with TMS as the internal reference. Elemental analysis were done at Atlantic Microlab Inc. UV-Vis spectra were collected on a Perkin Elmer Lambda 900 Spectrophotometer. Differential scanning calorimetric (DSC) and thermal gravimetric analysis (TGA) data were collected on Perkin Elmer DSC-6 and TGA-6 systems. Photoluminescence experiments were performed on an ISA Flouromax-3 luminescence spectrofluorometer in solution (THF).

Cyclovoltammetry: Electrochemical studies were performed on a Bioanalytical (BAS) Epsilon-100w tri-electrode cell system. Tree electrodes are a Pt working electrode, an ancillary Pt electrode, and a silver reference electrode (in a CH_3CN solution of 0.01 M $AgNO_3$ and 0.10 M tetrabutylammonium hexafluorophosphonate, TBA-HFP). Polymer samples were typically dissolved in hot solvent (typically o-Dichlorobenzene) and then coated onto Pt working electrode. The measurements were performed in 0.10 M TBA-HFP/acetonitrile solution purged with nitrogen gas. Between the experiments, surfaces of electrodes were cleaned or polished. Scan rate was 100mV/s. Ferrocene (2 mM in 0.10 M TBA-HFP/CH_3CN solution) was used as internal reference standard, and its HOMO level (-4.8 eV) was used as the reference level.[11-14]

Gel permeation Chromatography. Polymer molecular weights were measured by a Viscotek GPC system using a UV-VIS absorption detector at ambient temperature, tetrahydrafuran (THF) as the solvent, and polystyrene standards for conventional calibration.[15,23,24]

N-(n-hexyl)pyrrole (1). The procedure by Thorsten[15] was modified as follows: To a 250 ml 2-necks round bottom flask were added pyrrole (10g, 149mmol), 1-bromohexyl (149mmol, 24.6g), (n-Bu)$_4$NBr (149mmol, 48.03g), 100 mL CH_2Cl_2.The mixture was cooled to 0^oC in a nitrogen atmosphere. 100 mL of 50% NaOH was dropped into the mixture. The mixture was refluxed for 26 hours. The mixture was cooled to room temperature, diluted by 50 mL of water, and extracted with CH_2Cl_2. The CH_2Cl_2 extract was dried with $MgSO_4$, and filtered. The crude product was purified by column chromatography with silica gel and (2:3, CH_2Cl_2 : Hexane) to give 12.99 g of yellow pure product. Yield: 57.7 %. ^1H NMR ($CDCl_3$): δ (ppm) 0.88 (t, J=6.17 hz, 3H), 1.00-1.68 (m, 8H), 1.74 (quintet, J=6.40 Hz, 2H), 3.85 (t, J=7.16 Hz, 2H), 6.13 (t, J=1.32 Hz, 2H), 6.64 (t, J=2.07Hz, 2H). The spectra are given in the Supporting Information (SI).

N-(n-hexyl)-2,5-dibromopyrrole (2). The procedure by Thorsten[15] was modified as follows: To a 50 ml 2-necks round bottom flask were added **(1)** (1.96g, 0.0130mol), and anhydrous (20mL) THF. The flask was then cooled to -78 ^oC. NBS powder (0.026mol, 4.625g) was added. The resulting the mixture was stirred for 10 minutes, then warmed to room temperature, and stirred for one hour. After routine workup with hexane, the solvent was removed by vacuum rotatary evaporation to afford 3.99g crude product. Yield:100%. The crude product was used in next step. ^1H NMR ($CDCl_3$): δ (ppm) 0.88 (t, J=6.17 hz, 3H), 1.00-1.68 (m, 8H), 1.74 (quintet, J=6.40 Hz, 2H), 3.95 (t, J=6.78 Hz, 2H), 6.15 (d, J=1.70 Hz, 2H). The spectra are given in the Supporting Information (SI).

N-(n-hexyl)-2,5-dialdehydepyrrole (3). To a 50 mL two-neck round bottom flask were added **(2)** (3.99g, 0.013mol) and anhydrous THF (20ml).The mixture was cooled to -78 ^{o}C. n-BuLi (13 mL, 2.5 M) in 10ml THF was cooled to -78 ^{o}C and added drop-wise into the mixture. Five minutes later, DMF (0.039 mol, 2.85 g) was added. The mixture was stirred for 10 more minutes and poured into the separation funnel containing pure hexane (50 mL) and tap water (50 mL). The hexane extracts were combined and dried with MgSO$_4$, and filtered. The crude product was purified by column chromatography with silica gel and ethyl acetate /hexane (1/450) to give 1.04 g of pure liquid product (yield 53.5%). ^{1}H NMR (CDCl$_3$): δ (ppm) 0.88 (t, J=6.17 hz, 3H), 1.00-1.68 (m, 8H), 1.71 (quintet, J=5.65 Hz, 2H), 4.74 (t, J=9.72 Hz, 2H), 6.96 (d, J=3.01 Hz, 2H), 9.83 (s, 2H). ^{13}C NMR (CDCl$_3$): δ (ppm) 13.67, 22.07, 25.91, 31.14, 31.37, 46.55, 121.70, 135.78, 181.72. Anal. Calc.: C, 69.54; H 8.27; N, 6.76; Found: C, 69.01; H, 8.28; N, 6.69. The spectra are available in the Supporting Information (SI).

Poly(N-hexylpyrrolenevinylene-sulfonephenylenevinylene), P(pyrrole-SFPV). To a solution of **3** (100 mg, 0.4824 mmol) and **8** (381.37 mg, 0.5065 mmol) in 3mL of THF in a glove box was added t-BuOK (124 mg, 1.109 mmol in 2 mL of THF) over two minutes. The mixture was stirred for 15 more minutes, neutralized with a few drops of acetic acid, and dropped into methanol (50 mL). 250 mg of dark red polymer solid was obtained after filtration, methanol washing, and vacuum drying at 60 ^{o}C for 24 hours. Yield: 84.4%. ^{1}H NMR (CDCl$_3$): δ (ppm) 0.95 (m, 12H), 1.50-2.00 (m, 40 H), 3.12 (t, J=5.65 Hz, 2H), 3.85 (t, J=4.15 Hz, 2H), 4.20 (m, 4H), 6.68 (d, J=16.0 Hz, 2H), 6.95 (d, J=16.0 Hz), 2H), 7.10 (s, 2H), 7.18 (s, 1H), 8.18 (s, 1H) . (^{1}H NMR in **Figure 1.2.1**).

Poly(thienylenevinylene-sulfonephenylenevinylene), P(TV-SFPV). To a solution of **6** (100 mg, 0.714 mmol) and **8** (564.1 mg, 0.749 mmol) in 3 mL of THF in a glove box was added t-BuOK (193.4 mg, 1.723 mmol in 2 ml of THF) over two minutes. The mixture was stirred for one more hour, and the solution was taken out the glove box, neutralized with a few drops of acetic acid, and dropped into 50 mL of methanol. Dark red polymer solid was obtained after filtration, methanol and ethanol washing, and vacuum drying at 60 ^{0}C in 24 hours, yield: 300mg, 77.3%. ^{1}H NMR (CDCl$_3$): δ (ppm) 0.95 (m, 12H), 1.50-2.00 (m, 32 H), 3.12 (t, J=5.65 Hz, 2H), 3.85 (t, J=4.15 Hz, 2H), 4.12 (quintet, 2H), 4.20 (m, 4H), 7.10 (s, 2H), 7.18 (s, 1H), 7.45 (d, J=16.0 Hz, 2H), 7.88 (d, J=16.0 Hz), 2H), 8.18 (s, 1H) . (^{1}H NMR in **Figure 1.2.1**).

Poly(3,4-hexyloxythienylenevinylene-sulfonephenylenevinylene), P(OC6TV-SFPV). To a solution of **4** (100mg, 0.2937mmol) and **8** (323.2mg, 0.3231mmol) in 3mL of THF in a glove box was added t-BuOK (79.6 mg, 0.7093 mmol in 2 mL of THF) over two minutes. The mixture was stirred for 30 more minutes, then taken out the glove box, neutralized with a few drops of acetic acid, and dropped into 50 mL of methanol. Dark red polymer solid was obtained after filtration, methanol and ethanol washing, and vacuum drying at 60 ^{0}C in 24 hours, yield: 150 mg, 65.9%. ^{1}H NMR (CDCl$_3$): δ (ppm) 0.95 (m, 12H), 1.50-2.00 (m, 32 H), 3.12 (t, J=5.65 Hz, 2H), 3.85 (t, J=4.15 Hz, 2H), 4.20 (m, 4H), 7.18 (s, 1H), 7.45 (d, J=16.0 Hz, 2H), 7.88 (d, J=16.0 Hz), 2H), 8.18 (s, 1H) . (^{1}H NMR in **Figure 1.2.1**).

1.2.3 Results and Discussion
Synthesis of Monomers and Polymers.

The structures of all five sulfonylphenylenevinylene based copolymers (SFPVs) synthesized in our lab are shown in **Scheme 1.2.1**. All polymers have been synthesized from the acceptor type sulfone-phenylene diphosphonate monomer **8** [16,21] and different donor type dialdehyde co-monomers 3-7. Two of them, P(OC10PV-SFPV) and P(PV-SFPV), have been reported by us recently.[16] The dialdehyde **4** and **6** were synthesized based on literature procedures.[17,22] The dialdehyde **3** was prepared in three steps from pyrrole as shown in **Scheme 1.2.2**. Compound **1** was synthesized from pyrrole according to a literature procedure[15,18,19] with a hexyl side chain instead of a dodecyl side chain. Compound **2** was obtained from bromination of **1** using a literature procedure.[15,20] Purification of **2** was not performed due to limited stability of **2** in air. However, the crude product was pure enough to give a neat ^{1}H NMR spectrum (See **Figure 1.2.9** in supporting information) after a careful work-up. Finally, the monomer **3** was obtained from **2** by a di-formylation reaction (**Figure 1.2.7** in supporting information).
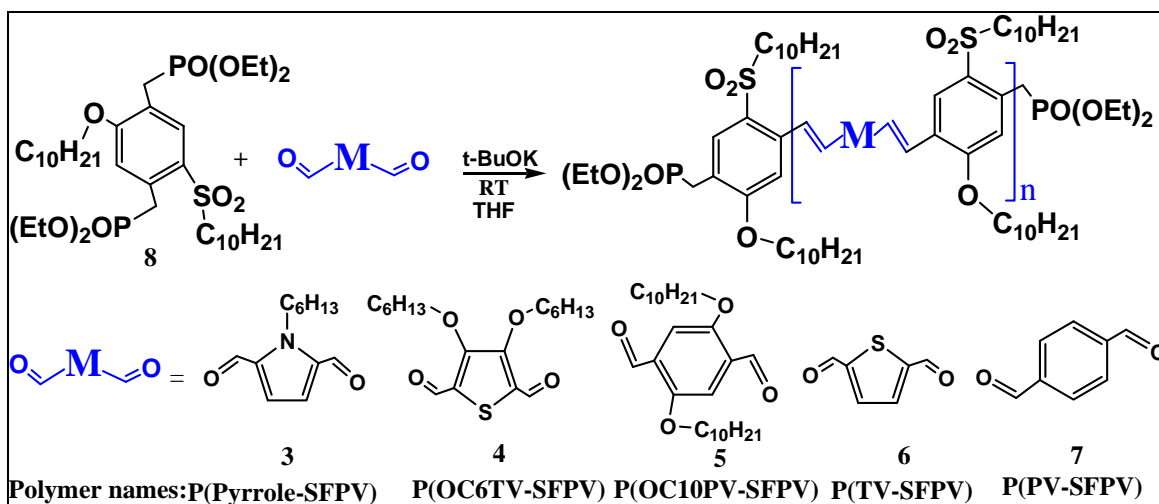
Scheme 1.2.1 Synthetic schemes of SFPVs from a common acceptor unit sulfone-substituted phenylene and five different donor units. P(OC10PV-SFPV) and P(PV-SFPV) were reported by us earlier.
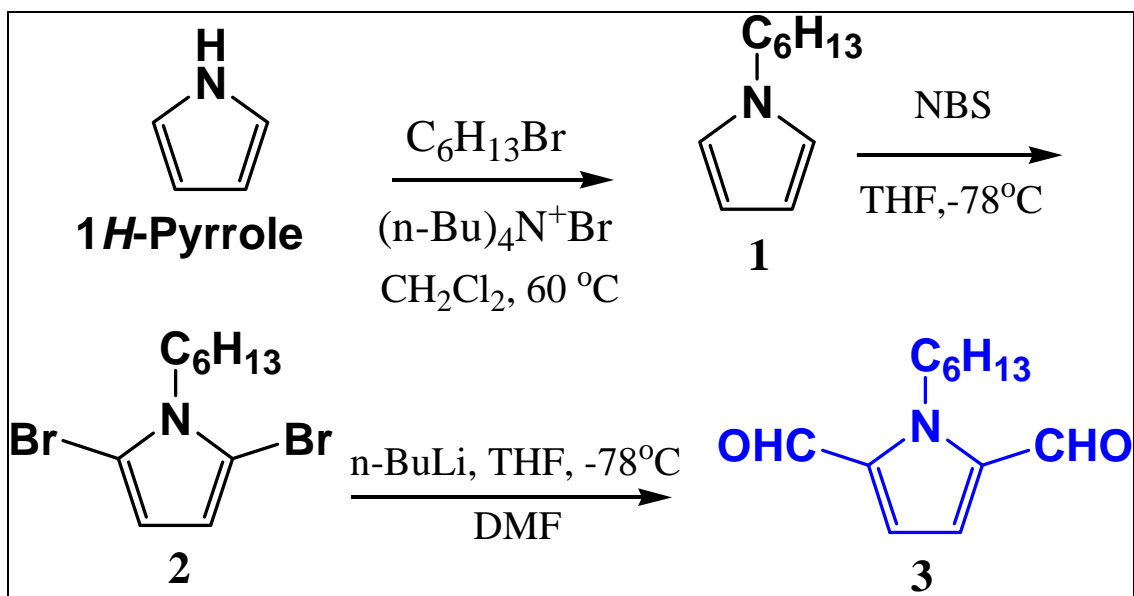
Scheme 1.2.2 Synthetic scheme of the dialdehyde monomer **3**.

The polymerization reactions for P(pyrrole-SFPV), P(OC6TV-SFPV), and P(TV-SFPV) were performed inside an inert gas glove box. The 5% excess of diphosphonate co-monomer was used to control the molecular weight of polymers. In ^{1}H NMR spectrum, **Figure 1.2.1**, the dialdehyde monomer was fully consumed as evidenced by the disappearance of the peaks at 9.83ppm, 10.10ppm, and 10.04ppm for **3, 4,** and **6** monomers, respectively (See ^{1}NMR spectra in **Figures 1.2.7, 1.2.11,** and **1.2.12** in Supporting Information). The diphosphonate peak (-**CH$_2$**-PO(OEt)$_2$, a doublet) of P(pyrrole-SFPV) polymer can be seen at 3.85 ppm in the spectrum as expected (enlarged ^{1}HNMR spectrum, **Figure 1.2.14a** in Supporting Information), and the diphosphonate peaks of P(OC6TV-SFPV) and P(TV-SFPV) polymers are seen at 3.32 ppm as expected (enlarged ^{1}H NMR spectrum, **Figure 1.2.14b-c** in Supporting Information). In the ^{1}H NMR spectrum of P(pyrrole-SFPV), two singlets at 7.18 ppm and 8.18 ppm represents two non identical phenyl protons, a singlet at 7.10 ppm corresponds to two identical pyrrole protons, and two doublets at 6.68 ppm and 6.95 ppm correspond to the newly formed C=C bond. In the ^{1}H NMR spectrum of P(OC6TV-SFPV), two singlet at 7.18 ppm and 8.18 ppm correspond to two non identical phenyl protons, and two doublets at 7.45 ppm and 7.80 ppm represent the newly formed of C=C bond. In the ^{1}H NMR spectrum of P(TV-SFPV), two singlet at 7.18 ppm and 8.18 ppm correspond to two non identical phenyl protons, a singlet at 7.08 ppm represents two identical thienyl protons, and two doublets at 7.45 ppm and 7.88 ppm corresponds to the newly formed C=C bond. Three conjugated co-polymers have formed cis and trans structures,[17] and their solubility were not high enough to obtain a clear ^{13}C NMR spectrum.
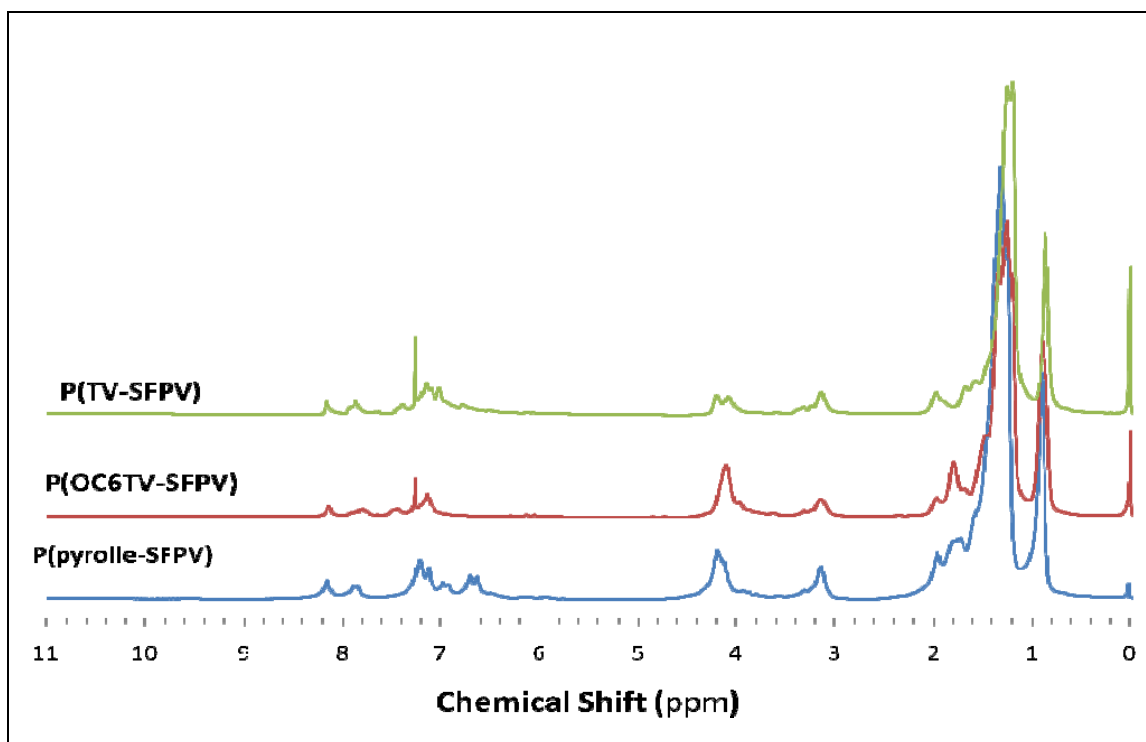
Figure 1.2.1 ^{1}H NMR spectra of the new SFPVs.

Chemical stability. These polymers are much more stable than similar vinylene-based polymers that have an S,S-dioxo-thiophene unit as the acceptor.[17] They are stable to the presence of t-BuOK and hydroxide bases, while S,S-dioxo-thiophene polymers can be easily bleached by these bases. Although both series of polymers carry sulfone (SO_2) groups, the later series of polymers have the sulfones directly attached on non-aromatic C=C bonds, making the C=C bonds much more electron-deficient and much more susceptible to Michael addition reactions.

Thermal Properties. DSC and TGA were used to study the decomposition behaviors of SFPV's. The DSC scans of polymers are shown in **Figure 1.2.2**. In the temperature range of room temperature (RT) to 300°C, none of the polymers exhibits a glass transition. P(pyrrole-SFPV) and P(OC6TV-SFPV) exhibit endothermic peaks at 265 and 285 °C and the onset decomposition peaks at 270 and 290°C, respectively. P(TV-SFPV) exhibits a decomposition peak with onset temperature of 310°C. No melting behaviors of these polymers were observed before decomposition. The TGA analyses of these polymers are shown on **Figure 1.2.3**. The weight loss onset temperatures of P(pyrrole-SFPV), P(OC6TV-SFPV), and P(TV-SFPV) are at 302°C, 292°C, and 300°C, respectively. Thermal as well as molecular weights data are also tabulated in **Table 1.2.2**.
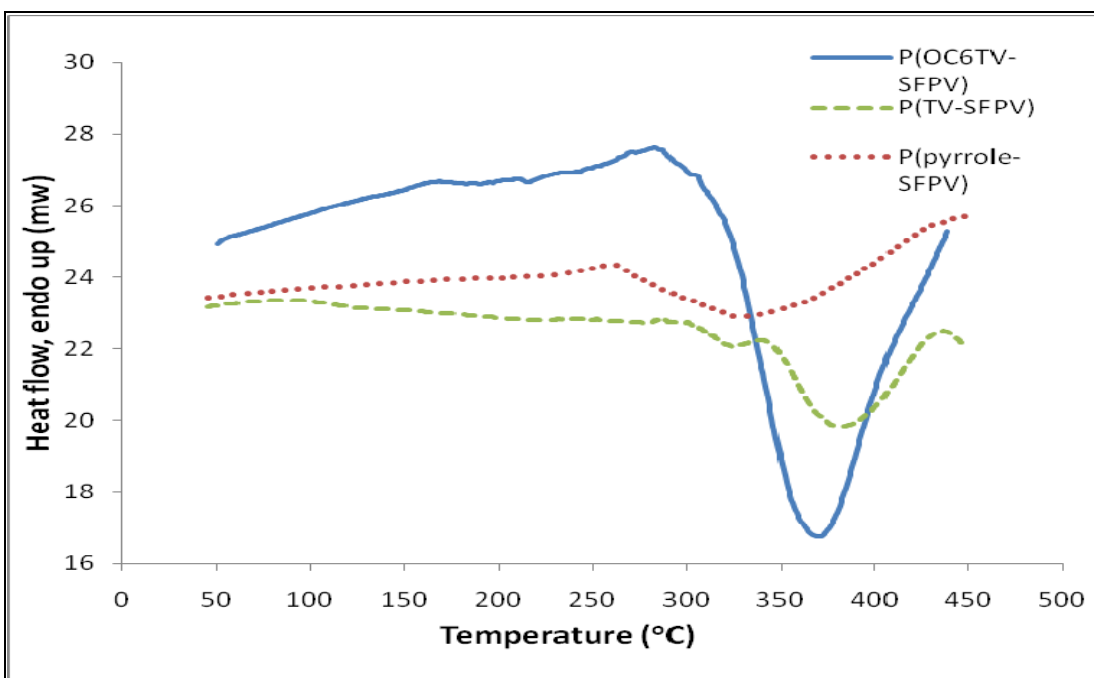
29

Figure 1.2.2 Differential Scanning Calorimetric (DSC) curves of the new SFPVs.
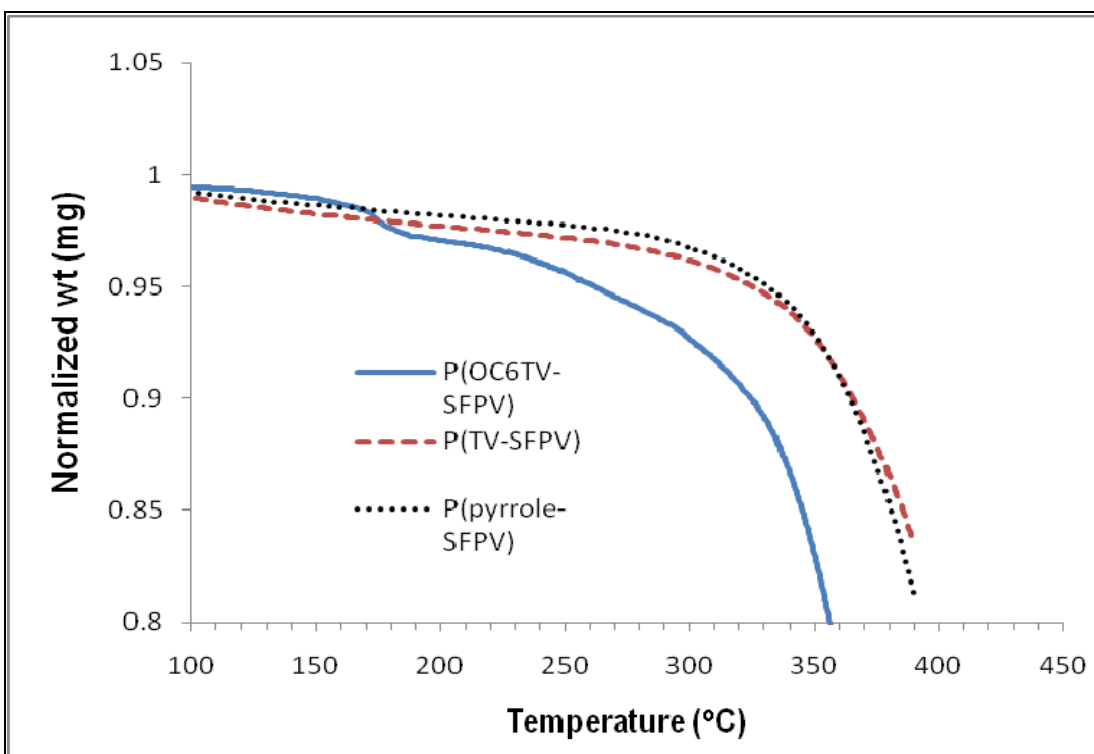

Figure 1.2.3 Thermal Gravity Analysis (TGA) of the new SFPVs.

Electrochemical and Optical Properties. UV-VIS spectrometer was used to obtain absorption peak wavelength (λ_{max}), and optical energy gaps (E_g^{opt}, calculated from absorption cutoff or onset wavelengths) of the polymers in THF solutions (**Figure 1.2.4**). Electrochemical energy gaps are calculated from the HOMO (based on the oxidation peak onset) and LUMO (based on the reduction peak onset) energies measured by cyclic-

30

voltammetry (**Figure 1.2.6**). These data are shown in **Table 1.2.1**. The optical energy gap decreases by 0.51 eV from P(PV-SFPV) to P(pyrrole-SFPV) due to both increasing electron donating ability of the donors from benzene to pyrrole, as well as the decreasing resonance energy of the donor moieties from pyrrole (22 Kcal/mol), thiophene (29 Kcal/mol), to benzene (36 Kcal/mol).[10] Alkoxy side groups enhance the electron-donating ability of the donor unit and result in a decrease in optical energy gap (0.11 eV) from P(**TV**-SFPV) to P(**OC6TV**-SFPV). The similar effect was also observed in two related polymers P(PV-SFPV) and P(**OC10PV**-SFPV) (see **Scheme 1.2.1** for structures and **Table 1.2.1** for energy gaps).

Photoluminescence in solution and GPC measurements. Molecular weights of these polymers were measured by GPC. M_n, M_w, and polydispersity (PD) data are shown in **Table 1.2.2**. PL spectra of these polymers in THF solution are shown in **Figure 1.2.5**. The different excitations (536, 485, and 480) were used to excite P(pyrrole-SFPV), P(OC6TV-SFPV), and P(TV-SFPV) polymers, respectively. The PL peak wavelengths of P(pyrrole-SFPV), P(OC6TV-SFPV), and P(TV-SFPV) are 620, 610, 590 nm, respectively.
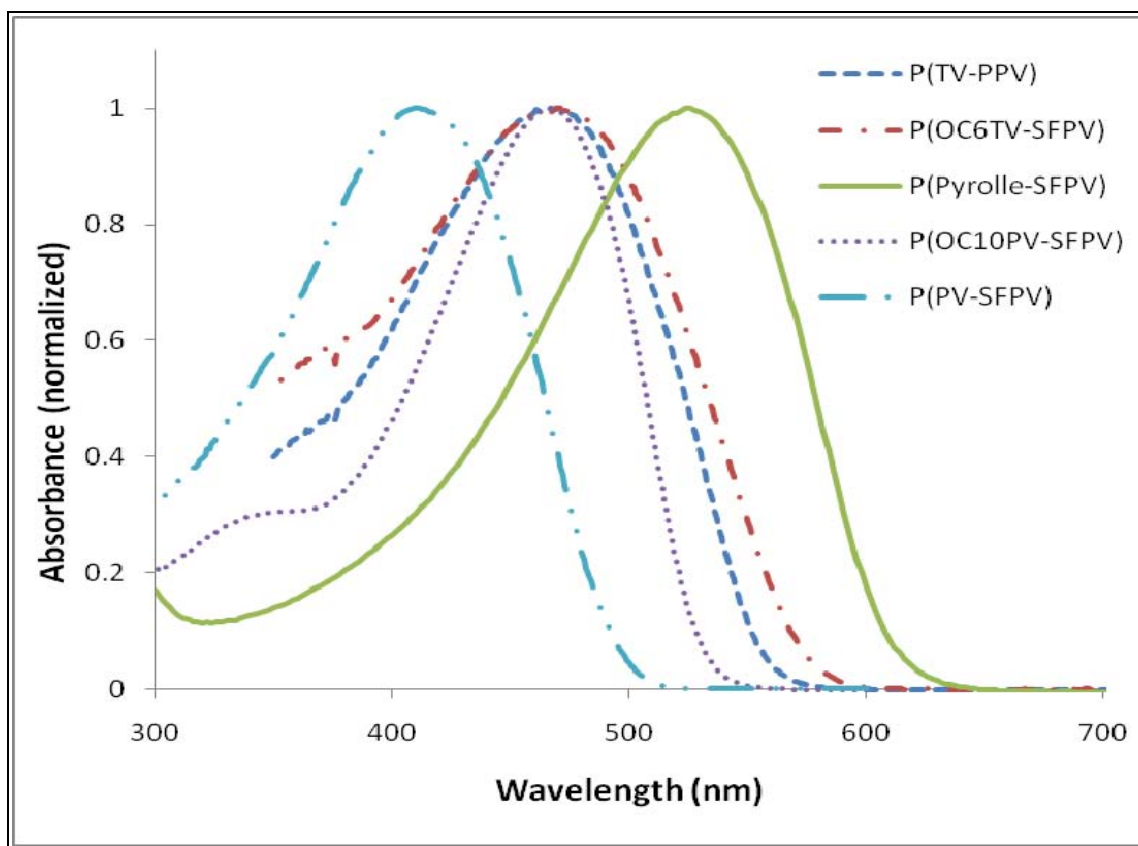

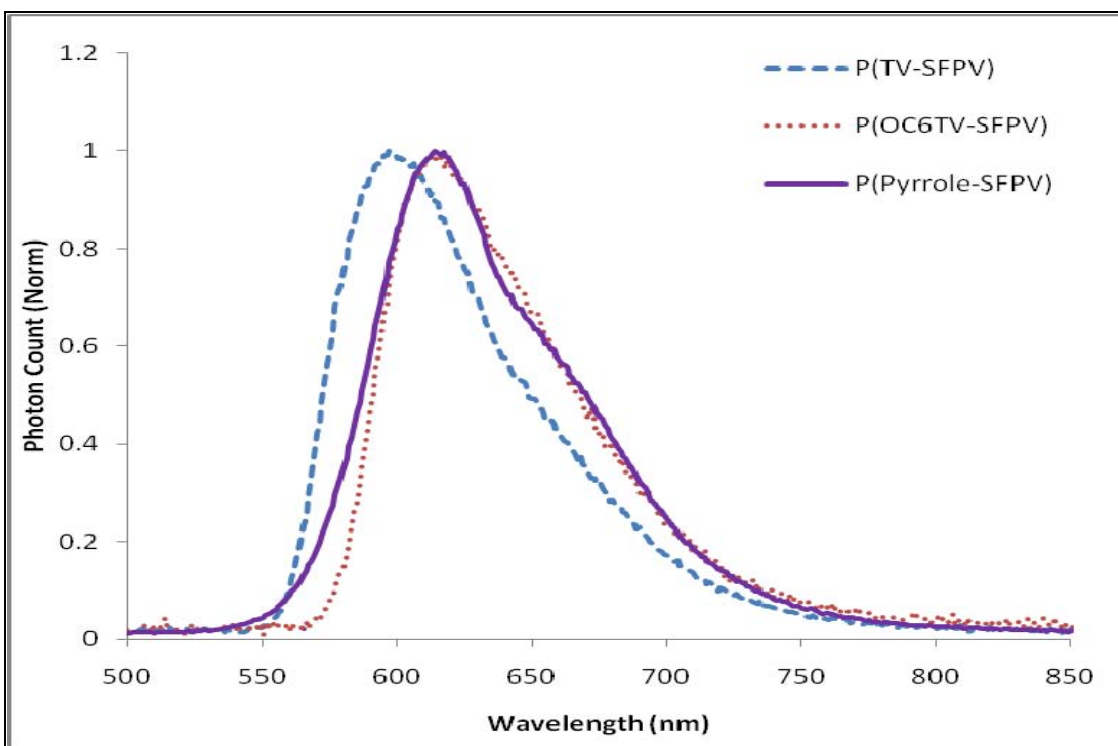**Figure 1.2.4** UV-vis spectra (normalized) of all SFPVs in THF.

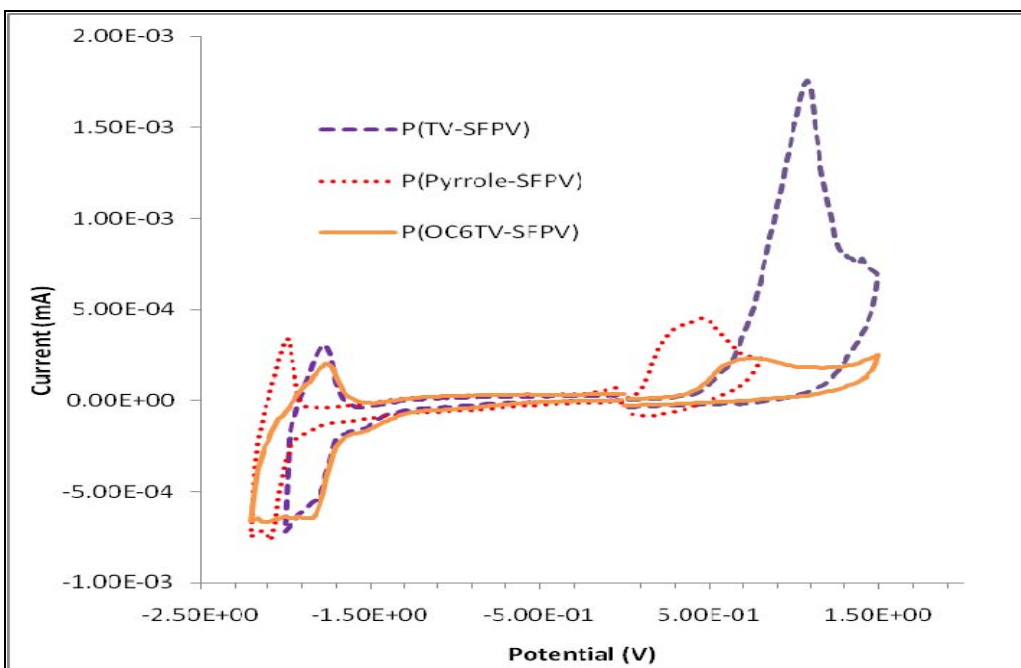**Figure 1.2.5** Normalized photoluminescence spectra of the new SFPVs in THF.

Figure 1.2.6 Cyclic Voltamograms (CV) of the new SFPV films coated on Pt wire. Reference electrode: Ag in 0.1M $AgNO_3$/MeCN.

SFPV-Polymers	λ^{abs}_{max}/nm In THF solution	λ_{cutoff} (nm) Onset	E^{opt}_{gap} (eV)	Oxid. Onset/ HOMO level (V/eV)	Redn. Onset /LUMO level (V/eV)	Electrical Energy gaps E^{el}_{gap} (eV)
P(pyrrole-SFPV)	536	640	1.94	0.10/-4.88	-1.94/-2.84	2.04
P(OC6TV-SFPV)	485	591	2.10	0.45/-5.23	-1.70/-3.08	2.15
P(TV-SFPV)	480	562	2.21	0.56/-5.34	-1.68/-3.10	2.24
P(OC10PV-SFPV)	465	535	2.32	0.54/-5.32	-1.90/-2.88	2.44
P(PV-SFPV)	409	506	2.45	0.69/-5.54	-1.78/-3.03	2.51

Table 1.2.1 Summary of optical properties and frontier orbital energy levels of all SFPVs.

SFPV-Polymers	Mw/Mn/PD	DSC Onset T(^{o}C) Endothermic peaks/Decomposition	TGA Onset T(^{o}C)
P(pyrrole-SFPV)	18099/7188/2.52	265/270	302
P(OC6TV-SFPV)	15457/4183/3.70	285/290	292
P(TV-SFPV)	5407/3364/1.61	--/310	300

Table 1.2.2 Summary of molecular weights and thermal properties of the new SFPVs.

1.2.4 Conclusions and Summary

A new series of more stable and processable sulfone acceptor derivatized phenylenevinylene-based conjugated polymers (SFPVs) containing different donor type comonomers have been successfully synthesized and characterized by the Horner-Emmons reaction. The solution optical energy gaps of these polymers are in the range of 1.94 - 2.48 eV, and the electrical energy gaps of these polymer thin films are in the range of 2.04-2.51 eV. This study shows that pyrrole is very effective in reducing energy gap due to a stronger electron donating ability of the nitrogen atom in the pyrrole ring, as well as its lower aromatic resonance energy compared to thiophene. The energy gap decreases by 0.51 eV from P(PV-SFPV) to P(pyrrole-SFPV) due to the increasing electron donating ability of the donors from benzene to pyrrole. The energy gap narrowing were also due to the decreasing resonance energy of the donor moieties from benzene (36 Kcal/mol), thiophene (29 Kcal/mol), to pyrrole (22 Kcal/mol). It is also shown that alkoxy substitution on the donor aromatic units has a significant effect on energy gap, *e.g.*, a reduction of 0.11 eV from P(TV-SFPV) to P(OC6TV-SFPV). In this work, we demonstrate an effective chemical strategy to lower energy gap in D-A coupled conjugated polymers without using a strong acceptor unit such as the S,S-dioxo-thiophene based comonomers. This strategy reduces the chance of certain unwanted side reactions, *e.g.*, Michael addition reaction to highly electron-deficient C=C bonds or its reactive proton, and therefore allows easier incorporation of such polymers into block copolymers for a variety of supramolecular optoelectronic device applications.[16,17]

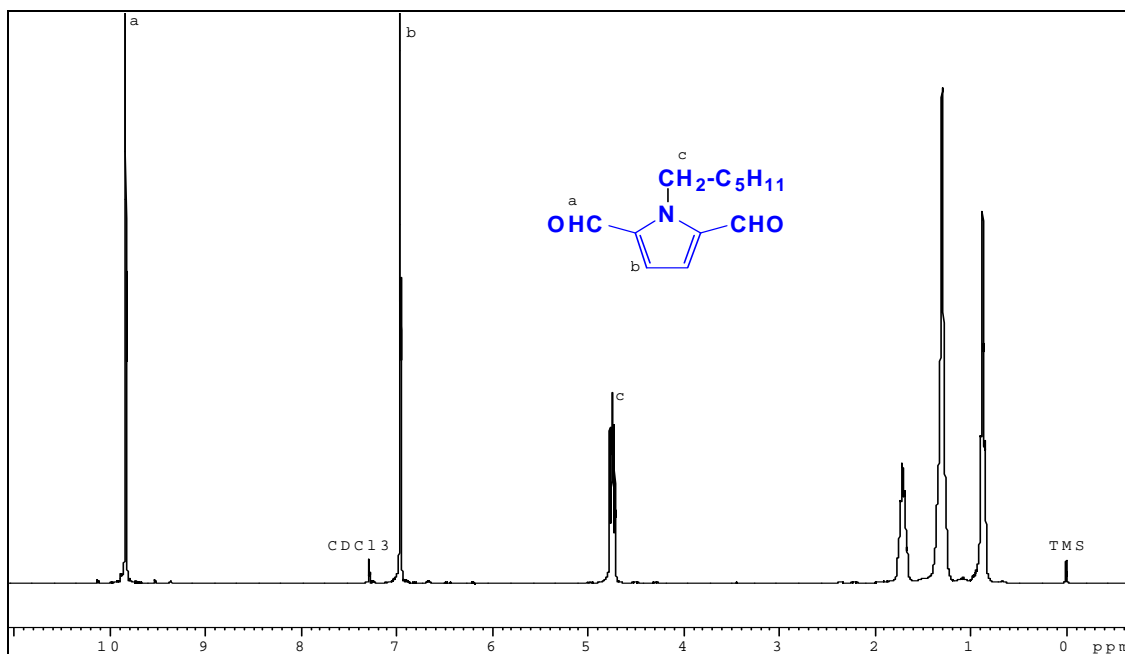**1.2.5 Supporting Information (SI):** ^{1}H and [13]H NMR spectra of all the precursors and the monomers:

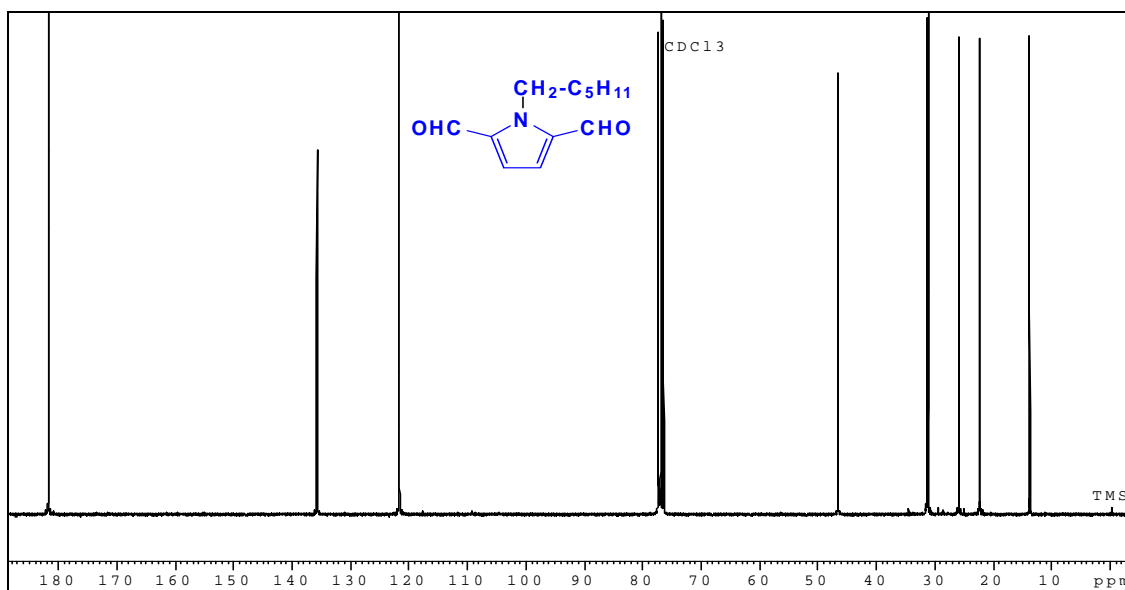**Figure 1.2.7** ^{1}H NMR of N-(n-hexyl)-2,5-dialdehydepyrrole **3**.

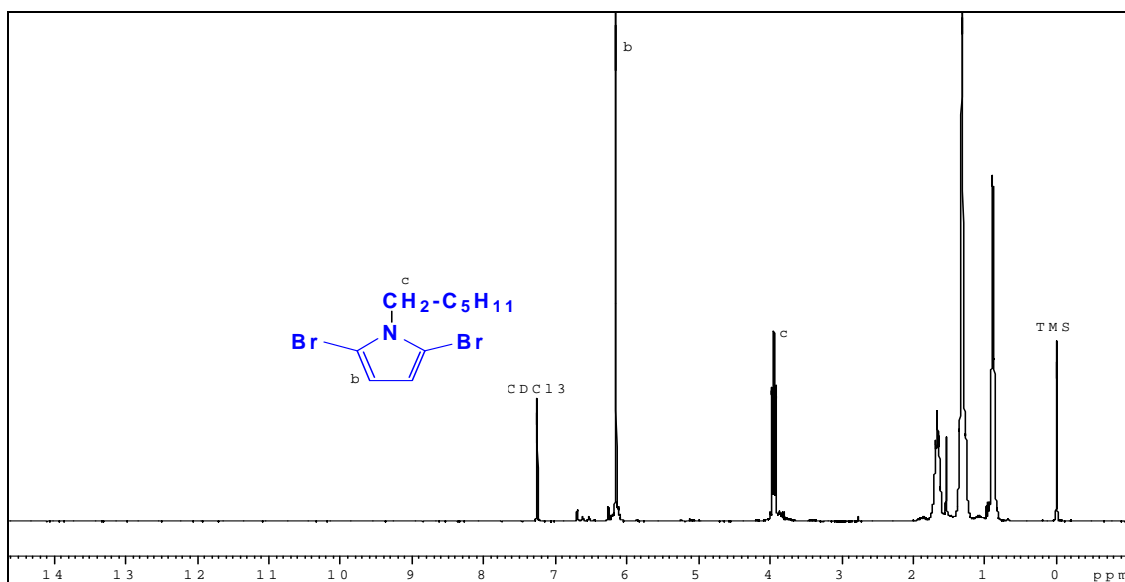**Figure 1.2.8** ^{13}C-NMR of N-(n-hexyl)-2,5-dialdehydepyrrole **3**.

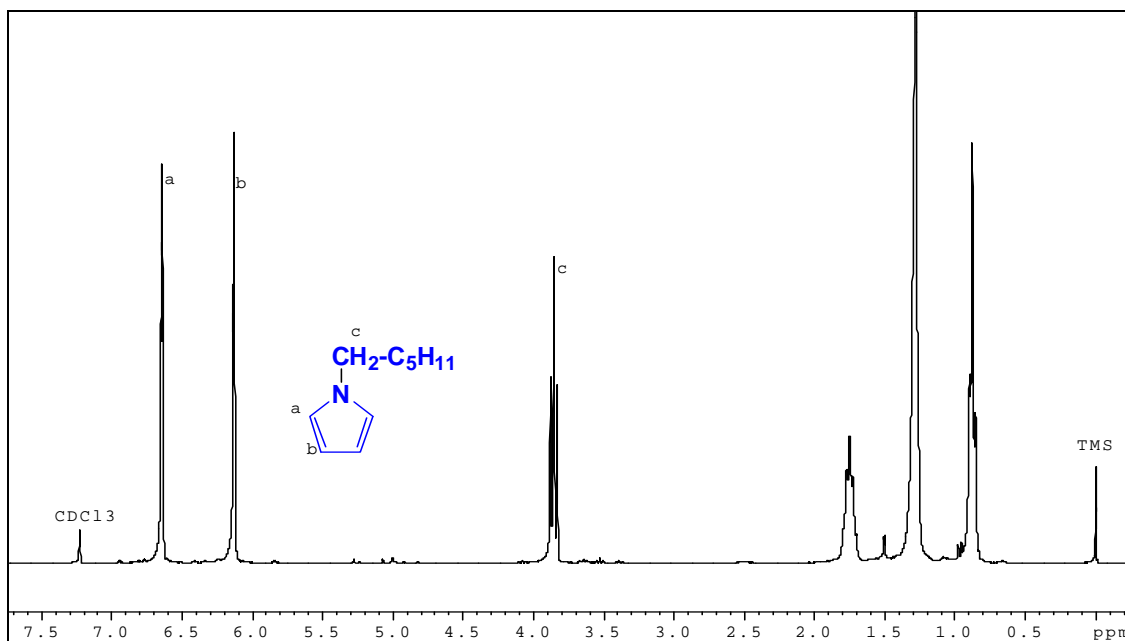**Figure 1.2.9** ^{1}H NMR of N-(n-hexyl)-2,5-pyrrole.

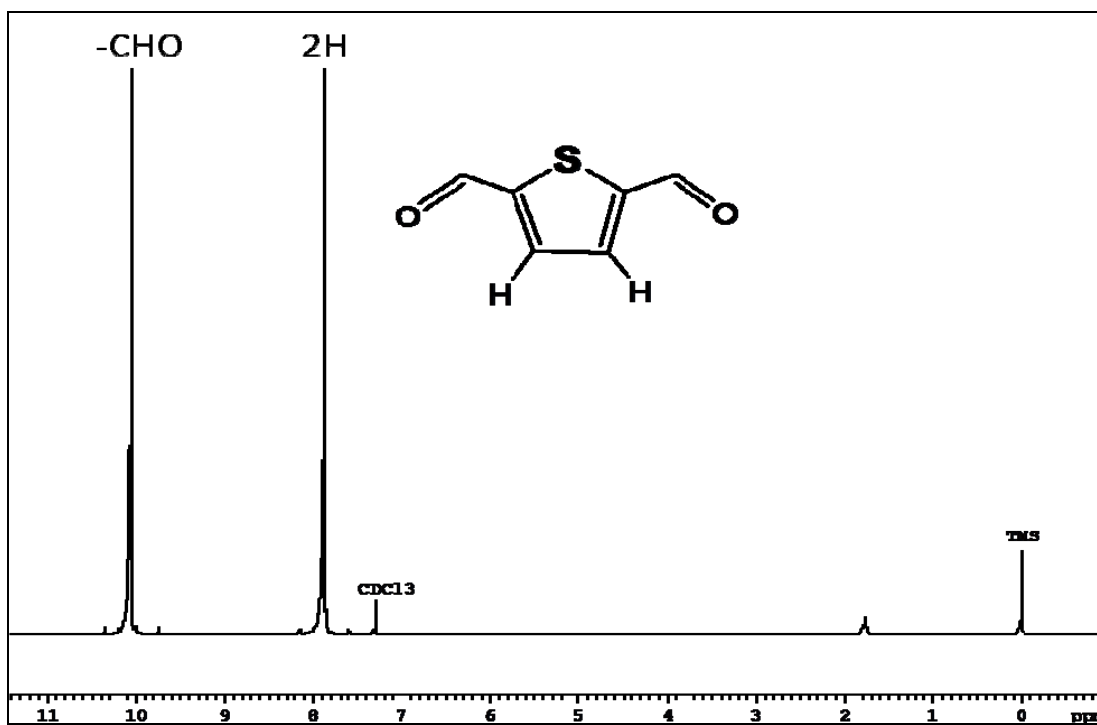**Figure 1.2.10** ^{1}H NMR of N-(n-hexyl)pyrrole.

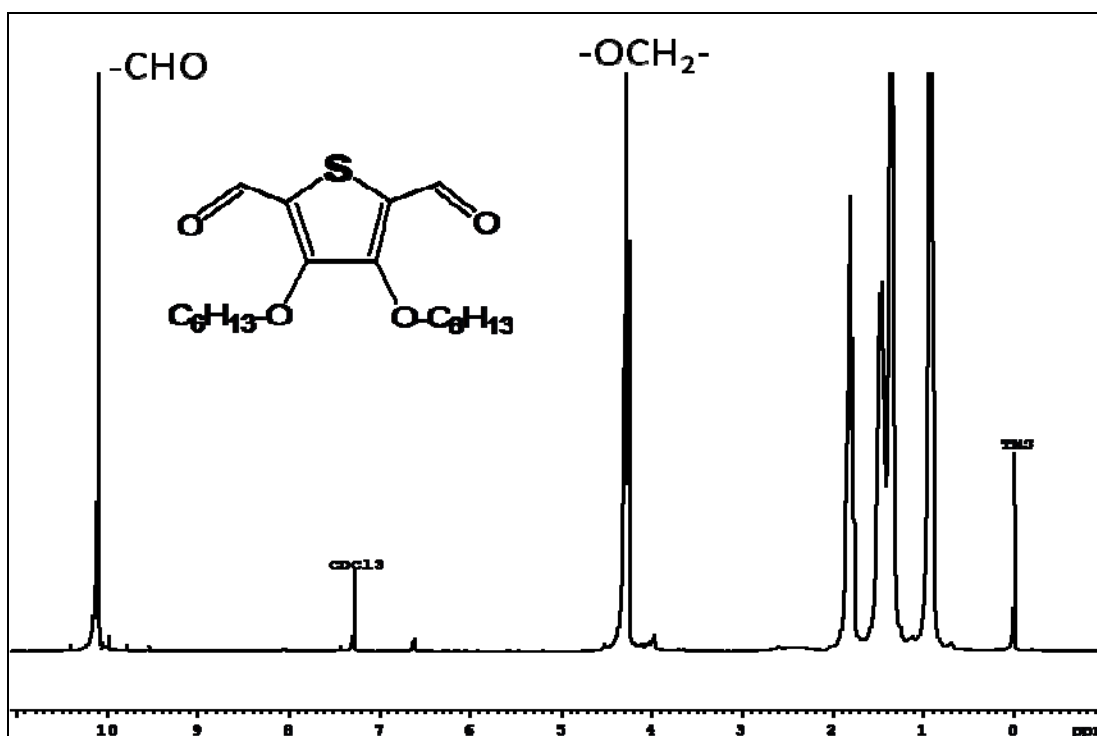**Figure 1.2.11** ^{1}H NMR of 2,5-dialdehydethiophene **6**.

Figure 1.2.12 ^{1}H NMR of 2,5-dialdehyde-3,4-bisdihexyloxythiophene **4**.
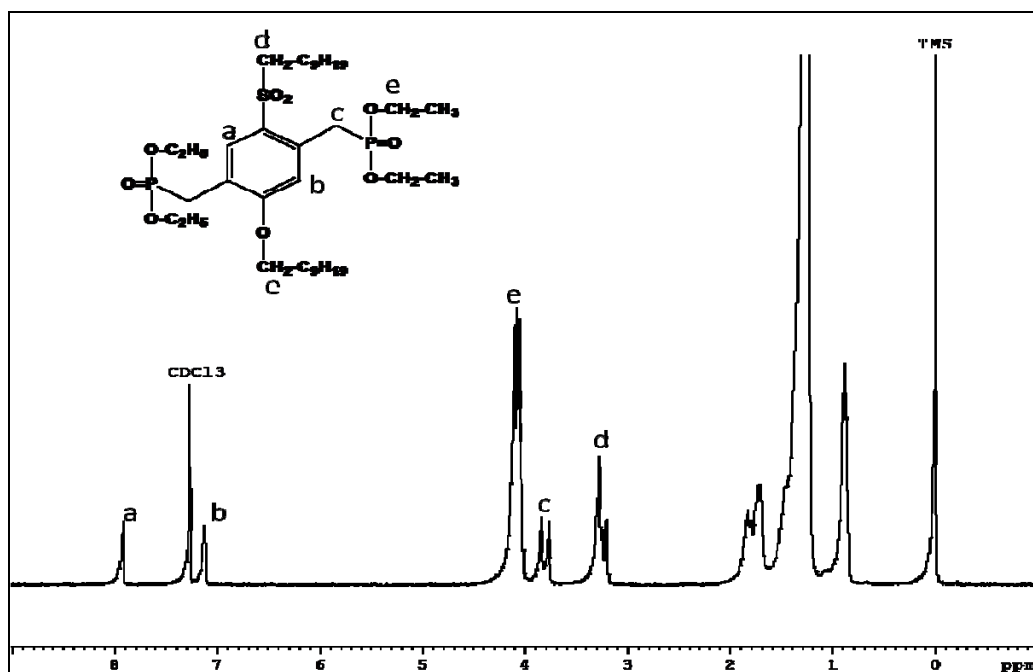
Figure 1.2.13 ^{1}H NMR of [2-(Decan-1-sulfonyl)-5-(decyloxy-4-(diethoxyphosphoryl-methyl))benzyl]phosphonic Acid Diethyl Ester **8.**
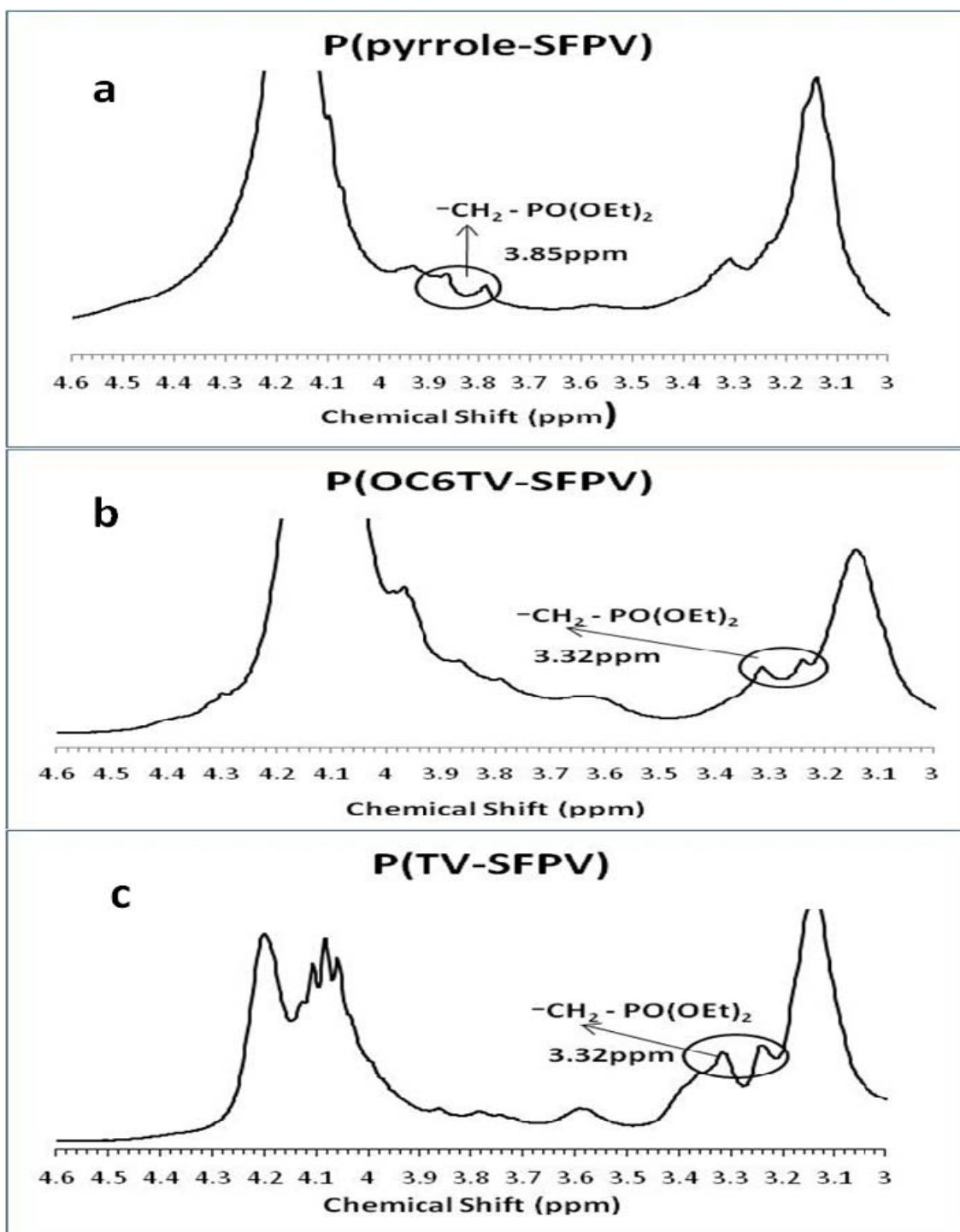
Figure 1.2.14 Enlarged ^{1}H NMR spectra of SFPVs.

1.2.6 References and Notes for Part 1.2

1. (a) Sun, S.; Sariciftci, S. Eds.; Organic Photovoltaic: Mechanism, Materials, and Devices; CRC Press: Boca Raton, FL, **2005** (ISBN: 978-0824759636). (b) Sun, S.; Dalton, L.; Eds.; In Introduction to Organic Electronic and Optoelectronic Materials and Devices; CRC Press: Boca Raton, FL, **2008**.
2. Barry, C. T.; Young-Gi, K.; Tracy, M.; Reynolds, J. *J. Am. Chem. Soc*. **2006**, *128*, 403-428.
3. Lewis, N. S., *Science*, **2007**, *315*, 198-801.
4. Roncali, J. *Chem. Rev*. **1997**, *97*, 173-205.
5. Darling, S. D., *Energy Environment. Science*, **2009**, *2*, 1266-1273.
6. Calinowski, J., *Organic Light Emitting Diodes: Principles, Characteristics, and Processes*; CRC Press **2004**, ISBN 978-0-8247-5947-6.
7. *Organic Light Emitting Materials and Devices*; Ed. Zhigang-Rick Li and Hong Meng; CRC Press, **2007**, ISBN 978-1-57444-574-9.
8. Henning Sirringhaus, in *Organic Field Effect Transistor*, Ed. Zhenan Bao and Jason Locklin, Chapter 2, CRC Press, **2007**, ISBN 978-0-8493-8080-8.
9. Hou, J.; Park, M.; Yang, Y. *Macromolecules*. **2008**, *41*, 6012-6018.
10. http://www.mhhe.com/physsci/chemistry/carey/student/olc/graphics/carey04oc/ref/ch11aromaticity.html. Chapter 11 : Arenes and Aromaticity.
11. Liu, M. *et al*., *Macromolecules*, **2002**, 35, 3532.
12. Ahn, T. *et al*., *Optical Mater.*, **2002**, 21, 191.
13. Bard, A. J. and Faulker, L. R., Electrochemical Methods-Fundamentals and Applications, Wiley, New York, **2000**, p. 634. ISBN: 978-0471-043720.
14. Koepp, H-M; Wendt, H.; Strchlow H., *Electrochem*.,**1990**, *64*, 483.
15. Brockmann, T. W.; Tour, Jame M. *J. Am. Chem. Soc*. **1995**, *117(16),* 4437-4447.
16. Zhang, C.; Choi, S.; Haliburton, J., *Macromolcules*, **2006**, *39*, 4317-4326.
17. Zhang, C.; Nguyen, T; Sun, J; Li, R.; Black, S.; Bonner, C.; Sun, S., *Macromolecules*, **2009**, *42*, 663-670.
18. Wang, N.; Teo, K.; Anderson, H. Can. *J. Chem*. **1977**, 55, 4112.
19. Hamaide, T. *Synth commun*. **1990**, *28(18)*, 2913.
20. Khoury, Y.; Kovacic, P.; H.M. *J. Polym. Sci. Lett*. **1981**, *19*, 395.
21. Wang, B.; Wasielewski, M. R. *J. Am. Chem. Soc*. **1997**, *119*, 12-21.
22. Akoudad, S.; Frere, P.; Mercier, N.; Roncali, J. *J. Org. Chem*. **1999**, *64*, 4267-4272.
23. Benoit, M.; Grubisic, F.; Remppr, J. *J. Polym. Sci. Part B*. **1967**, *5*, 753.
24. www.viscotek.com

1.3 Poly(3-Dodedyl-2,5-Thienylenevinylene) Based Low Energy Gap Conjugated Polymers (C12-PTV) with Taylored Regio Regularity

Abstract: Regioregular (RR) conjugated polymers are critical for electronic and optoelectronic properties of polymer based semiconducting devices. Monosubstituted polythienylvinylene (PTV), a relatively low band-gap conjugated polymer, has been reportedly synthesized using the Stille coupling reaction between 3-dodecyl-2,5-dibromothiophene and (E)-1,2-bis(tributylstannyl)ethylene. Although a small fraction of the product shows good (~90%) regioregularity, the whole product (S-C12-PTV) is consisted of mostly unidentified structures. To gain better control of the polymer structure and regioregularity, a difunctionalized C12-thiophene monomer, 3-dodecyl-5-formyl-thiophen-2-ylmethyl)-phosphonic acid diethyl ester, has been polymerized in near quantitative yield via the Horner-Emmons reaction. The full (100%) regio-regularity of the resulting polymer (HE-C12-PTV) has been confirmed by its ^{1}H and ^{13}C NMR spectra. The full regio-regularity is also reflected in its strong tendency to crystallize and practically no solubility in boiling hexane, in sharp contrast to S-C12-PTV. UV-vis absorption spectroscopy, fluorescence spectroscopy, Cyclovoltammetry, thermal analysis (DSC & TGA) and X-ray diffraction have been used to characterize both polymers. UV-vis absorption spectra of the HE-C12-PTV chloroform solutions of different concentrations show well-resolved vibronic structures with an absorption maximum at 577 nm and a prominent shoulder at 614 nm. The optical band gaps are 1.80 eV in chloroform solution and 1.65 eV in film. The HOMO/LUMO energy levels of the HE-C12-PTV film were found to be at -4.98 eV and –2.88 eV, respectively. The electrochemical band gap of the polymer in the film is estimated to be 2.1 eV. The DSC curve shows a pronounced melting peak at 205°C. XRD study shows that a decent crystalline structure is formed without any annealing of the as-cast films.

1.3.1 Introduction

Polythienylenevinylenes (PTVs) are an important class of low band gap polymers and have been investigated for optoelectronic applications.[1] Substituted PTVs have been synthesized using several methods, including Ni-catalyzed Grignard coupling of 1,2-bis(3,4-dibutoxythiophene)ethylene with 1,2-dichloroethylene,[2] precursor polymer route via bis(sulfoxomethyl) derivative of 3,4-dialkoxythiophenes,[3] Stille coupling reactions[4] Heck coupling reaction,[4a] and Horner-Emmons reaction.[5] Most of the reported substituted PTVs have two side chains on each thiophene unit. Disubstitution improves solubility, but, tends to prohibit tight π-stacking[6] which is crucial to some opto-electronic applications such as photovoltaic and LED.

Mono n-dodecyl-substituted PTVs have been reportedly synthesized by the Stille coupling reaction between dibromothiophene and 1,2-bis(tributyltin)ethylene and by the Heck coupling reaction (**Scheme 1.3.1**).[4a] The Stille coupling was considered a better method in terms of structural regioregularity.[4a] However, even with this method, a decent regioregularity (~90%) was reported only for a small fraction (9.5%, hexane-insoluble) of the Stille coupling product (S-C12-PTV).[4a]

The Horner-Emmons reaction has been widely used to synthesize vinylene-based polymers, including symmetrically substituted poly(p-phenylenevinylene)s (PPVs),[7] regioregular RO-PPVs[8] and 3,4-disubstituted PTV[9]. In this work, this highly reliable reaction is utilized to synthesize monosubstituted C12-PTV (HE-C12-PTV) from a

difunctionalized monomer, 3-dodecyl-5-formyl-thiophen-2-ylmethyl)-phosphonic acid diethyl ester (**Scheme 1.3.2**) in a nearly quantitative yield. This unsymmetrically functionalized monomer, plus the high reliability of the reaction, leads to full head-to-tail regioregularity. Full content S-C12-PTV is also synthesized using the literature procedure.[4a] HE-C12-PTV and S-C12-PTV are compared by using a number of analysis techniques, including NMR, UV-vis absorption, thermal analysis, Cyclovoltammetry, and XRD. The results indicates that S-C12-PTV has very low structural regularity, much lower crystallinity (in film) and contains structural defects that cause the polymer to decompose at much lower temperatures. The chemistry reported here for fully regioregular C12-PTV can be modified for the synthesis of regioregularity-controllable C12-PTV which allows for further investigation of this polymer for optoelectronic applications.[10]
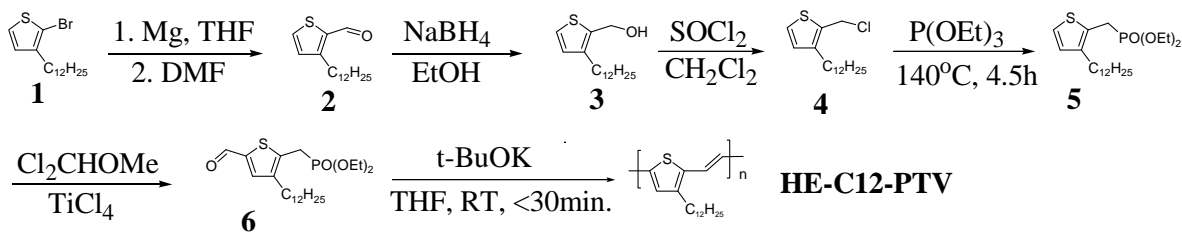
Stille coupling method:
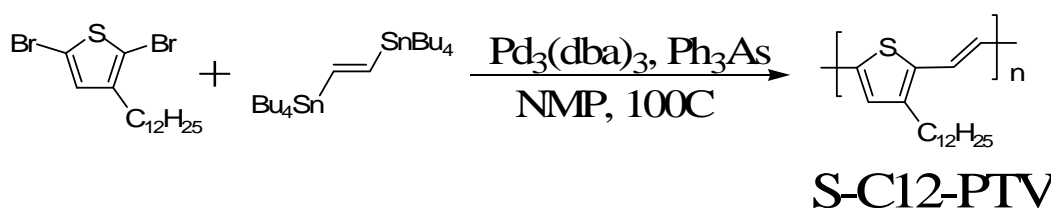
S-C12-PTV

Heck coupling method:
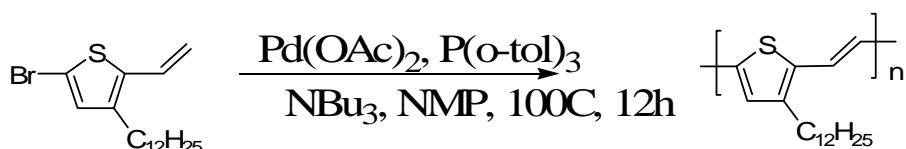
Scheme 1.3.1 Literature synthesis of C12-PTV.[4a]

Scheme 1.3.2 Synthesis of the fully regioregular C12-PTV.

1.3.2 Experimental

Starting materials, instrumentation, and general methods

All starting materials, reagents and solvents were purchased from commercial sources (mostly from Sigma-Aldrich and Fisher-Scientific) and used directly unless noted otherwise. NMR spectral data were obtained from a Bruker Avance 300 MHz spectrometer with TMS as the internal reference. Elemental analysis is performed by Atlantic Microlab Inc. UV-vis absorption data were collected on a Varian Cary-5 spectrophotometer. Thermal analysis is performed on a Perkin-Elmer TGA6/DSC6 system. The polymer molecular weights were measured on a Viscotek T60A/LR40 triple-detector GPC system at ambient temperature. Polystyrene standards were used for calibration.

Electrochemical studies were performed on a Bioanalytical (BAS) Epsilon-100w tri-electrode cell system. Three electrodes are a Pt working electrode, an ancillary Pt electrode, and a silver reference electrode (in a CH_3CN solution of 0.01 M $AgNO_3$ and 0.1 M TBA-HFP). The polymer samples were dissolved in hot solvents (such as o-dichlorobenzene) and then coated onto Pt working electrode. The measurements were performed in 0.1 M TBA-HFP solution in acetonitrile. Between the experiments, the surface of the electrodes were cleaned or polished. Scan rate is 100mV/s. Ferrocene (2 mM in 0.10M TBA-HFP/CH_3CN solution) is used as an internal reference standard and its HOMO level of -4.8 eV is used in calculations.

3-Dodecylthiophene-2-carboxaldehyde (2). A literature procedure[16] is used with minor modifications. A mixture of 2-bromo-3-dodecylthiophene (64.76 mmol, 21.45 g), Mg (1.652 g) and anhydrous THF (60 mL) is heated under reflux. Methylmagnesium bromide solution (3M in ether, 3 mL) is added to initiate the reaction. 2.5 h later, the mixture is cooled to RT, and DMF (5.5 mL, anhydrous) is then added via a syringe over 5 minutes. Fifteen minutes later, the reaction mixture is poured into a stirred mixture of hexanes (200 mL) and 2N HCl (70 ml). The hexanes is separated and washed with water two times and with aqueous $NaHCO_3$ solution one time. The hexanes extract is dried with $MgSO_4$, and then condensed. The crude product is purified by silica gel column chromatography using EtOAc/hexanes mixture (starting from pure hexane to 1:50 v/v) as the eluent. Yield: 92.4%. ^{1}H NMR ($CDCl_3$): Same as reported for 3-decylthiophene-2-carboxaldehyde, except the expected difference in aliphatic proton count.

3-Dodecyl-thiophene-2-methanol (3). 3-Dodecylthiophene-2-carboxaldehyde (8.93g, 31.8 mmol) is dissolved in 50 mL of ethanol. A solution of 222 mg of potassium hydroxide and 0.3612 g of $NaBH_4$ in 2 ml of water is added while the reaction mixture is stirred vigorously. One hour later, an NMR analysis of the reaction mixture showed that 40 % of the starting material remained. An additional solution of 222 mg of KOH and 0.3612 g of $NaBH_4$ in 2 ml of water is added. The organic layer is separated with hexanes (50 ml x 3) and dried over anhydrous $MgSO_4$. The solvent is removed by rotary evaporation. Yield: 99%. ^{1}H NMR spectrum of the crude product showed that the purity is 96%. The crude product is used in the next reaction. ^{1}H NMR ($CDCl_3$): Same as reported for 3-decylthiophene-2-methanol,[16] except the expected difference in aliphatic proton count.

2-Chloromethyl-3-dodecylthiophene (4). Thionyl chloride (2.36 ml, 36.43 mmol) is added over 1.5 minutes to a solution of 3-dodecyl-thiophene-2-methanol (8.23 g, 29.2 mmol), triethylamine (12.9 mL, 87.5 mmol) and methylene chloride (50 mL) cooled in an

ice bath. The solution is stirred for 30 minutes, then, poured to ice/hexanes. The mixture is acidified with 30 mL of 2N aq. HCl. The hexanes extract is washed with water to neutral, dried with MgSO$_4$, and condensed to give 9.40 g of crude product (theoretical yield: 8.76 g), >95% pure by both proton and carbon NMR spectra. ^{1}H NMR (CDCl$_3$): δ 0.88 (t, 3H, J=7.4Hz), 1.2-1.4 (m, 18H), 1.63 (m, 2H), 2.61 (t, 2H, J 7.4Hz), 4.77 (s, 2H, CH$_2$Cl), 6.85 (d, 1H, J=5.1Hz), 7.22 (d, 1H, J=5.1Hz). ^{13}C NMR (CDCl$_3$): δ 14.13, 22.71, 28.22, 29.55 (a few peaks overlapped), 30.90, 31.94, 46.20, 125.13, 129.00, 132.66, 142.49. The product is used in the next step without further purification (due to limited stability in silica gel column).

(3-Dodecyl-thiophen-2-ylmethyl)-phosphonic acid diethyl ester (5). A mixture of 2-chloromethyl-3-dodecylthiophene (9.40 g crude, 29.2 mmol) and triethyl phosphite (8.10 g, 44.4 mmol) is stirred at 140 °C for 4.5 hours. ^{1}H NMR analysis of the reaction mixture indicated that the reaction is complete and neat. Excess triethyl phosphite is removed by vacuum distillation. The crude product, showing only little impurities in aromatic region, is purified by column chromatography on silica gel using 1/12 (v/v) ethyl acetate/hexanes mixture as eluent. Yield: 5.0 g, 43%. Some product may have decomposed in the column during the long separation process. ^{1}H NMR (CDCl$_3$): δ 0.88 (t, 3H, J=7.4Hz), 1.1-1.4 (m, 24H), 1.58 (m, 2H), 2.56 (t, 2H, J=7.5Hz), 3.25 (t, 2H, J=20.7Hz, -CH$_2$P), 4.04 (m, 4H, P-O-CH$_2$-), 6.80 (d, 1H, J=5.3Hz), 7.06 (d, 1H, J=5.3Hz). ^{13}C NMR (CDCl$_3$): δ 13.81, 16.20/16.27 (d, OCH$_2$CH$_3$), 25.61, 27.53, 28.35, 29.21, 28.45, 29.5, 30.34, 32.84, 62.11 (d, J=7.1Hz), 122.95 (d, J=4.4Hz), 126.05 (d, J=11Hz), 128.40 (d, J=3.8Hz), 140.64 (d, J=9.9Hz). Anal. Calcd.: C, 61.37; H, 9.13; S, 7.45. Found: C, 61.09; H, 9.22; S, 7.31.

3-Dodecyl-5-formyl-thiophen-2-ylmethyl)-phosphonic acid diethyl ester (6). Titanium tetrachloride (1.20 ml, 10.9 mmol) is added dropwise to a ice-cooled mixture of (3-dodecyl-thiophen-2-ylmethyl)-phosphonic acid diethyl ester (1.07 g, 2.66 mmol), α,α-dichloromethyl methyl ether (0.321 g, 2.81 mmol) and methylene chloride (10 ml) over 10 minutes. The solution is stirred in the ice bath for 3.5 h, and then transferred into a separation funnel with NaHCO$_3$ solution and hexanes already added. The hexane phase is washed with brine two times and dried over anhydrous MgSO$_4$. The solvent is removed by rotary evaporation. Proton NMR of crude product showed no side reactions, and the yield is quantitative. Still, a silica gel column chromatography using ethyl acetate/hexanes mixture as eluent (with R$_f$ = 1/8~16 for the product) is performed to ensure high purity for the product (>99% by NMR, supported by the elemental analysis result). ^{1}H NMR (CDCl$_3$): δ 0.88 (t, 3H, J=7.4Hz), 1.1-1.4 (m, 24H), 1.58 (m, 2H), 2.60 (t, 2H, J=7.0Hz), 3.34 (d, 2H, J=21.66Hz, -CH$_2$P), 4.10 (m, 4H, P-O-CH$_2$-), 7.55 (s, 1H), 9.81 (s, 1H, CHO). ^{13}C NMR (CDCl$_3$): δ 14.13, 16.41 (d, J=6.0Hz, CH$_2$P), 22.69, 26.44, 28.20, 28.34, 29.35, 29.44, 29.49, 29.58, 29.64, 29.67, 30.18(d, J=1.6Hz, OCH$_2$CH$_3$), 31.92, 62.62 (d, J=6.1Hz, OCH$_2$CH$_3$), 137.70 (d, J=4.4Hz), 138.11 (d, J=12.1Hz), 141.14 (d, J=3.8Hz), 142.65 (d, J=8.8Hz), 182.57. Anal. Calcd. C, 61.37; H, 9.10; S, 7.32. Found: C, 61.09; H, 9.22; S, 7.31.

C12-PTV In a glove box, a solution of t-BuOK (1.2 eq, 88.6 mg) in THF (3mL) is added over 3 min to a solution of 3-dodecyl-5-formyl-thiophen-2-ylmethyl)-phosphonic acid diethyl ester (263 mg, 0.611 mmol) in THF (10 mL) at room temperature. The solution became blue almost immediately after addition of the base, and polymer precipitate appeared in less than five minutes. Thirty minutes after addition, the reaction mixture is dropped into methanol. The polymer product is collected by filtration. Yield:

0.157g, 93%. ^{1}H NMR (CDCl$_3$): δ 0.88 (t, 3H), 1.2-1.4 (m, 18H), 1.62 (m, 2H), 2.62 (t, 2H), 6.77 (s, 1H), 6.86 (d, 1H, J=15.8Hz), 6.98 (d, 1H, J=15.8Hz). ^{13}C NMR (CDCl$_3$): δ 14.05, 22.73, 28.54, 29.41, 29.45, 29.57 (two peaks overlapped here), 29.68, 29.73, 29.77, 30.84, 32.01, 120.07, 121.03, 129.17, 135.63, 140.65, 142.49.

1.3.3   Results and Discussion
Synthesis of C12-PTVs.

HE-C12-PTV is synthesized in six steps (**Scheme 1.3.2**) from 2-bromo-3-dodecylthiophene[11] (**1**). The selectivity of the reaction for 2-bromination is 97% according to the ^{13}C NMR analysis of the crude product. After the bromide is converted into carboxaldehyde, the two isomeric aldehydes were separated by column chromatography. Conversion of **3** into **4** is very fast and neat with thionyl chloride at ~10°C. However, due to the similarity between the NMR spectra of **3** and **4**, misjudgment of the reaction progress can happen if the ^{1}H NMR spectrum of the reaction product is not examined carefully. **4** is converted via the Arbuzov reaction into the phosphonate **5** which is formylated by Cl$_2$CHOMe/TiCl$_4$ to give the monomer **6** in a quantitative yield.[12] Polymerization of monomer **6** is very fast at room temperature with t-BuOK as the base and is completed in less than half an hour. Yields above 90% are routinely obtained. However, it is found that the reverse addition resulted in no polymer product or incomplete reaction. This can be explained in the following: when the monomer is added to the base, all monomer molecules are deprotonated at the Th-C$\underline{H}_2$-P carbon immediately, and the CHO group in a deprotonated **6** is no longer reactive toward the carbanion in another monomer or an oligomer.

S-C12-PTV is synthesized using the literature procedure.[4a] The full content of the product (ppt in MeOH, 65% yield) is used in the characterization and comparison below.

Characterization of HE-C12-PTV and S-C12-PTV

Solubility. S-C12-PTV is almost completely soluble in hexane, while HE-C12-PTV is only soluble in solvents such as chloroform and 1,2-dichlorobenzene (DCB). At elevated temperatures (*e.g.* 90°C), HE-C12-PTV can be dissolved in 1,2-dichlorobenzene at a concentration of 2 wt/vol%, sufficiently high for film casting. However, the polymer crystallizes as soon as the solution is applied onto glass substrates. This high tendency for crystallization is a result of its high structural regularity and high purity as discussed below.

NMR spectra and regioregularity. The polymerization for HE-C12-PTV only involves one monomer with unsymmetrical difunctionalities. This, coupled with high reliability of the Horner-Emmons reaction,[7] ensured head-to-tail linkage and full regioregularity. This is supported by the appearance of a clean singlet for the thienylenic proton (c) and two sets of clean doublets for the two ethenic protons (a and b) in ^{1}H NMR spectrum (**Figure 1.3.1**) and only six peaks in the aromatic region of the ^{13}C NMR spectrum (**Figure 1.3.1**). Although the Horner-Emmons reaction is known to produce cis C=C bond (as a minor product) in certain polymers such as PPV,[7] only trans C=C bond exists in the synthesized HE-C12-PTV. This is supported by two observations: 1. only one Th–C$\underline{H}_2$ peak is seen in the ^{1}H NMR spectrum. 2. The ^{1}H NMR peaks in the aromatic region matches with the main peaks of C12-PTV produced via the Heck coupling reaction, which is known to produce predominantly *trans* C=C bond (and, unfortunately, a significant amount of α-linkage).[4a]
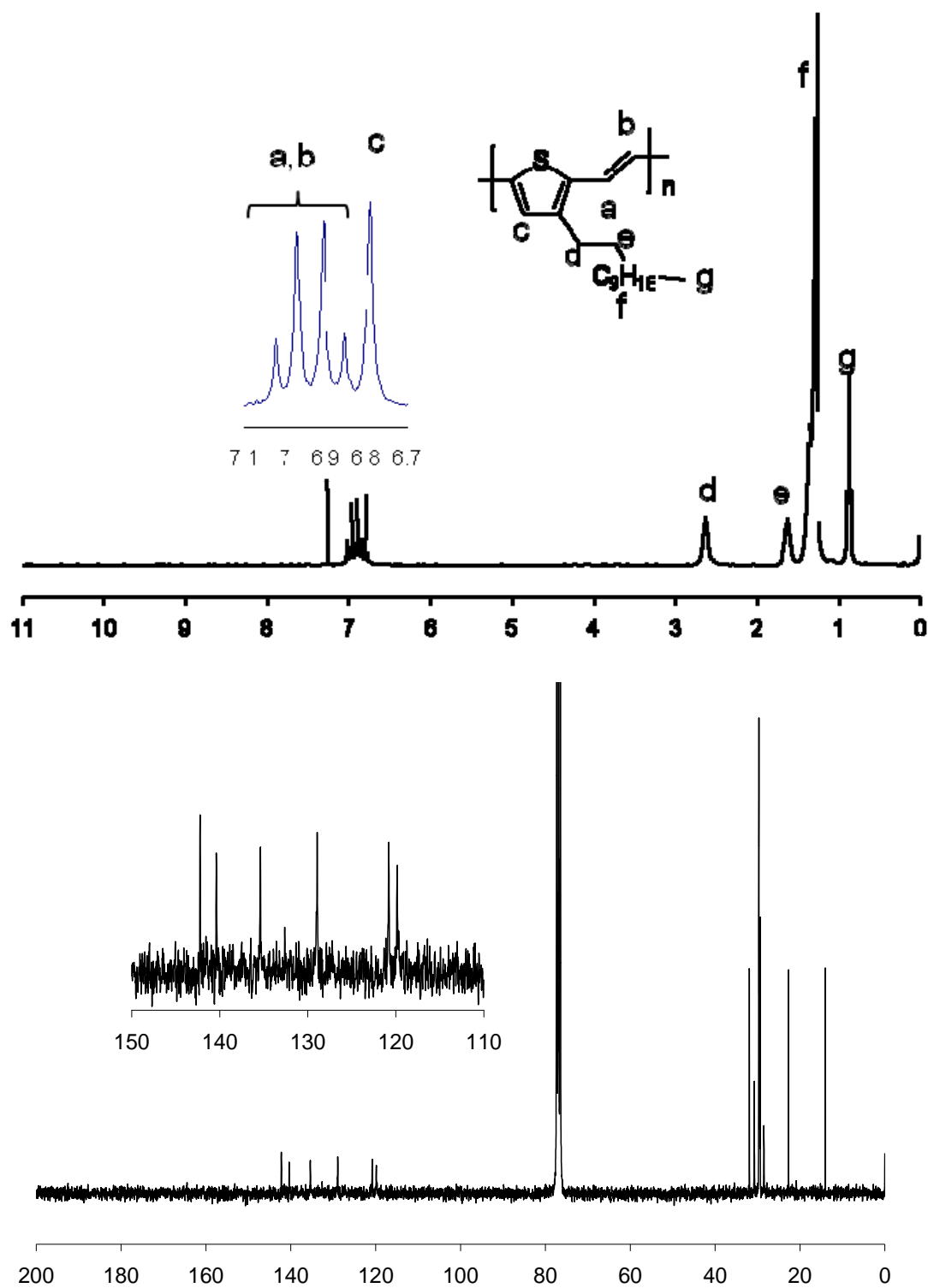
Figure 1.3.1 ^{1}H and ^{13}C NMR spectra of HE-C12-PTV in CDCl$_3$ at 60°C.
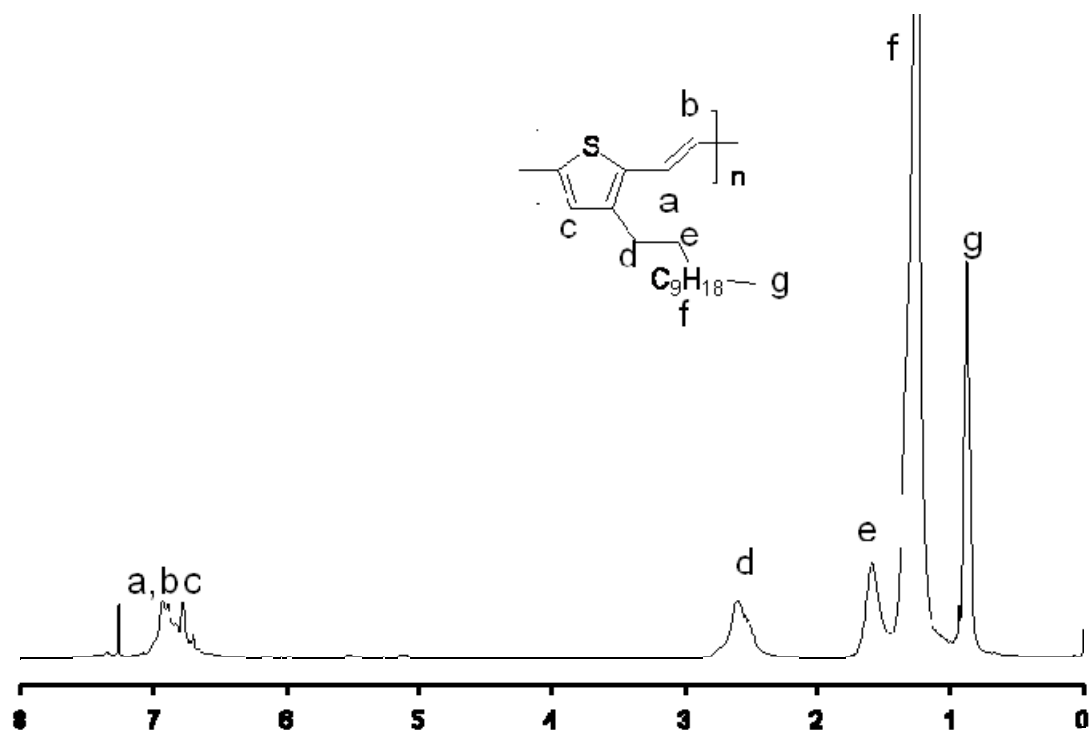
Figure 1.3.2 ^{1}H NMR spectrum of S-C12-PTV in CDCl$_3$ at room temperature.

In the ^{1}H NMR spectrum of S-C12-PTV (**Figure 1.3.2**, an NMR spectrum of full-content Stille C12-PTV, not available in the literature), although three peaks at 6.77, 6.88 and 6.93 ppm from the regioregular segments in the polymer can be seen (corresponding to protons c, a and b), a broad bump, where the three peaks sit on, is dominant in the aromatic region. This bump and the broad Th–C$\underline{H}_2$ peak (proton d) around 2.65 ppm are indications of structural complexity in the polymer.

Molecular weight (MW) by GPC. Due to the limited solubility of HE-C12-PTV in THF at the ambient temperature, the polymer product precipitates from the reaction mixture. The number average MW (M_n) of HE-C12-PTV is relatively low (7.2K). Its polydispersity is 2.9. On the other hand, S-C12-PTV has a M_n of 8.7K and polydispersity of 2.4.

Optical and Electrochemical Properties. UV-vis absorption spectra of HE-C12-PTV in chloroform solution (which has a violet blue color) of different concentrations (0.01 mM and 1 mM in chlolroform) and in thin film (drop-cast from the o-dichlorobenzene solution) are shown in **Figure 1.3.3**. The absorption curves of the solutions of two concentrations show maxima at the same wavelength (577 nm) and both have a prominent shoulder at 614 nm. A shoulder peak in the absorption spectrum of the high concentration (1mM) is seen at 665nm, which is absent when the concentration is low. The shoulder peak is attributed to aggregation of the polymer in chloroform solution,[13] and matches well with the similar shoulder peak in the film absorption spectrum (666 nm). The thin film has a λ_{max} of 574 nm, and a band edge at 752nm (1.65 eV), red-shifted by 62 nm (0.15eV) from the band edge (690 nm, 1.80 eV) of the chloroform solution (0.01 mM).
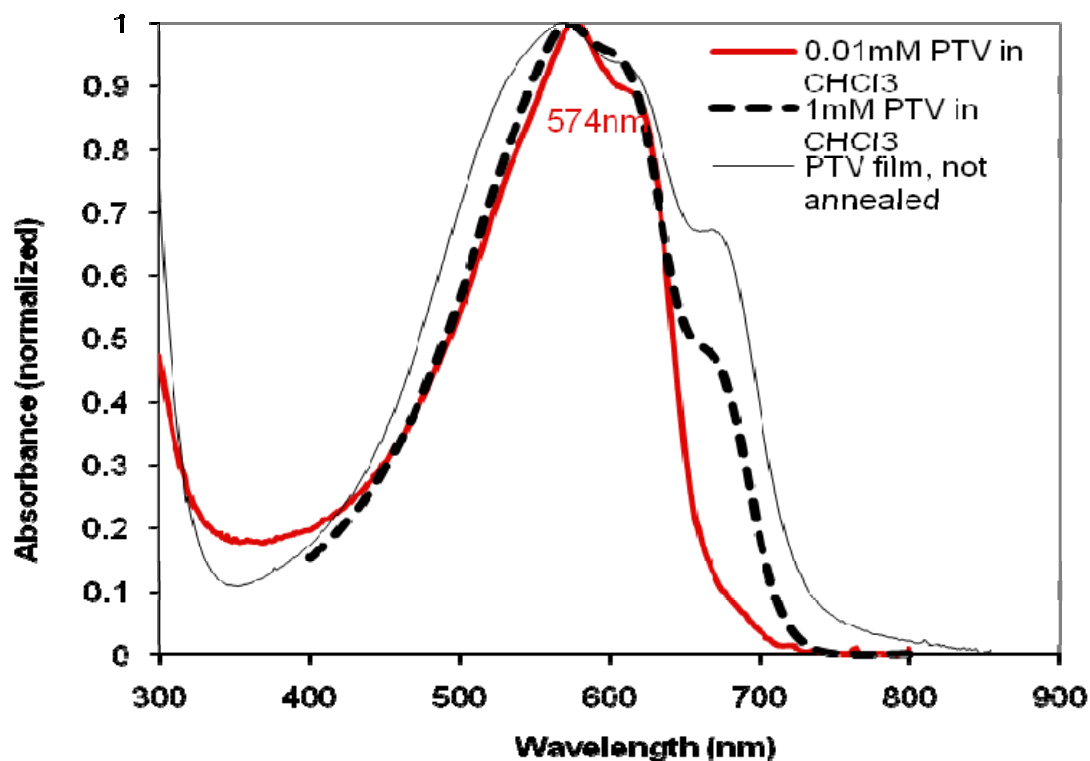
Figure 1.3.3 UV-vis absorption spectra of HE-C12-PTV in chloroform and film.

UV-vis absorption spectra of S-C12-PTV chloroform solutions (which have a violet color) and film are shown in **Figure 1.3.4**. No fine structure is seen and a 22-nm blue shift in the peak wavelength is observed for the optical absorption in the film as compared to that in the chloroform. The blue shift is an indication of lack of π-π interaction in the solid state, likely a result of poor regularity and structural defects in the polymer. Compared to the absorption peak of HE-C12-PTV (574nm) or the hexane-insoluble fraction of S-C12-PTV (576nm) in chloroform,[4a] the λ_{max} of S-C12-PTV in chloroform is blue shifted by 22-24 nm. This indicates that the absorption peak of hexane-soluble fraction of S-C12-PTV is at a shorter wavelength and dominates the absorption profile of the whole product. Accordingly, the absorption band edge of the film (735nm, 1.69eV) is blue-shifted by 17 nm as compared to that of the HE-C12-PTV film.
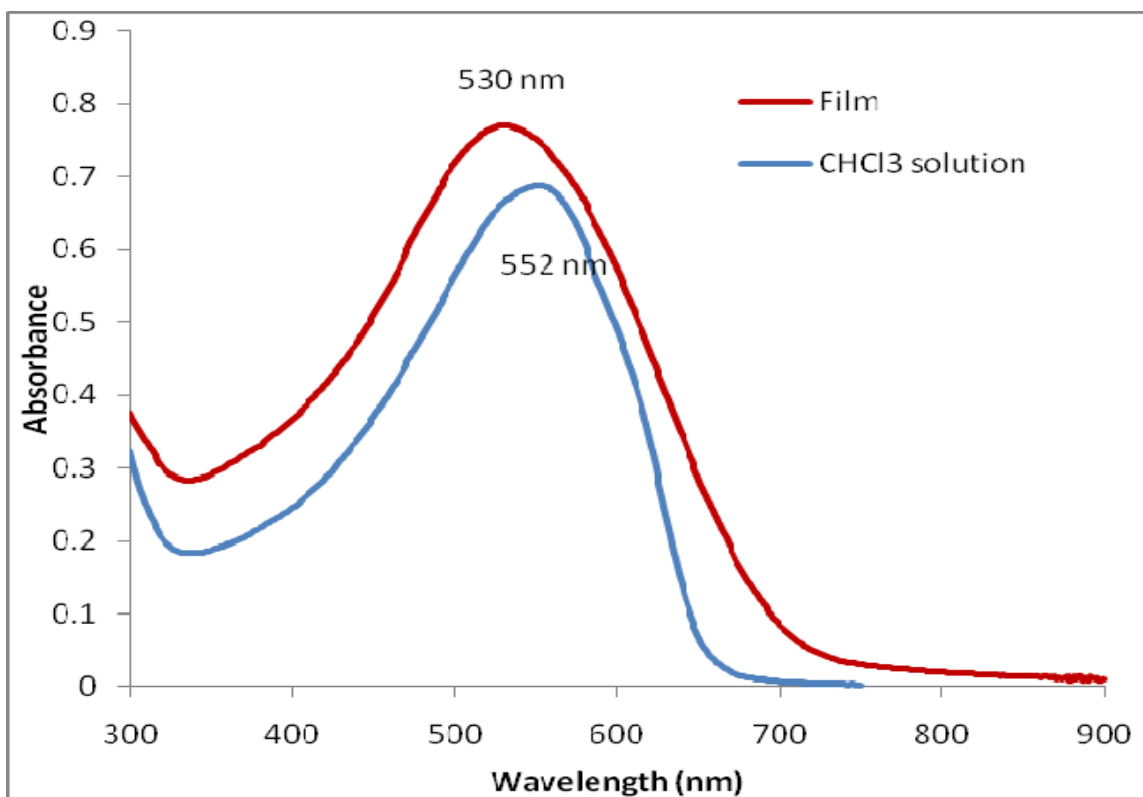
Figure 1.3.4 UV-vis absorption spectra of S-C12-PTV in chloroform solutions and film.

C12-PTVs have very weak photoluminescence, not measurable on a commercial florescence spectrometer. No PL spectrum has been reported in the literature. Using an ISA Fluoromax-3 luminescence spectrofluorometer and a customary photoinduced absorption spectroscopic setup, which consists of a Newport Oriel Cornerstone 1/4 m monochromator together with various diffraction gratings and optical filters to span the spectrum from 0.2 to 3.0 eV, PL spectrum of HE-C12-PTV was successfully obtained (**Figure 1.3.5**) from its dilute solution in o-dichlorobenzene. The shoulder peaks on the long wavelength slope are due to the vibronic structures of the polymer. Aggregation of the polymer, another possible origin of the shoulder peaks, is ruled out as the concentration of the solution is below 0.01 mM.
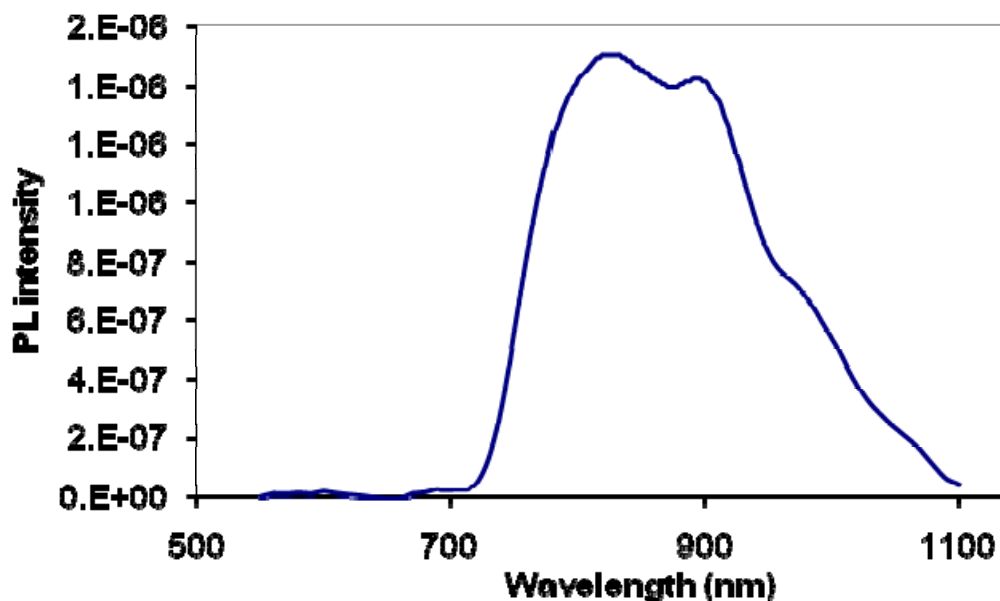
Figure 1.3.5 Photoluminescence spectrum of HE-C12-PTV. The photo excitation is provided by a cw Ar+ laser (488 nm, 2.54 eV).

Cyclovoltammetry (CV) is used to identify the HOMO/LUMO energies based on the correlation between oxidation/reduction potentials and the HOMO/LUMO levels. The CV scan of C12-PTV film coated on Pt working electrode is shown in **Figure 1.3.6**. The HOMO/LUMO values were found to be -4.98 eV and -2.88eV respectively. The electrochemical energy gap ($E_{g,el}$) is estimated to be 2.07 eV, which is larger than the optical band gap (1.65 eV) $E_{g,el}$ is larger because the electrode potential must be lower than the HOMO of the neutral polymer for the oxidation to happen and must be higher than the LUMO of the neutral polymer for the electron to transfer from the electrode into the LUMO orbital. The redox of the polymer in the potential range of 0 to 0.8V is completely reversible at least for nine cycles performed, while in the range of 0 to –2.2V, the redox is irreversible. This indicates that the polymer is stable at oxidized state and not stable at the reduced state. The CV behavior of S-C12-PTV is similar to HE-C12-PTV (the results are listed in **Table 1.3.1**).
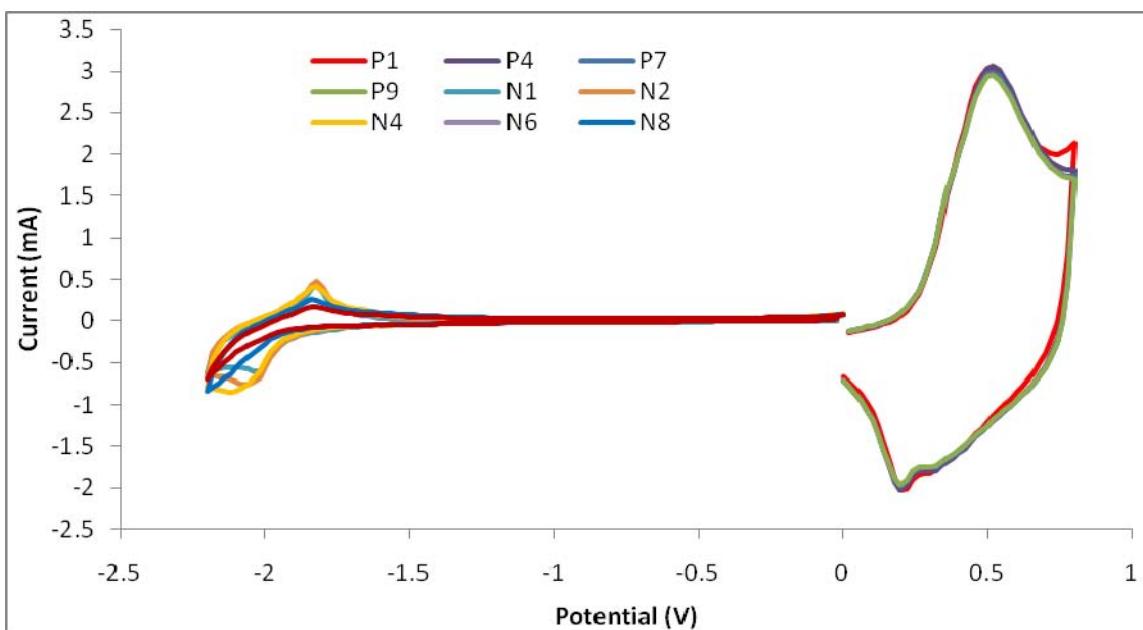
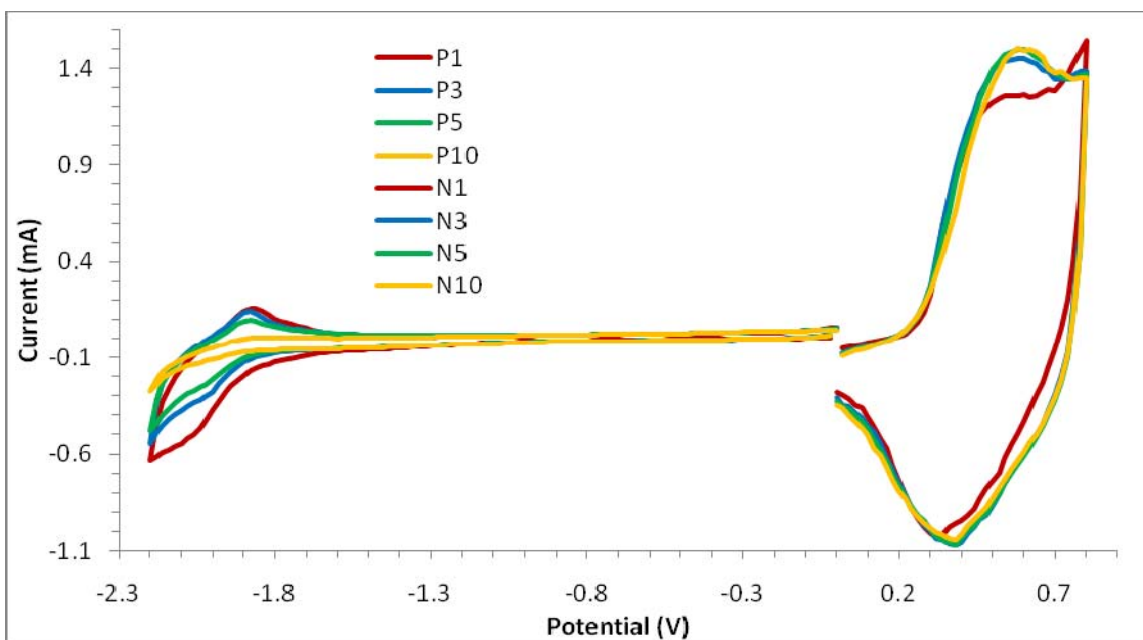**Figure 1.3.6** Cyclovoltammograph of HT-HT C12-PTV film coated on Pt wire. Reference electrode: Ag in 0.1M AgNO₃.

Figure 1.3.7 Cyclovoltammograph of S-C12-PTV film coated on Pt wire. Reference electrode: Ag in 0.1M AgNO₃.

Table 1.3.1 Properties of C12-PTVs

	Mn/PDI	λ_{max} CHCl$_3$/film	E_g^{opt} (film)	E_{ox}/E_{red} onset (V)	HOMO/LUMO and $E_{g,el}$ (eV) (film)	T_d (^{o}C)
HE-C12-PTV	7.2K/2.9	577/574	1.65	0.16/-1.94	2.07	326
S-C12-PTV	8.7K/2.4	552/530	1.69	0.22/-1.76	1.98	158

Thermal Analysis and Stability Tests. The phase transition and thermal stability were examined by differential scanning calorimetry (DSC), thermal gravimetric analysis (TGA) combined with NMR analysis. The DSC curve (**Figure 1.3.8**) shows a pronounced melting peak at 205°C for HE-C12-PTV. The melting is confirmed by visual inspection of a sample heated to a temperature (230°C) above the melting range. ^{1}H NMR analysis of a sample heated at 280°C both for 10 minutes in the DSC under N$_2$ atmosphere shows no decomposition. So, the endothermic slope between 230°C and 280°C is not due to a chemical reaction process, but rather a physical transition (presumably a transition from liquid crystal phase to isotropic liquid). The onset at 326°C of an exothermic transition (with a peak at 358°C) indicates the beginning of chemical decomposition of the polymer, most likely crosslinking reactions involving non-aromatic C=C bonds as confirmed by the insolubility of the sample after heating at 350°C. The weight loss onset temperature is determined from TGA scan (**Figure 1.3.9**) to be 373 ^{o}C. In the DSC curve of S-C12-PTV, no melting peak can be seen. Its TGA curve shows an early weight loss with an onset temperature at about 158 ^{o}C and 10% weight loss at 219 ^{o}C. It was also found that the polymer becomes insoluble after 3 months of storage at room temperature in dark (not observed for HE-C12-PTV under the same condition). The fact that S-C12-PTV has a much lower thermal stability suggests that S-C12-PTV contains significant amount of structure defect which is not stable and can cause the polymer to crosslink even at room temperatures.
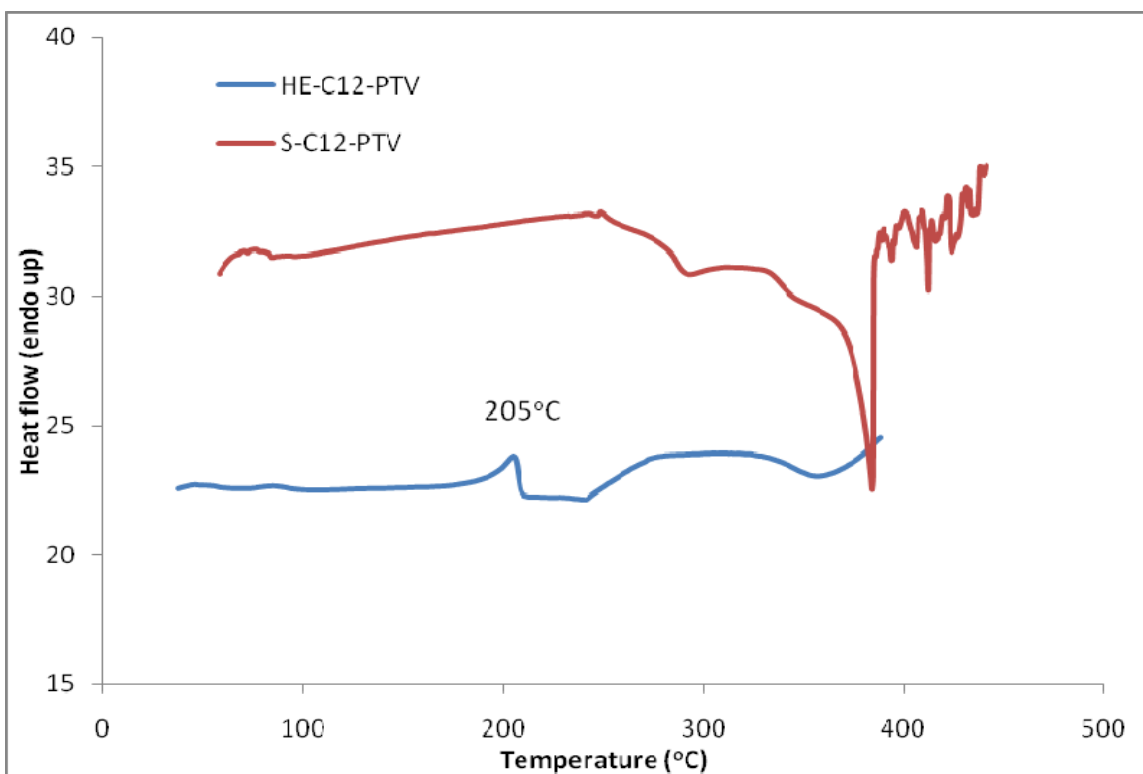
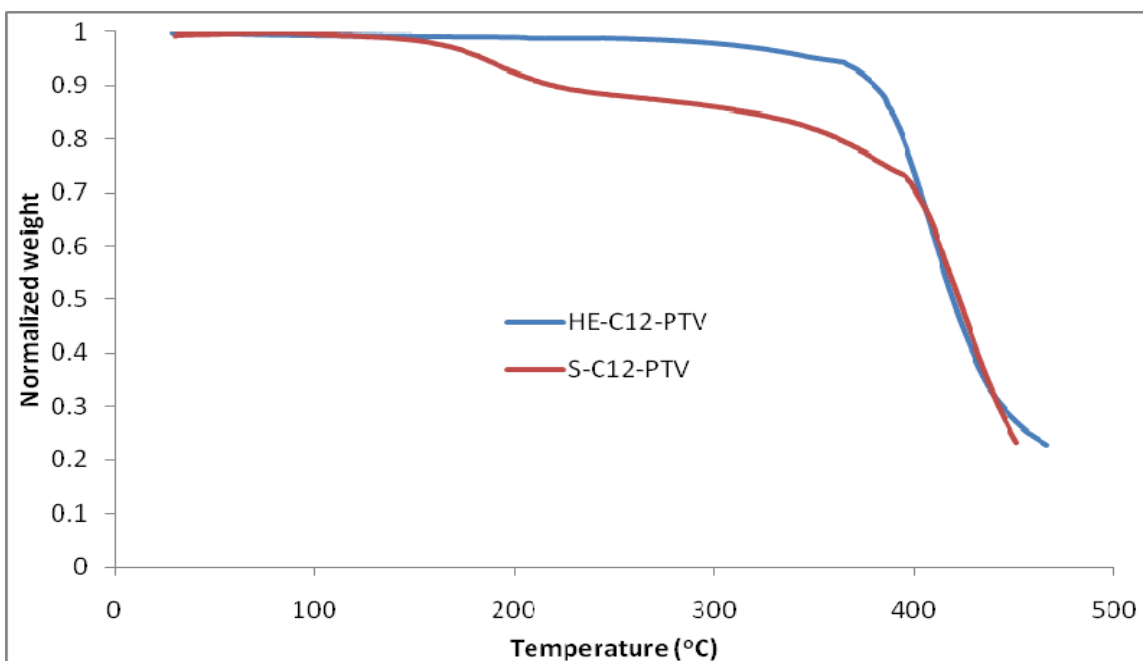**Figure 1.3.8** DSC curve of HT-HT C12-PTV power sample in N_2 at a scan rate of 10 ^{o}C/min.

Figure 1.3.9 TGA curve of HT-HT C12-PTV powder sample in N_2 at a scan rate of 10°C/min.

X-Ray diffraction (XRD) measurements. Wide angle out-of-plane diffraction pattern is obtained on XRD Spectra are recorded using Rigaku X-Ray Diffractometer (Model D/max-2200) (Cu Kα radiation, λ=1.5406Å) for as-cast C12-PTV films on glass

substrate from hot o-dichlorobenzene solution (**Figure 1.3.10**). The average thickness of the films is ~2 μm. Similar peaks are seen for both HE- and S- C12-PTV films. However, the peaks for S-C12-PTV film is much weaker, in agreement with the lack of distinct melting peak in the DSC scan. A calculation based on the first diffraction peak (100) gives an interlayer spacing of 17.6 Å, which is smaller than the d-spacing of 27.19 Å in HT-poly(3-dodecylthiophene) (P3DDT) film[14] by a factor of 1.54. The distance is consistent with structural models, where the side-chains of C12-PTV are interdigitated or closed packed and tilted toward the backbone.
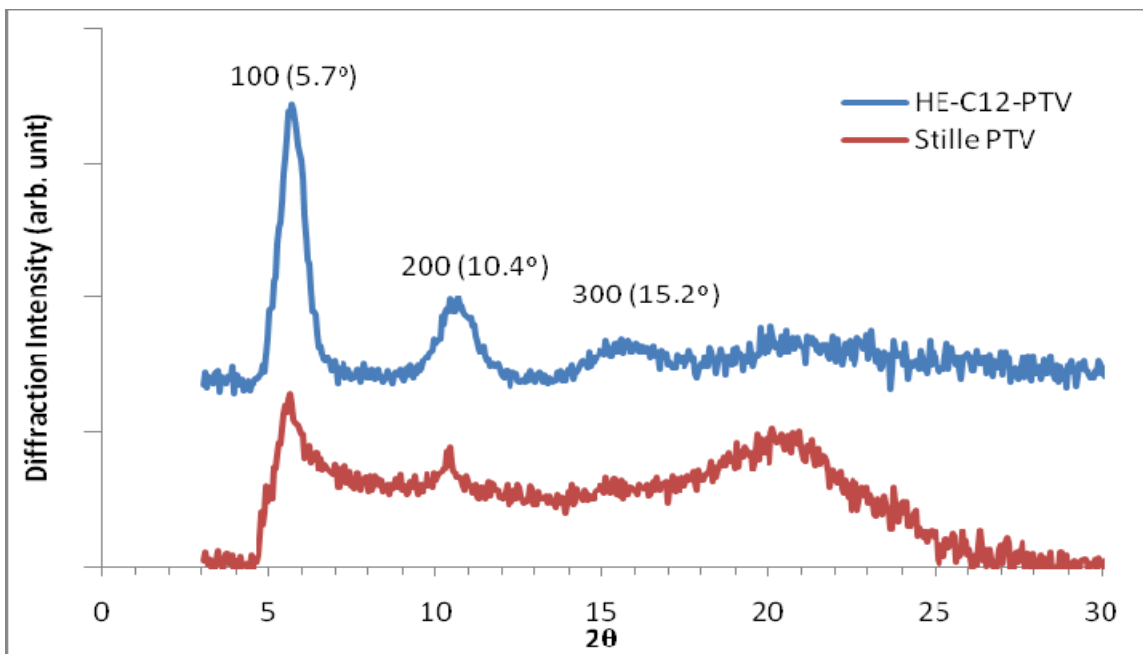

Figure 1.3.10 Wide angle X-Ray diffraction pattern of an as-cast C12-PTV film (thickness ~2 μm) drop-cast from o-dichlorobenzene solutions.

Mobility Measurement. S-C12-PTV films of 300 nm thickness was spin-coated from its 2wt% solution in 1,2-DCB onto ITO/glass slides. The active area is ~4 mm^2 of thermally deposited Au film (50 nm thick). Under the step voltage of 20 V, the transient current is dominated by SCLC as demonstrated in the insert of **Figure 1.3.11(b)**. The time elapse at peak transient current (t_1) is about 20 μs. The circuit response time (t=RC, R=1 Kohm, and C=0.3 nF) is about 0.3 μs, much smaller than t_1. The mobility (μ)[15] is calculated to be ~2×10^{-6} cm^2/Vs from $\mu = \dfrac{0.786d^2}{t_1 V}$ with d = 300 nm, t_1 = 20 μs, and V = 20 V.

The mobility measurement was also attempted for HE-C12-PTV, however, the polymer crystallizes so fast during film casting that good quality films could not be prepared and reliable/meaningful data could not be obtained. The chemistry to control the regioregularity and processibility of HE-C12-PTV has been developed.[10] More systematic investigation of the effect of regioregularity on mobility and solar cell device performance is currently underway.
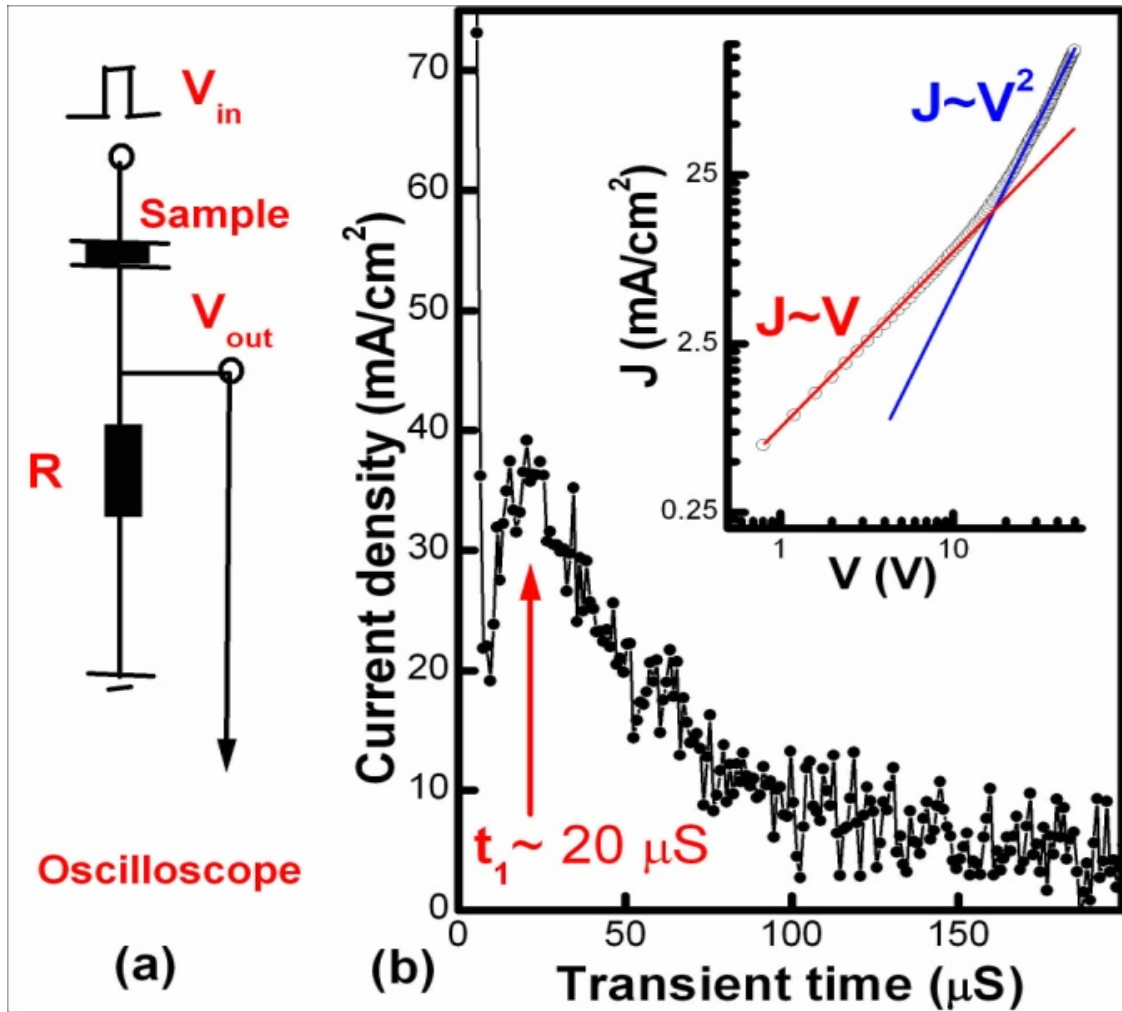
Figure 1.3.11 The measurement circuit and the plot of the transient current as a function of time. A step voltage (20 V with duration time of 1 ms and repetition rate of 100 Hz.) from signal generator (SRS model DS345) is applied to device as an input voltage (V_{in}). The transient current is measured through a serial resistor of 1K Ohm. The correspondent output voltage (V_{out}) is then sent to a digital oscilloscope (Tektronix TDS360).

1.3.4 Conclusions and Summary

Fully regioregular HT-HT C12-PTV has been synthesized and characterized by NMR, UV-vis absorption spectroscopy, fluorescence spectroscopy, cyclovoltammetry, thermal analysis and XRD. Full regioregularity is ensured by a combination of three measures: the polymerization scheme which only involves one monomer with asymmetric difunctionalities, high reliability of the Horner-Emmons reaction, and the high purity of the monomer. UV-vis absorption spectra of the HT-HT C12-PTV chloroform solutions of different concentrations show well-resolved vibronic structure with an absorption maximum at 577 nm and a prominent shoulder at 614 nm. The band edge is 690 nm (1.80 eV, optical band gap). The band edge of the electronic transition in thin film is 752nm (1.65 eV). The PL intensity of C12-PTV is very weak with a peak at 662 nm. The HOMO/LUMO energy levels of the C12-PTV film were found to be -5.03 eV and -3.63eV respectively. The electrochemical band gap is estimated to be 1.4 eV. The DSC curve shows a pronounced melting peak at 205°C followed by an endothermic transition of LC phase to isotropic liquid in the temperature range of 242-280°C. The onset temperature of chemical decomposition of the polymer is about 326°C by DSC, while the onset temperature of polymer disintegration is about 373°C as determined by TGA.

The polymerization scheme adopted here allows systematic tuning of regioregularity by simply adding a certain amount of co-monomer which is an isomer of compound **6**. Systematic studies on the effect of regioregularity control versus C12-PTV solubility, film morphology, and performance of solar cells are currently under way and to be reported separately.

1.3.5 References and Notes for Part 1.3

1. A. P. Smith, R. R. Smith, B. E. Taylor and M. F. Durstock, *Chem. Mater.* 2004, **16**, 4687-4692; K. Van De Wetering, C. Brochon, C. Ngov and G. Hadziioannou, *Macromol.* 2006, **39**, 4289 – 4297; F. Banishoeib, A. Henckens, S. Fourier, G. Vanhooyland, M. Breselge, J. Manca, T. J. Cleij, L. Lutsen, D. Vanderzande, L. H. Nguyen, H. Neugebauer and N. S. Sariciftci. *Thin Solid Films* 2008, 516(12), 3978-3988; J. Hou, Z. Tan, Y. He, C. Yang and Y. Li. *Macromol.* 2006, 39(14), 4657-4662.
2. M. L. Blohm, J. E. Pickett and P. C. Van Dort, *Macromol.* 1993, 26, 2704-2710.
3. H. Cheng and R. L. Elsenbaumer. *Chem. Commun.* 1995, 1451-2.
4. a) R. S. Loewe and R. D. McCullough. *Chem. Mater.* 2000, *12*, 3214. b) E. E. Havinga, C. M. J. Mutsaers and L. W. Jenneskens, *Chem. Mater.* 1996, 8, 769-776.
5. K. Van De Wetering, C. Brochon, C. Ngov and G. Hadziioannou. *Macromol.* 2006, 39, 4289 – 4297.
6. Good crystal packing for dialkyl substituted thiophene polymers has not been reported in the literature.
7. C. Zhang, S. Choi, J. Haliburton, T. Cleveland, R. Li, S. Sun, A. Ledbetter and C. Bonner, Jr. *Macromol.* 2006, 39, 4317-4326.
8. Y. Suzuki, K. Hashimoto, and K. Tajima. *Macromol.* 2007, 40, 6521-6528.
9. K. Van De Wetering, C. Brochon, C. Ngov and G. Hadziioannou. *Macromol.* 2006, **39**, 4289 – 4297.
10. C. Zhang, E. Annih, R. Li, S.-S. Sun. *Proc. SPIE* 2009, 7213 (Photovoltaic and Display Materials), Paper 7213-8.
11. P. Baeuerle, F. Pfau, H. Schlupp, F. Wuerthner, K. U. Gaudl, C. Balparda, and F. Miguel. *J. Chem. Soc., Perkin Trans. 2: Phy. Org. Chem.* 1993, 489-494.
12. C. Zhang, A. W. Harper and L. R. Dalton. *Syn. Commun.*, 2001, 31(9), 1361-1365.
13. A. V. Gavrilenko, T. D. Matos, C. E. Bonner, S.-S. Sun, C. Zhang and V. I. Gavrilenko. *J. Phys. Chem.,* C. 2008, 112(21), 7908-7912.
14. T.-A. Chen, X. Wu and R. D. Rieke. *J. Am Chem. Soc.* 1995, 117, 233-244.
15. M. A. Lampert and P. Mark, *Current Injection in Solids*, Academic Press, New York, P112-138 (1970). D. Poplavskyy, J. Nelson, and D. C. Bradley, *Macromol. Symp*. 2004, **212,** 415-420.
16. M. He, T. M. Leslie and J. A. Sinicropi. *Chem. Mater.* 2002, 14, 4662-4668.

1.4 Development of A Novel DBA Type Block Copolymer for Potential High Efficiency Optoelectronic Applications

1.4.1 Introduction

Donor-Bridge-Acceptor (DBA) (**Scheme 1.4.1**) type block copolymers (where D is a conjugated donor block, A is a conjugated acceptor block, and B is a non conjugated flexible bridge unit) have the potential to form a D/A bicontinuous phase separated nanostructures that are very promising for high efficiency polymer optoelectronic particularly photovoltaic detector and solar cell applications. In an earlier work, we developed and reported a (DBAB)n type of conjugated block copolymer system.[1-2] A major disadvantage of the (DBAB)n type of block copolymer system is that it is not easy to form a large uniform domain of D/A bicontinuous nano morphology due to block size differences between each blocks, either D or A blocks. However, in a DBA system, even if the D or A block sizes are different as a result of the polymer polydispersity character, due to free intermolecular spaces between each individual DBA block copolymer unit, the difference of the donor or acceptor block sizes can be easily compensated or accommodated by the same block unit of the other DBA units, or simply by the free D or A blocks intentionally added.[3] The synthesis of DBA turns out to be much more challenging than the (DBAB)n primarily due to the need for different functionalized D and A monomers and mono end functionalized polymer blocks.
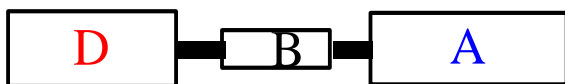
Scheme 1.4.1 Schematic of a DBA block copolymer. D is a conjugated donor block with higher LUMO/HOMO energies, and A is an acceptor block with lower LUMO/HOMO energies compared to A. B is a non-conjugated and flexible short linkage unit.

1.4.2 Synthesis of donor and acceptor blocks

The synthetic route shown in **Scheme 1.4.2** was designed for the synthesis of PPV-based donor and acceptor blocks. Monomers are di-functionalized with aldehyde on one side and phosphonate groups at the other side of the monomer, and these monomers can be polymerized via the Horner-Emmons reaction. Phosphonate terminators will be used to ensure that the phosphonate group is in slight excess so that the polymers will only have phosphonate end group to couple with the aldehyde bridge units. The amount of the terminator can be adjusted to control molecular weight of resulting polymer blocks.
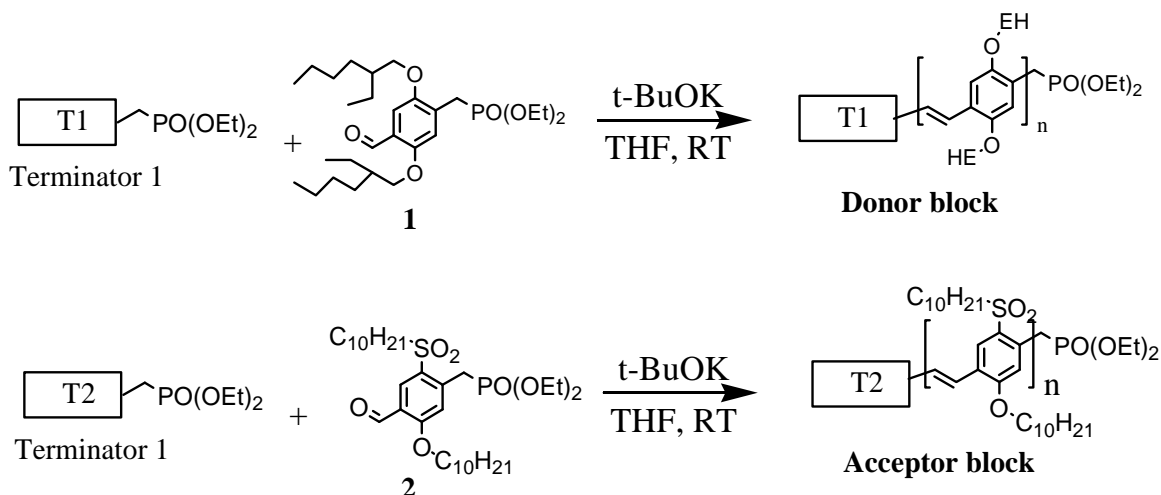
Scheme 1.4.2 General synthetic schemes for PPV based donor and acceptor blocks.

Synthesis of the donor block

The synthesis of donor block involves three sub-tasks: 1) Synthesis of donor monomer, 2) Synthesis of terminators, and 3) Polymerization.

The synthesis of monomer **1** is shown in **Scheme 1.4.3**. The 2-ethylhexyl is used instead of a straight alkyl group as regioregular C10O-PPV was found not soluble. The NMR spectrum of monomer **1** is shown in **Figure 1.4.1**.
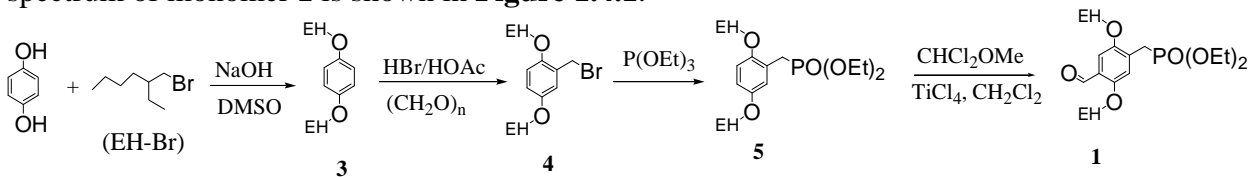
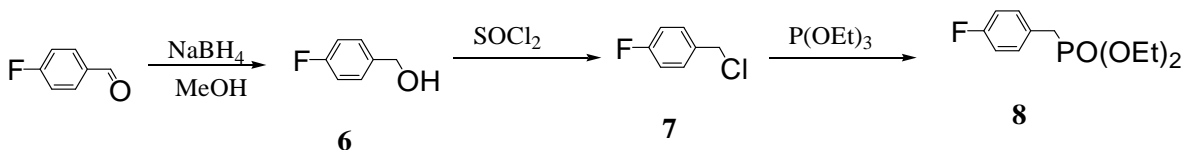**Scheme 1.4.3** Synthesis of the donor monomer **1.**
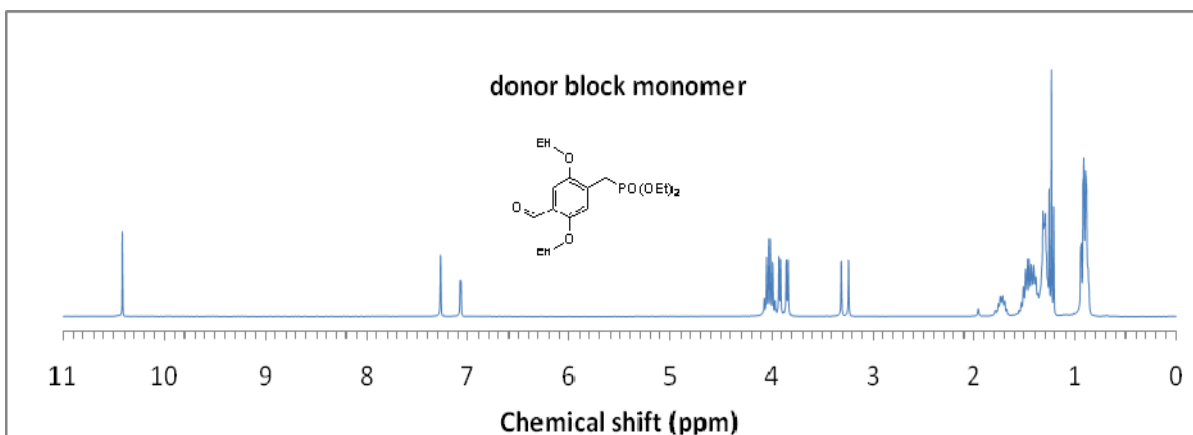
Figure 1.4.1 ^{1}H NMR of donor monomer **1.**

Polymerization of monomer 1 in presence of terminator 5. When t-BuOK was added to a solution of **5** and **1** in THF, a high molecular weight polymer (judged by the way it precipitated in MeOH) was obtained. However, no phosphonate group was seen in its NMR spectrum. Presumably, the P-CH$_2$ group in the terminator cannot compete for t-

BuOK added, and therefore, does not participate in polymerization. In an effort to avoid the problem, the solution of **5** and **1** was added to an excess of t-BuOK/THF solution. A phosphonate-terminated donor polymer was obtained, however, the amount of phosphonate was less than expected. Likely, t-BuOK is not strong enough to fully deprotonate terminator **5** and therefore the terminator:monomer ratio is smaller than the feed ratio.

It became clear that a good terminator of higher acidity should be used. A new terminator was designed to have an electron-withdrawing fluorine substituted at the para position (compound **8**) and was successfully synthesized (**Scheme 1.4.4**, **Figure 1.4.2**).

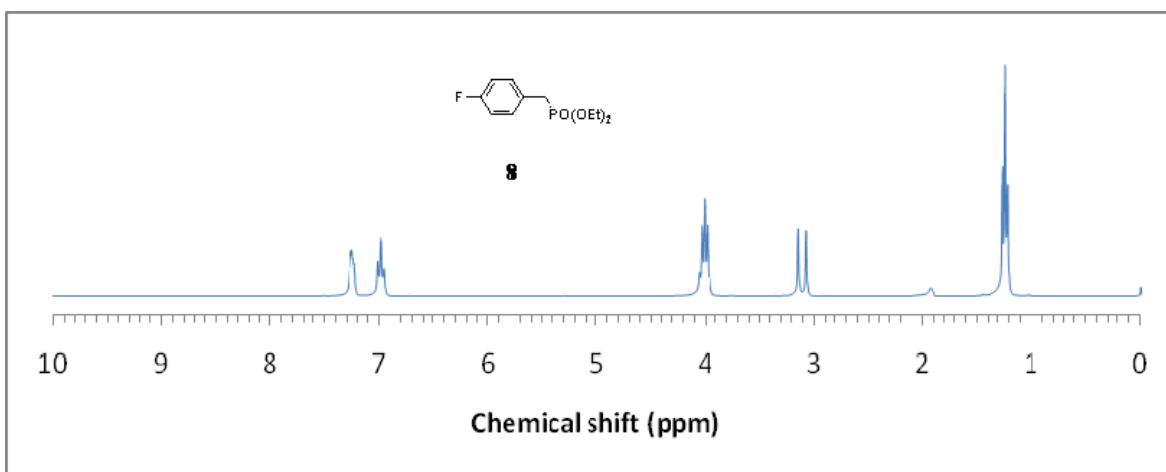**Scheme 1.4.4** Synthesis of the donor monomer **8**.

Figure 1.4.2 ^{1}H NMR of terminator **8**

Polymerization of monomer 1 in presence of terminator 8. With the use of new terminator **8**, standard mixing of reactants (t-BuOK added to a solution of **4** and **7**) worked well and yielded a donor polymer block with sufficient amount of CH$_2$-PO(OEt)$_2$. (see NMR spectrum the donor block in **Figure 1.4.3**).
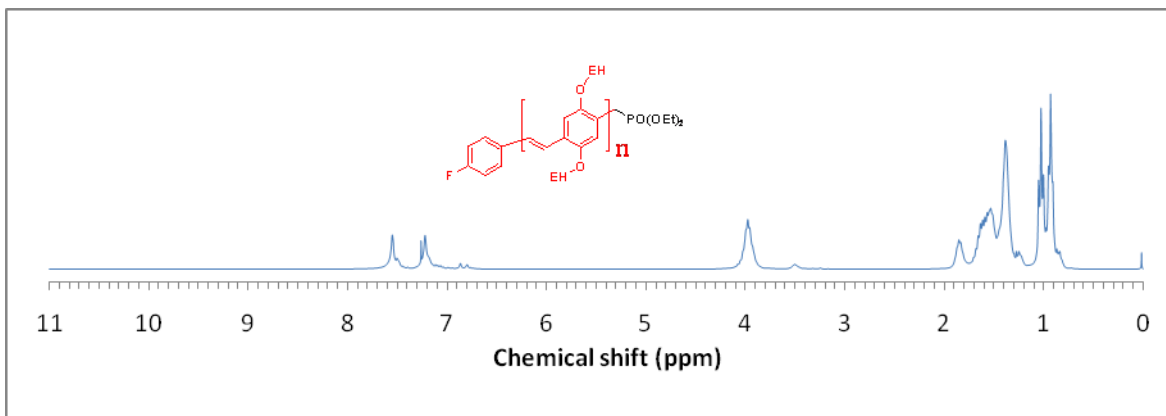

Figure 1.4.3 ^{1}H NMR spectrum of phosphonate-terminated donor block.

Synthesis of the acceptor block

It turned out that the acceptor monomer is much more difficult to obtain than expected. Several schemes were investigated before a working scheme was identified. Unsuccessful schemes will be discussed shortly before the working scheme is presented.

Scheme 1.4.4 was first investigated and failed at the last step. Compound **9** has been reported by us earlier [2]. The selectivity of the mono reduction of dialdehyde **9** was very high (81.5%) and the monomer isomeric product can be removed by silica gel column chromatography. Unfortunately, Arbuzov reaction of **11** with triethyl phosphate to produce **2**, one of the most frequently used reaction in our lab, did not work under different conditions. Severe side reactions happened.
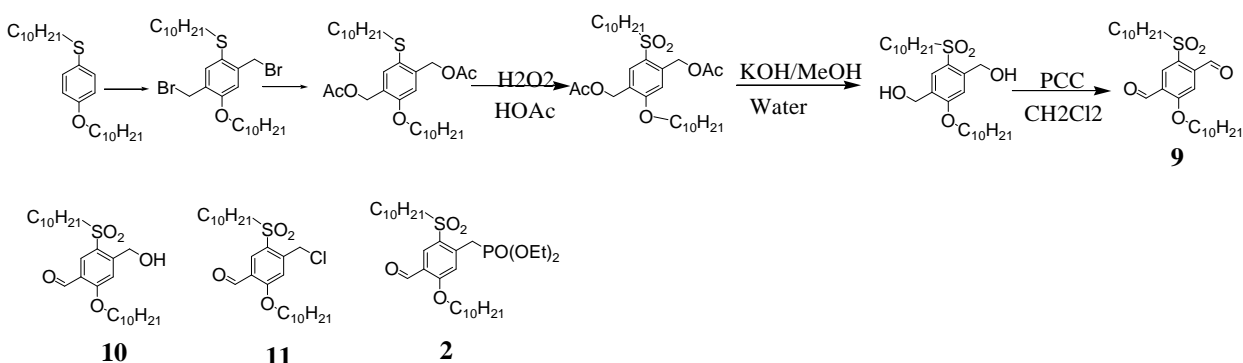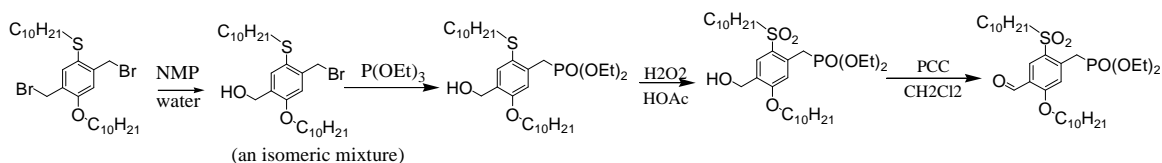

Scheme 1.4.4 The first failed scheme for acceptor monomer synthesis.

We then attempted **Scheme 1.4.5** to synthesize unsymmetrically functionalized dimer **16** from reaction of isomeric mixture (**13**) (prepared from mono-protection of dialdehyde **12** [2]) and diphosphonate compound **14** [3]. Unexpectedly, only trimer **15** was obtained which were not desired. Clearly, the desired product **16** is much more acidic than **14**, and therefore, continued to react with remaining **13** to give **15**.
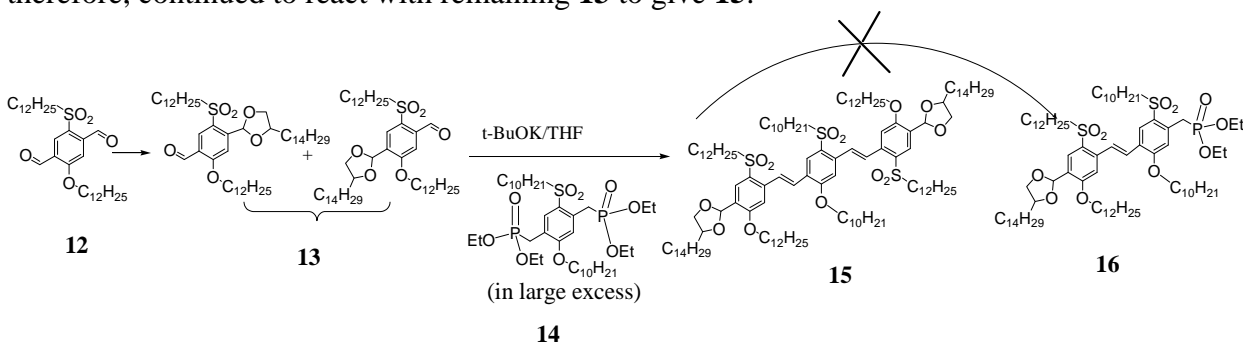

Scheme 1.4.5 The second failed scheme for acceptor monomer synthesis.

The third scheme for acceptor monomer synthesis (**Scheme 1.4.6**) failed as the step 1 product mixture (mono-bromo compounds) decomposed during purification in the silica gel column.

Scheme 1.4.6 The third failed scheme for acceptor monomer synthesis.

The successful synthesis of the acceptor monomer was eventually established via **Scheme 1.4.7**. This scheme was not considered first as it was believed that the phosphonate group could not survive wildly different and very harsh reaction conditions used in the long sequence of reactions: 1. Strong acid (HBr at 60C for 7h), 2. Wet polar solvent at 90°C, 3. Oxidizing/acid condition/high temperature (H2O2/HOAc/90C), 4. Strong base/alcohol (KOH/EtOH). With careful control of reaction times, the phosphonate survive all the conditions. Mono bromomethylation and the Arbuzov reaction of **17** produces phosphonate compound **18** (Purification was only possible after the phosphonate step). The NMR data of acceptor monomer **22** is shown in **Figure 1.4.4**.
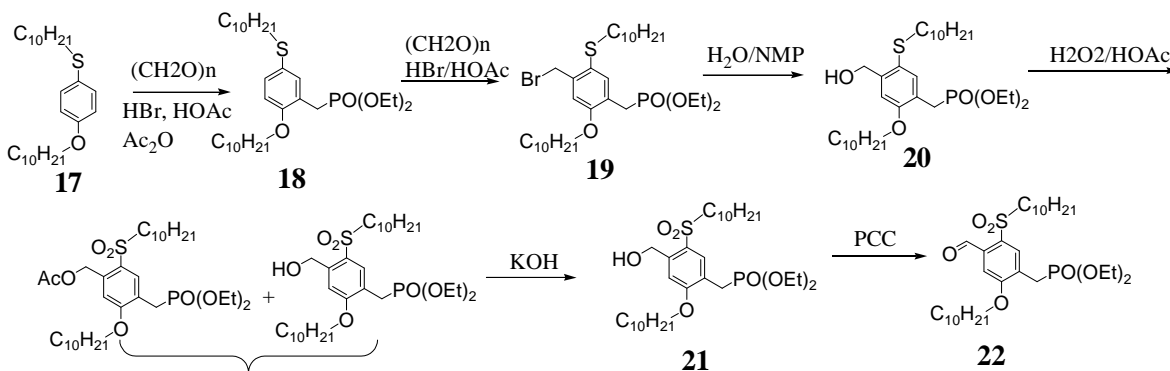
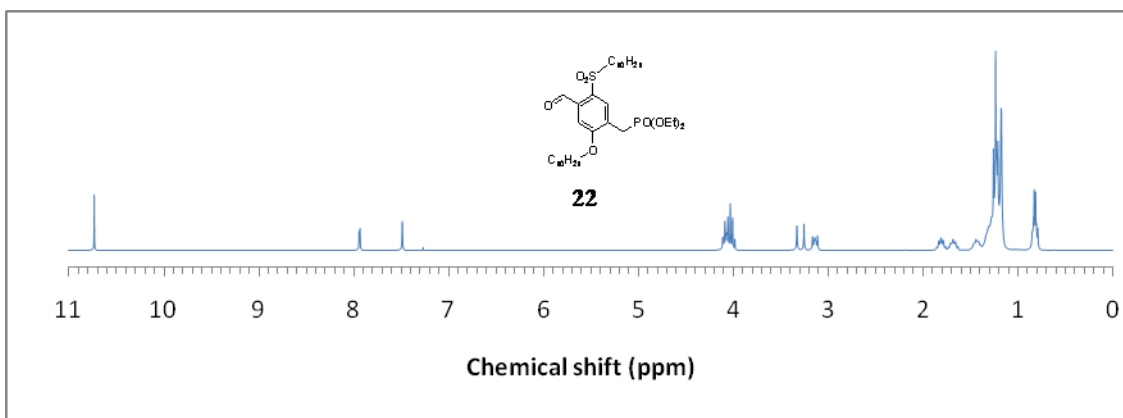**Scheme 1.4.7** The successful scheme for acceptor monomer synthesis.

Figure 1.4.4 NMR data of the acceptor monomer **22.**

1.4.3 Synthesis of the DBA Block Copolymer

The donor block was first reacted with 15 times excess dialdehyde bridge unit **23** to be end-capped with a bridge unit as shown in **Scheme 1.4.8**. The ^{1}H spectrum of the product (DB) is shown in **Figure 1.4.5**. It is clearly seen that the phosphonate group is

gone, and an aldehyde group emerged. DB was further reacted with the acceptor block to give the final product: DBA. The aldehyde group and phosphonate group at the end of the acceptor are no longer seen in the ^{1}H spectrum of DBA (**Figure 1.4.5**).
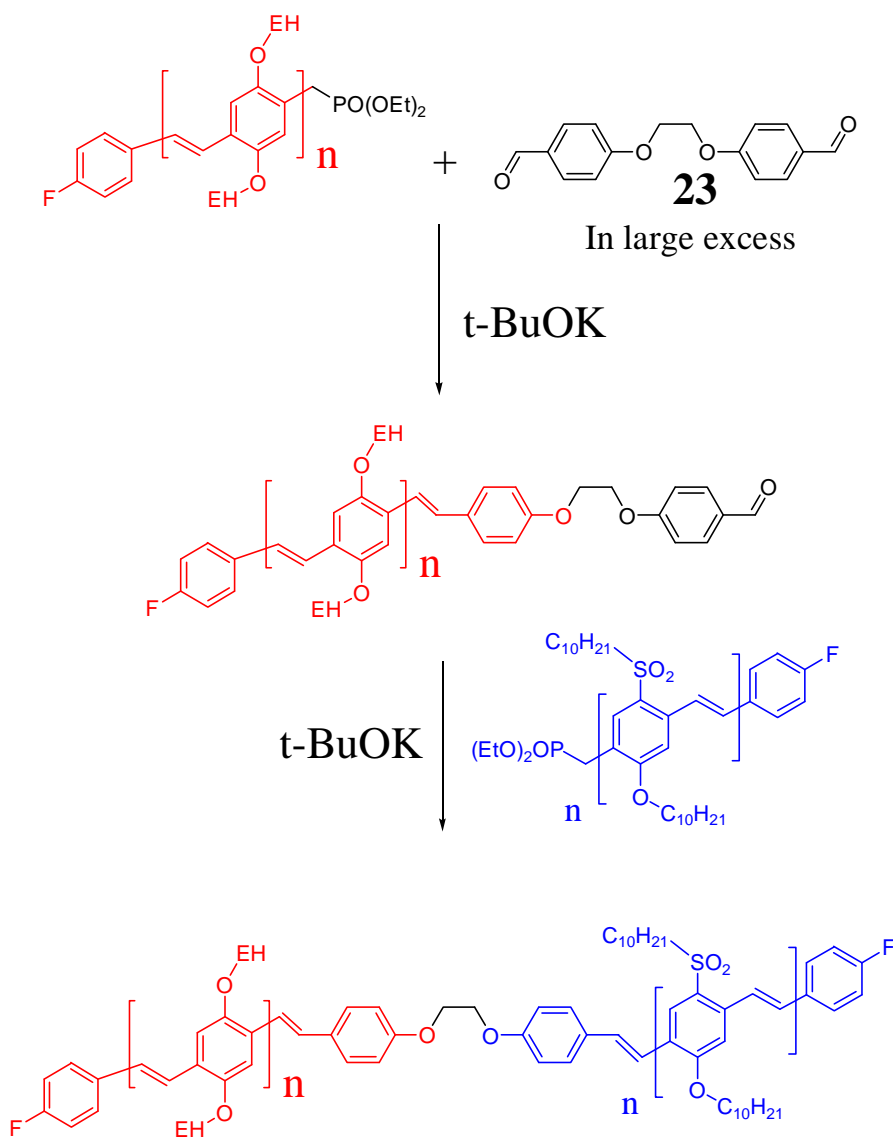
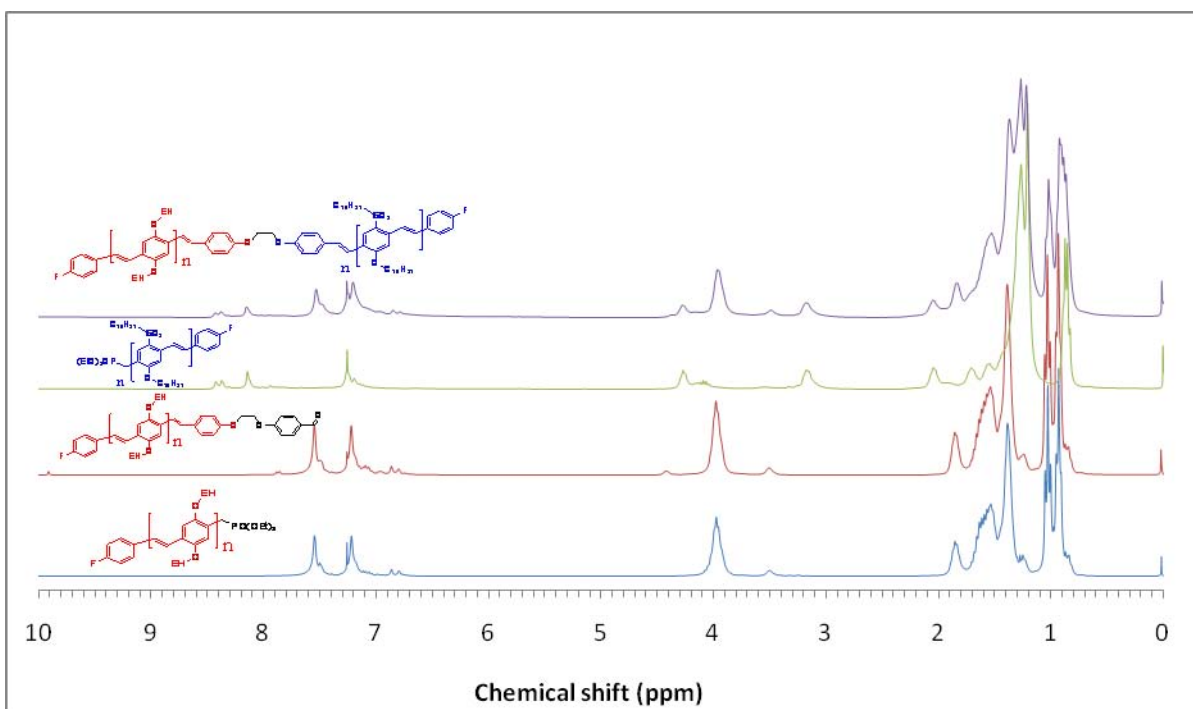**Scheme 1.4.8** The scheme for DBA synthesis.

Figure 1.4.5 ^{1}H NMR spectrum of the donor block D, donor + bridge DB, acceptor A, and DBA block polymer.

DBA Block Copolymer Synthetic Procedures

1,4-Bis-(2-ethyl-hexyloxy)-benzene (3): To a 1L round-bottom flask were added DMSO (300mL), hydroquinone (20 g) and 2-ethylhexyl bromide (95.19g, 0.49 mole). A solution of NaOH (23.3g)/water (22g) was then added drop wise to the vigorously stirred mixture heated in 90 ^{o}C oil bath. After addition, the reaction mixture was stirred for another 30 min. The product was extracted with hexane and washed with water. The crude product was purified with a flash silica gel column to afford 52g pure product. Yield: 86%.

2-Bromomethyl-1,4-bis-(2-ethyl-hexyloxy)-benzene (4): A mixture of 1,4-bis-(2-ethyl-hexyloxy)-benzene **3** (50.88g, 0.152 mol), paraformaldehyde (5.48g, 0.183 mol), glacial acetic acid (110g) and 30% HBr/HOAc (82 mL) was heated in 60 ^{o}C oil for 4h. The product was extracted with hexane and washed with water and sodium bicarbonate solution. The hexane extract was dried with magnesium sulfate and then condensed for use in the next step without separation of 1,4-bis-(2-ethyl-hexyloxy)-benzene (15% by ^{1}H NMR spectrum), mono bromomethylated (77%) and dibromomethylated (8%) products.

[2,5-Bis-(2-ethyl-hexyloxy)-benzyl]-phosphonic acid diethyl ester (5): A mixture of above crude product **4** (30.26g, 70.8 mmol) and triethyl phosphite (16.47g, 99.1 mmol) was stirred and heated in a 140 $^{\circ}$C oil bath for 2.5 h. The remaining triethyl phosphate was removed by distillation. The residue was purified with a silica gel column using 1:6 EtOAc/Hexanes as the eluent to afford 24.0g colorless oil **5**. Yield 70% (for two steps).

[2,5-Bis-(2-ethyl-hexyloxy)-4-formyl-benzyl]-phosphonic acid diethyl ester (1): To an ice bath –cooled solution of [2,5-bis-(2-ethyl-hexyloxy)-benzyl]-phosphonic acid diethyl ester **5** (4.847g, 10 mmol), methylene chloride (30 mL) and a-dichloromethyl methyl ether (1.38g, 12 mmol), titanium tetrachloride (6.64g, 35 mmol) was added drop wise over two minutes. The color changed to dark red instantly. One hour later, ^{1}H NMR analysis of the reaction mixture indicated the complete of the reaction. The reaction mixture was then poured into a stirred mixture of K_2CO_3 (8.42g), water (200 mL) and ice (50g) in a 1L beaker. The product was extracted with 200mL hexanes, and purified with a silica gel column. Yield: 48%.

The donor block. In a glove box, to a vigorously mixture of [5-(decane-1-sulfonyl)-2-decyloxy-4-formyl-benzyl]-phosphonic acid diethyl ester **1** (3 mmol, 1.538g SC), 1/20 eq, (4-fluoro-benzyl)-phosphonic acid diethyl ester **8** (36.9 mg, 0.150 mmol) and THF (15 mL) was added drop wise a solution of t-BuOK (469mg, 1.20 eq)/THF (23 mL). After the addition, the solution was stirred for five minutes, and was dropped into MeOH. Polymer was collected by filtration and dried. 1.113g, yield: 93.45%.

2-Bromomethyl-1-decyloxy-4-decylsulfanyl-benzene (An intermediate). A mixture of 1-decyloxy-4-decylsulfanyl-benzene **17** (8.044 g, 19.78 mmol), paraformaldehyde (2.37 g, 4 mol eq), glacial acetic acid (8 g), acetic anhydride (4g) and 33% HBr/HOAc (13g) was stirred at 90 $^{\circ}$C for two hours. The reaction mixture was diluted with 100 mL water, then extracted with hexanes. The hexanes extract was washed with water, then dilute aqueous NaHCO_3, dried and condensed to give brown oil which was used in the next step without purification.

(2-Decyloxy-5-decylsulfanyl-benzyl)-phosphonic acid diethyl ester (18). In a glove box, a solution of all crude 2-bromomethyl-1-decyloxy-4-decylsulfanyl-benzene and triethyl phosphate (4.58 g, 1.4 eq) was stirred at 125°C for 14h. After remove remaining phosphate, the crude product was purified by a silica gel column using hexane/ethyl acetate as eluent to give 7.70 g colorless oil. Yield: 69.9%.

(4-Bromomethyl-2-decyloxy-5-decylsulfanyl-benzyl)-phosphonic acid diethyl ester (19). A vigorously stirred mixture of (2-decyloxy-5-decylsulfanyl-benzyl)-phosphonic acid diethyl ester **18** (5.65 g), paraformaldehyde (2 g), trifluroacetic acid (10 mL), trifluoroacetic anhydride (3.5 g) and 33% HBr/HOAc (6 mL) was stirred at 60 ^{o}C for 6.5h. The hexanes extract was washed with water, then dilute aqueous NaHCO$_3$, dried and condensed to give brown oil which was used in the next step without purification.

(2-Decyloxy-5-decylsulfanyl-4-hydroxymethyl-benzyl)-phosphonic acid diethyl ester (20). A vigorously stirred mixture of crude (4-bromomethyl-2-decyloxy-5-decylsulfanyl-benzyl)-phosphonic acid diethyl ester **19** obtained in the procedure above, sodium bicarbonate (2.5g), 1-methyl-pyrolidinone (50 g) and water (5 g) was heated in a 90 ^{o}C oil bath for two and half hours. The reaction mixture was diluted with 100 mL water, then extracted with hexanes. The hexanes extract was washed with water, dried with MgSO$_4$ and condensed by rotary evaporation. Purification by silica gel chromatograph afforded 3.2 g (95% pure).

[5-(Decane-1-sulfonyl)-2-decyloxy-4-hydroxymethyl-benzyl]-phosphonic acid diethyl ester (21). A mixture of (2-decyloxy-5-decylsulfanyl-4-hydroxymethyl-benzyl)-phosphonic acid diethyl ester **20** (3.2g, 95% pure), 50% H$_2$O$_2$ (1.3 g), and glacial HOAc (3mL) was stirred for twenty minutes at RT, then at 90 ^{o}C for 35 min. HOAc and H$_2$O$_2$ was removed under 100mbar at 90 ^{o}C for 10m. The product was extracted by hexanes (40mLx2). The extract was then washed with aqueous Na$_2$CO$_3$, and water once, dried with MgSO4, and condensed to give 3.666g crude product. The crude product was treated with a mixture of KOH (3 g)/water (7g)/EtOH (40mL) at RT for two and half minutes. After adding NaHCO$_3$ (6 g), the mixture was condensed on a rotary evaporator in 40 ^{o}C water bath under reduced pressure. The residue was extracted with ether. The extract was

dried and condensed to give 3.35g crude product which was pure enough to be used in the next step.

[5-(Decane-1-sulfonyl)-2-decyloxy-4-formyl-benzyl]-phosphonic acid diethyl ester (2). A mixture of [5-(decane-1-sulfonyl)-2-decyloxy-4-hydroxymethyl-benzyl]-phosphonic acid diethyl ester **21** (3.35 g), methylene chloride (12 mL) and pyridinium chlorochromate (1.5 g) was stirred at RT for 4 h. Solvent was removed by rotary evaporation under 500 mbar until the solution become sticky. Hexane extract of the residue was washed with aqueous $NaHCO_3$, and dried and condensed. Purification by silica gel column chromatograph using 1/6 EtOAc/Hexanes as the eluent afforded 1.85 g pure product. Yield: 57.9 % for three steps from (2-decyloxy-5-decylsulfanyl-4-hydroxymethyl-benzyl)-phosphonic acid diethyl ester (3.2g, 95% pure).

The acceptor block. In a glove box, a mixture of [5-(decane-1-sulfonyl)-2-decyloxy-4-hydroxymethyl-benzyl]-phosphonic acid diethyl ester **2** (1.000 g) + (4-fluoro-benzyl)-phosphonic acid diethyl ester **8** (19.6mg , 1/20 eq) and THF (6mL) in 100 mL flask was vigorously stirred while t-BuOK (1.05 eq)/THF (5mL) was added over two minutes. Three minutes after the addition, the reaction mixture was dropped into stirred MeOH. Polymer product was collected by filtration and dried at $60^{o}C$ in vacuum for two days. 735 mg, 95.5%

Phosphonate-terminated DEH-PPV + bridge: In a glove box, a mixture of the donor polymer block (0.43g), the bridge compound (0.164 g) and THF (7.5 mL) was heated until the polymer was fully dissolved. After being cooled for five minutes, t-BuOK (38 mg)/THF (1mL) was added over ten seconds. After being stirred for 30 s. The reaction was quenched with 30% HOAc (0.1 mL) MeOH. The mixture was dropped into MeOH and the polymer product was collected by filtration: 415mg.

DBA Block Copolymer, CBP3.1a. In a glove box, to a stirred mixture of the donor-bridge (300 mg), the acceptor polymer (400 mg) and THF (13 g) was added t-BuOK (65.8 mg/1 g THF). After being stirred for five minutes after the addition, the reaction mixture was dropped into stirred MeOH. Polymer product was collected by filtration and dried at $60^{o}C$ in vacuum for two days. Yield: 684mg.

1.4.4 Physical Characterizations of the New DBA Block Copolymer

The UV-VIS absorption spectrum of the donor, acceptor and DBA block copolymer is shown in **Figure 1.4.6**. Since it appears the DBA UV-VIS curve is a simple overlap of the donor and acceptor UV-VIS curves, no ground state charge transfer or "chemical doping" occurs between the donor and the acceptor block. A photovoltaic polymer should be a "chemical doping" system. **Figure 1.4.7** exhibits photoluminescence (PL) spectra of donor block (D), acceptor block (A), and DBA block copolymer in chloroform solution. From concentration correlated calculations, it is found that at least 56% PL is quenched in DBA solution as compared to pristine donor, while no quenching is detected in 1uM D/A blend solution. These preliminary PL data provided evidences of photo induced electron transfer from the donor block to the acceptor block via the bridge unit! **Figure 1.4.8** exhibit the DSC data of the three polymer systems where there is no clear glass transition observed before the polymer decomposes at about 300°C, these are common in conjugated polymers. **Figure 1.4.9** exhibits the thermal gravimetric analysis (TGA) results and shows the DBA is thermally stable up to about 300°C. **Figure 1.4.10** exhibit the CV data of the D and A. Combined UV-VIS and CV data reveal the donor D has a LUMO/HOMO of -3.1eV/-5.3eV, and A has a LUMO/HOMO of -3.0eV/-5.5eV.
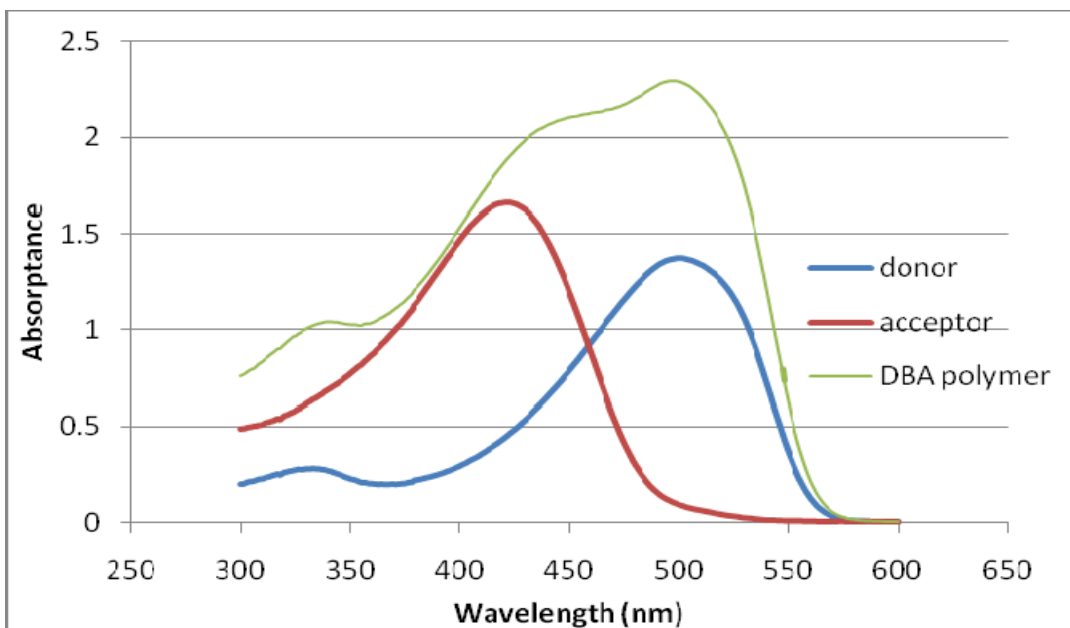

Figure 1.4.6 UV-VIS absorption spectrum (Donor Eg: 2.21eV; Acceptor Eg: 2.53eV).
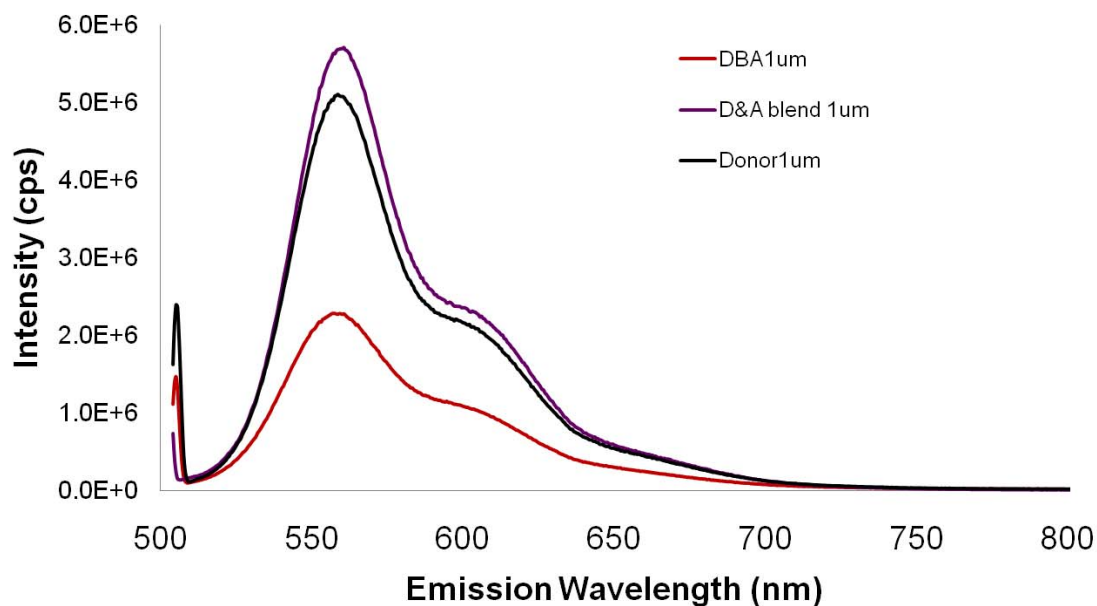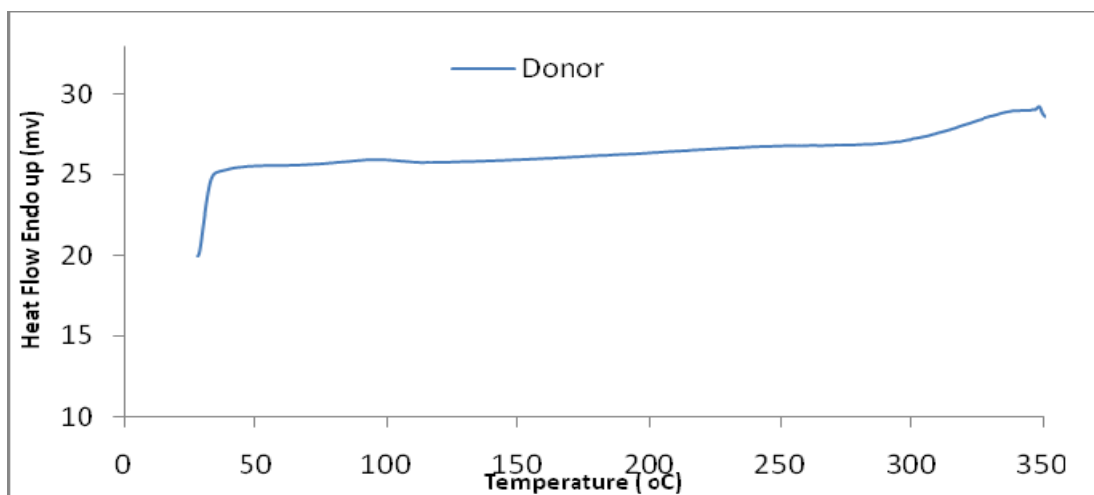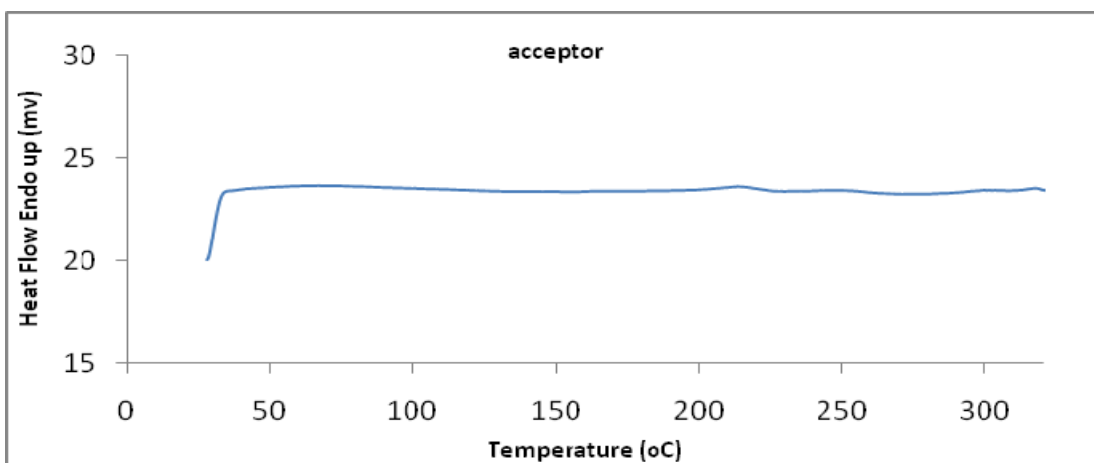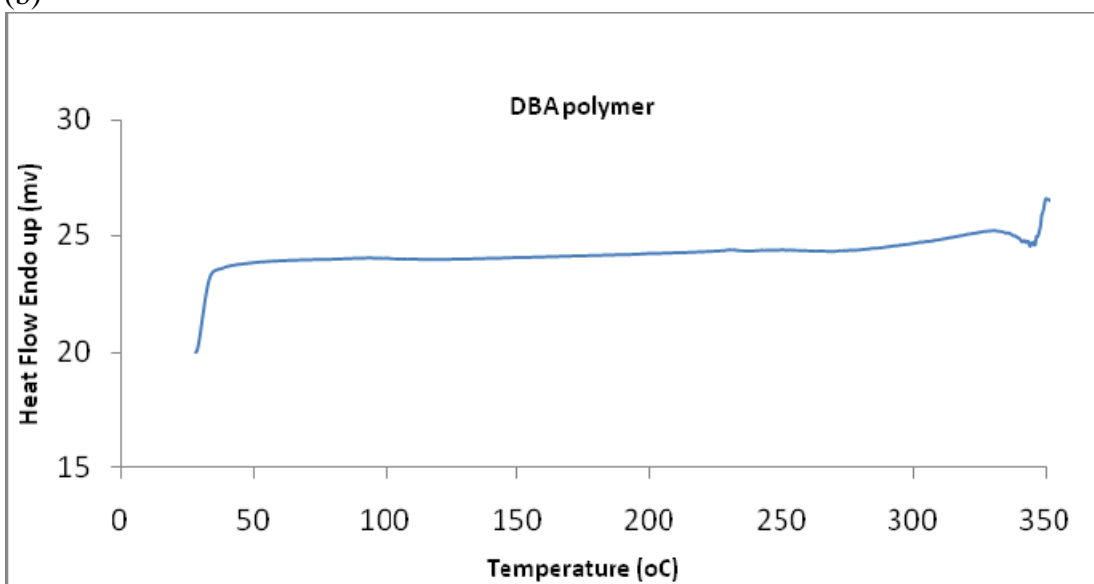
Figure 1.4.7 Photoluminescence (PL) spectra of D, D/A blend, and DBA block copolymer in CHCl$_3$ solution. It is found that 56% PL is quenched in DBA solution, while no quenching is detected in 1uM D/A blend solution.
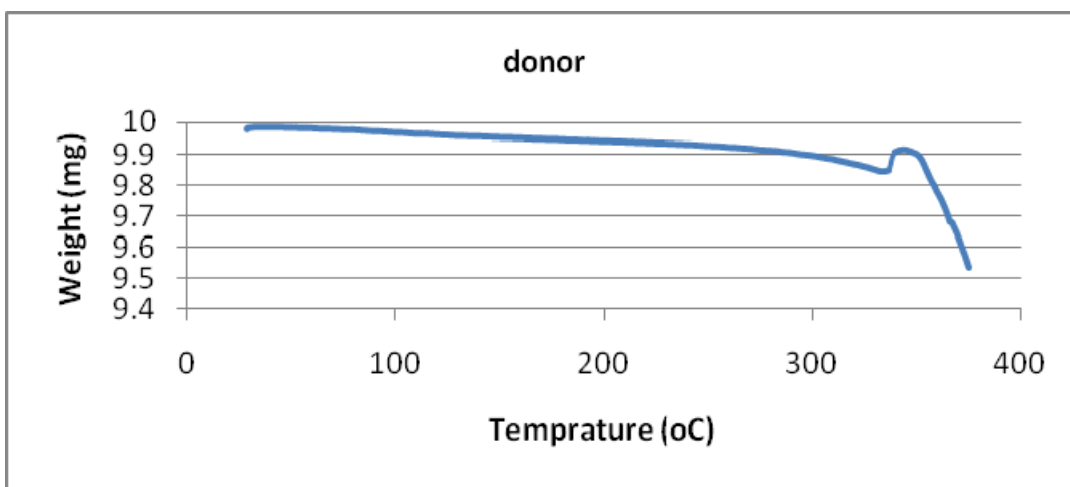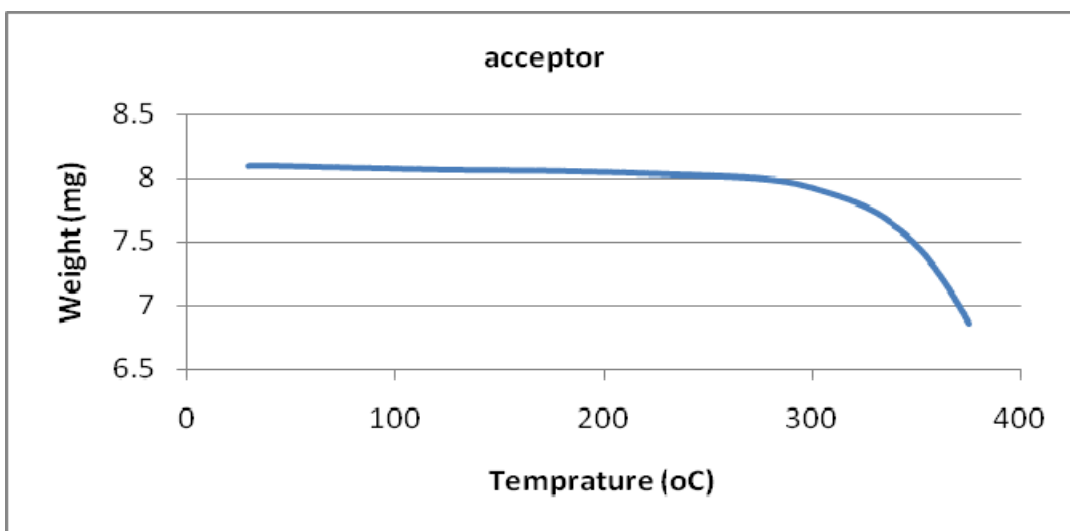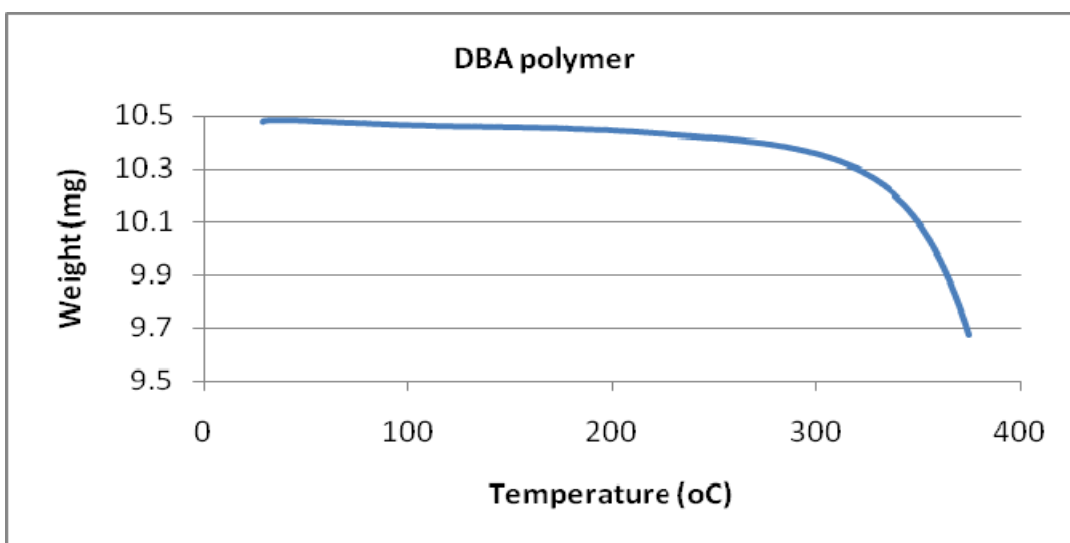

(a)

(b)

(c)

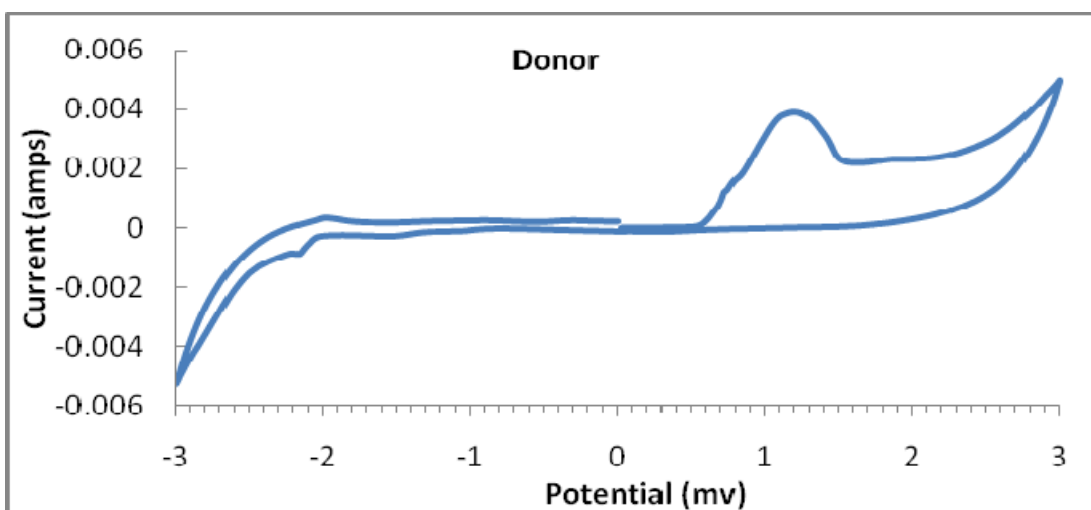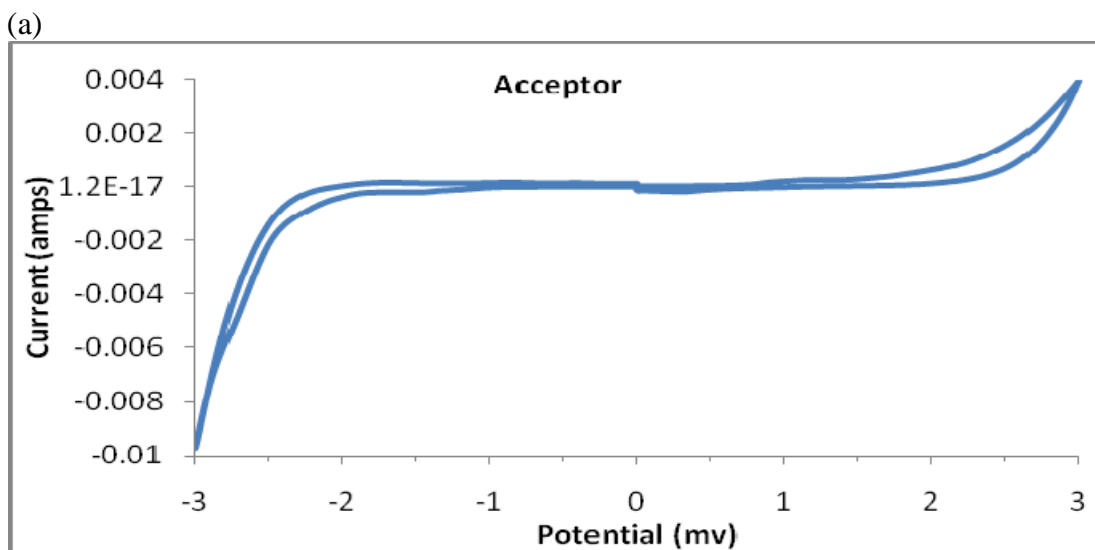**Figure 1.4.8** DSC curves of (a) donor, (b) acceptor and (c) DBA.

(a)

(b)

(c)

Figure 1.4.9 TGA curves of (a) donor, (b) acceptor and (c) DBA.

(a)

(b)
Figure 1.4.10 Cyclic Voltammetry (CV) curves of (a) donor and (b) acceptor.

1.4.5   Conclusions and Summary
The successful synthesis and characterization of the first DBA conjugated block copolymer system opened a new opportunity of controlling the morphology (and therefore the electronic/optical properties) of the polymer semiconductors at the molecular scale. Such block copolymer systems are essential for a variety of polymeric electronic and optoelectronic applications where the molecular orientations and pathways are essential.

1.4.6   Notes and References for Part 1.4
1. Zhang C, Choi S, Haliburton J, Cleveland T, Li R, Sun S, Ledbetter A, Bonner C. *Macromolecules*. **2006**, 39, 4317-4326.
2. Sun, S.-S.; Zhang, C.; Ledbetter, A.; Choi, S.; Seo, K.; Bonner, Jr., C. E.; Drees, M. and Sariciftci, N. S. *Appl. Phys. Lett.* **2007**, 90, 043117.
3. Zhang, C and Sun, S., "Organic and Polymeric Photovoltaic Materials and Devices", in *Introduction to Organic Electronic and Optoelectronic Materials and Devices*, eds: Sun, S. and Dalton, L., CRC Press/Taylor & Francis: Boca Raton, Florida, USA, **2008,** Chapter 14, pp 401-420.

2.   QUANTUM DOTS CRAFTED CARBON NANOTUBES (TASK #2, UD)

Sub-awardee (UD) developed and studied quantum dots crafted carbon nanotubes for potential optoelectronic applications. Specifically, **Figure 2.1(a)** shows a typical SEM image of the CdS-MWNTs nanocomposites, which clearly reveals the coupling of CdS quantum dots (QDs) along the MWNTs. Although the diameters of these QDs are in the range of 10-30 nm, most of the particles have a diameter of about 15 nm. It is already known that inorganic semiconducting quantum dots (QDs) have a different band gap with a size distribution, hence, emitting color can be controlled by size of QDs in light emitting diodes (LEDs). It is known that 15 nm size of CdS quantum dots has a 4.5 eV of electron affinity with a 2.4 eV of bandgap. A low lowest unoccupied molecular orbital (LUMO) value of CdS quantum dots can help electron transfer by reducing the energy barrier between 1-(3-methoxycarbonyl)propyl-1-phenyl(6,6)-methanofullerene (PCBM) and cathode (Al). Additionally, 6.9 eV of highest occupied molecular orbital (HOMO) value of CdS can force holes to transfer to anode not to reach cathode, as shown in **Figure 2.1(c)**. **Figure 2.1(b)** showed UV-vis absorption spectra of CdS-CNT composites in methanol suspension.
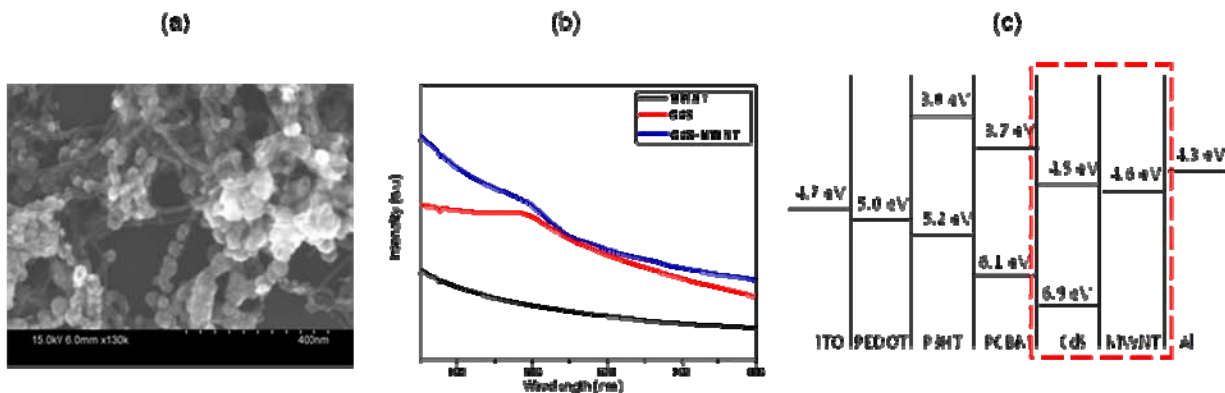

Figure 2.1 (a) SEM image of CdS-MWNTs composites, (b) UV-vis absorption spectra of MWNT, CdS, and CdS-MWNT nanocomposites in methanol, and (c) energy diagram of active materials including two electrodes in PVCs.

While MWNTs gave a featureless absorption, pure CdS and CdS-MWNTs nanocomposites exhibited the maximum peak at 485 nm and 497 nm, respectively, which implies charge transfer happens between CdS QDs and MWNTs in the ground state. Additionally, 12 nm of red shift from CdS-MWNTs nanocomposites may be due to electron delocalization property from MWNTs. **Figure 2.1(c)** shows the energy diagram of active materials including two electrodes for fabrication of solar cells. As mentioned before, CdS quantum dots can not only help the electron transfer by reducing energy barrier between PCBM and cathode but also force holes not to reach cathode derived from low HOMO value, after charge separation. Due to excellent electrical properties and large surface area, moreover, MWNTs can improve charge carrier mobility and increase exciton dissociation area.

3. PRELIMINARY OE DEVICE STUDIES (PROJECT TASK #3)

Project awardee (Professor Sun's group at NSU) has collaborated with sub-awardee (Professor Dai's group at UD, now at CWRU, and Dai's co-workers/collaborators) on fabricating and studying a number of optoelectronic solar cell devices using NSU developed polymers (polymer samples include 55-C12-PTV, SFPTV or P(C6OTV-SFTV), and "CBP" or the (-DBAB-)$_n$ block copolymer system developed at NSU earlier) with QD-CNTs developed from Dai's group. **Figures 3.1-8** exhibit preliminary data of such studies.

Performance of Solar Cells with Low Bandgap Polymers- C12PTV-0.5 % (CdS-CNT)

Figure 2. Performance of solar cells with the low bandgap polymer (C12PTV, spin coating, 400/1000 rpm, ~40 s) and 0.5 % CdS-CNT.
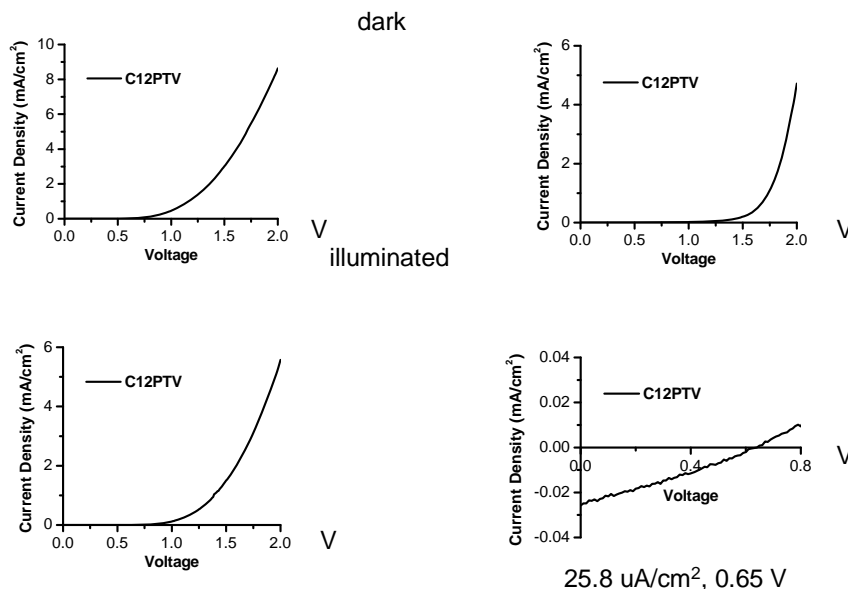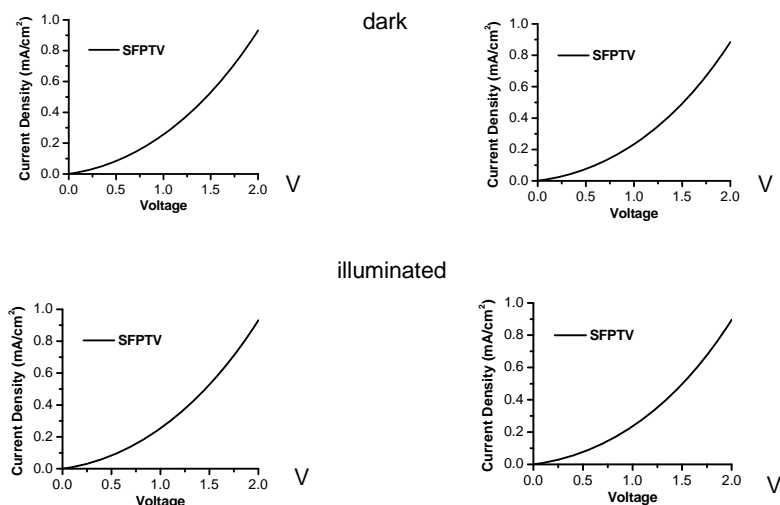
Figure 3.1 Preliminary results of the 55-C12-PTV/CdS-CNT solar cells photo J-V data (CNT concentrations of 0.5% by weight).

Performance of Solar Cells with Low Bandgap Polymers-SFPTV-0.5 % (CdS-CNT)

Un-thermal annealed   Thermal annealed

dark

illuminated

Performance of solar cells with the low bandgap polymer (SFPTV, spin coating, 400/1000 rpm, ~40 s) and 0.5 % CdS-CNT.

Figure 3.2 Preliminary results of the SF-PTV/CdS-CNT solar cells photo J-V data (CNT concentrations of 0.5%).

Performance of Solar Cells with Low Bandgap Polymers-CBP-0.5 % (CdS-CNT)

Un-thermal annealed   Thermal annealed
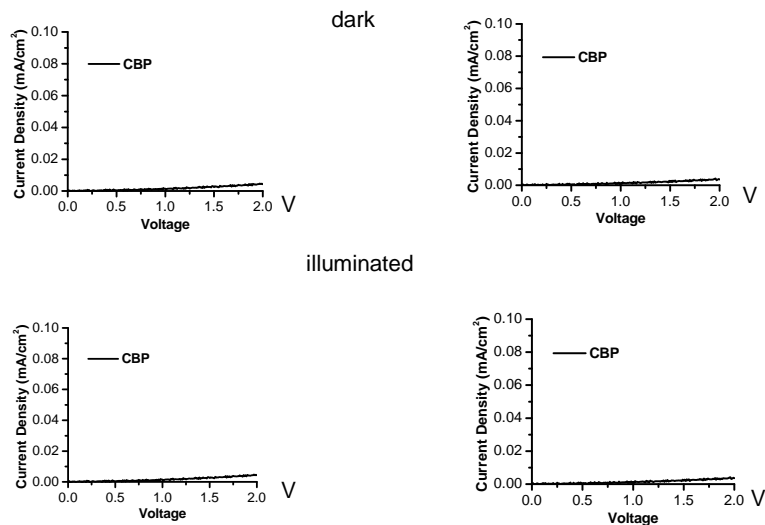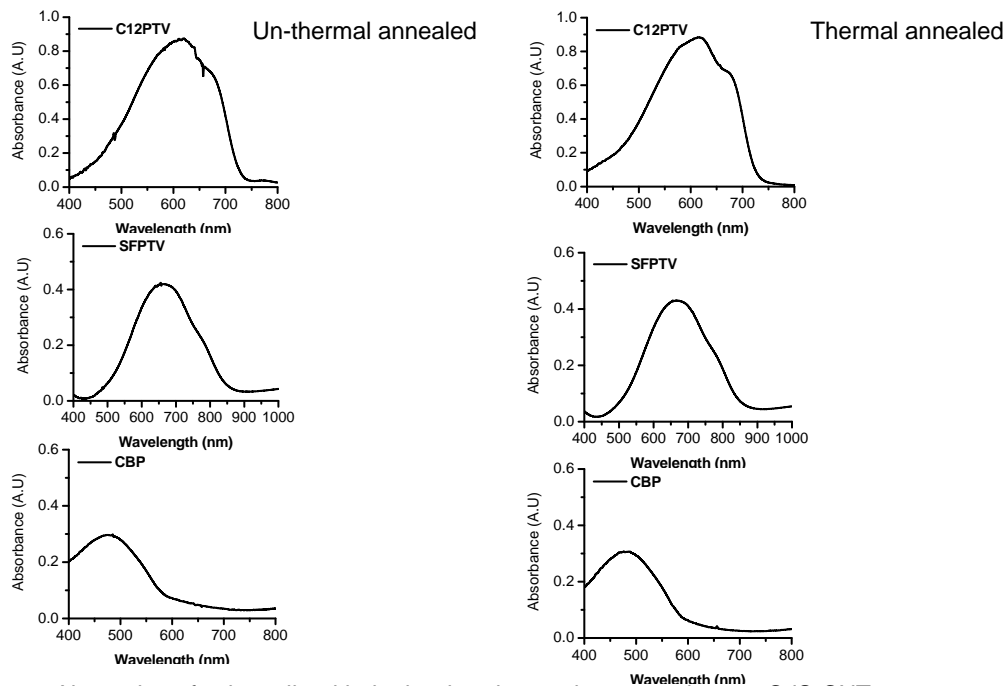
dark

illuminated

Performance of solar cells with the low bandgap polymer (CBP, spin coating, 400/1000 rpm, ~40 s) and 0.5 % CdS-CNT.

Figure 3.3 Preliminary results of the CBP/CdS-CNT solar cells photo J-V data (CNT concentrations of 0.5%).

Absorption of Solar Cells with Low Bandgap Polymers and 0.5 % (CdS-CNT)

Un-thermal annealed

Thermal annealed

Absorption of solar cells with the low bandgap polymers and 0.5 % CdS-CNT.

Figure 3.4 Absorption of the Polymer/CdS-CNT solar cells (CNT concentrations of 0.5%).

Performance of Solar Cells with Low Bandgap Polymers-C12PTV-1, 2 and 5 % (CdS-CNT)

dark

1 %

2%

5 %

illuminated
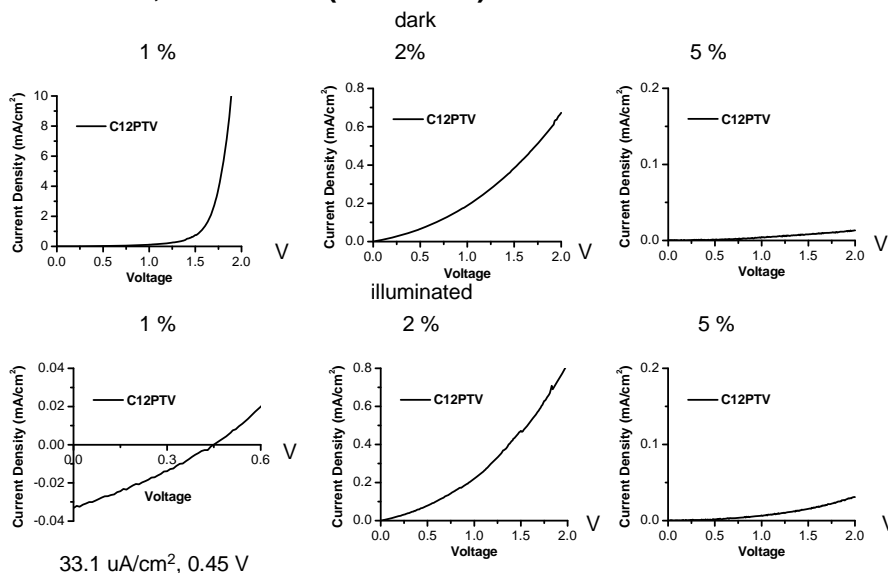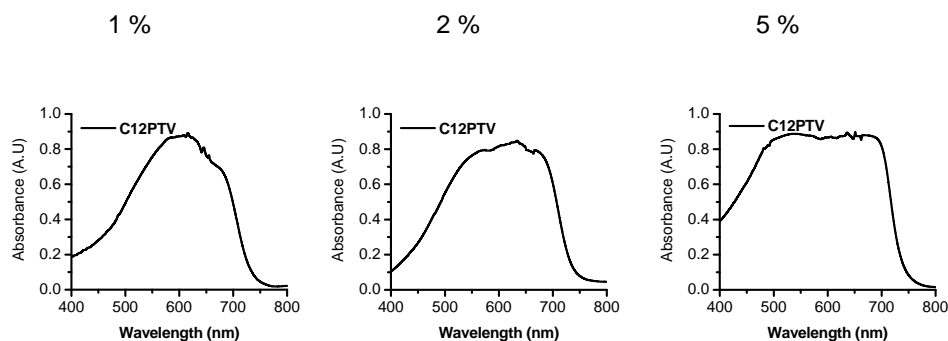
1 %

2 %

5 %

33.1 uA/cm^2, 0.45 V

Figure 6. Performance of solar cells with the low bandgap polymer (C12PTV, spin coating, 400/1000 rpm, ~40 s) plus 1, 2 and 5 % CdS-CNT under the thermal annealed condition.

Figure 3.5 Preliminary results of the 55-C12-PTV/CdS-CNT solar cells photo J-V data (CNT concentrations of 1-5%).

Absorption of Solar Cells with Low Bandgap Polymers and 1, 2 and 5 % (CdS-CNT)

1 %   2 %   5 %

Absorption of solar cells with the low bandgap polymers and 1, 2 and 5 % CdS-CNT.

Figure 3.6 Absorption of the 55-C12-PTV/CdS-CNT solar cells (CNT concentrations of 1-5%).

Performance of Solar Cells with Low Bandgap Polymers-C12PTV-0.5 and 1 % CNT

dark

0.5 %   1 %

illuminated

0.5 %   1 %

15.8 uA/cm^2, 0.55 V   24.9 uA/cm^2, 0.37 V

Performance of solar cells with the low bandgap polymer (C12PTV, spin coating, 400/1000 rpm, ~40 s) plus 0.5 and 1 % CNT under the thermal annealed condition.

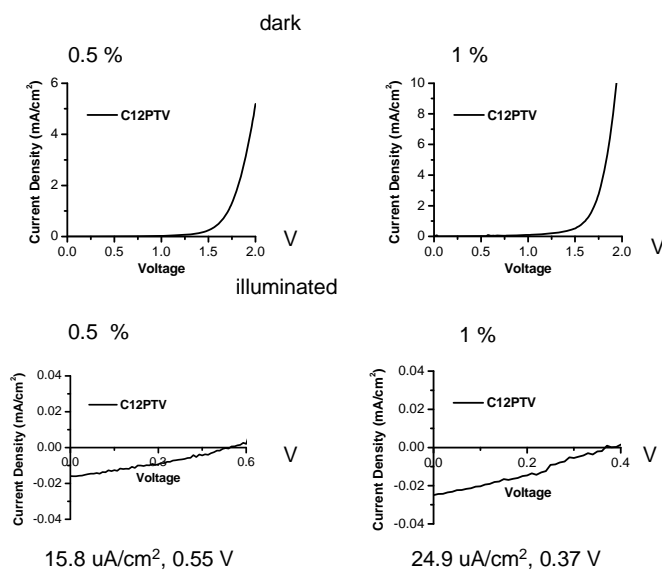**Figure 3.7** Preliminary results of the 55-C12-PTV/CNT (no QD) solar cells photo J-V data (CNT concentrations of 0.5-1%).

76

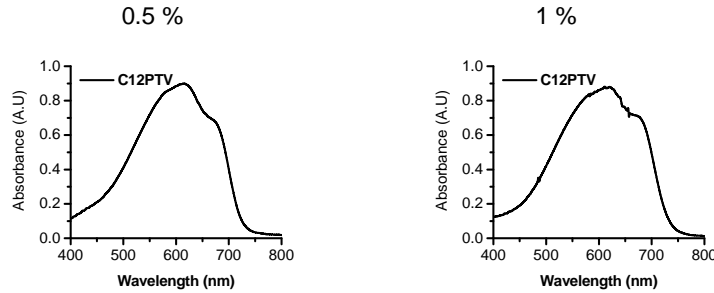## Absorption of Solar Cells with Low Bandgap Polymers and 0.5 and 1 % CNT

Figure 9. Absorption of solar cells with the low bandgap polymers plus 0.5 and 1 % CNT.

Figure 3.8 Absorption of the 55-C12-PTV/CNT solar cells (CNT concentrations of 0.5-1%).

Polymer/QD-CNT cell fabrication and characterization procedures: The indium tin oxide （ITO） substrates were cleaned by ultrasonic treatment in detergent, deionized water, acetone and isopropyl alcohol sequentially, each for ten minutes, followed by O_2 plasma treatment for 30 min. The PEDOT:PSS thin layer was spin-coated on cleaned ITO substrates at a spin speed of 2000 rpm for 30 s. Substrates were then baked at 140 °C for 20 min. Samples were transferred to the glove box to deposit active layers for Polymer/(CdS-CNT) blends. The sample of 2.5 mg (CdS-CNT) was put into 1 ml $CHCl_3$ and sonicated for two hours. 10, 20, 40 or 100 µl of such solution was added into 1 ml polymer solution (5 mg/ml in $CHCl_3$) to make polymer/QD-CNT blend cells (with 0.5, 1, 2 or 5% wt CdS-CNT loaded cells). The blend active layer was deposited on top of PEDOT:PSS layer via spin-coating at 400/1000 rpm for ~ 40 s. LiF (8 Å) and Al (200 nm) layers were then evaporated on top of active layer in vacuum. Thermal annealing was carried out at 80 °C for about one hour in the glove box. The current–voltage J-V characteristics were measured via a Keithley 2400 source-measure unit. A solar simulator with Xenon lamp (Newport, ~100 mW/cm^2, AM 1.5) was used as the light source to characterize the solar cells' performances. The absorption spectra were measured on an Agilent 8453 UV-Vis spectrophotometer.

In summary: from preliminary and no yet optimized OE device experimental results, it appears 0.5-1% wt QD-CNT or CNT with 55-C12-PTV polymer cells exhibit typical photo diode J-V curves, while all other cells exhibit non-diode (or typical resistor type) curves. While we are still investigating the causes of the non-diode behavior, there are

several possible contributing factors. For instance, it may be due to probable short circuits caused by the metallic CNTs connecting two electrodes, as it is well known that typical CNT samples contain a mixture of metallic and semiconducting CNTs. Additionally, the semiconducting charge mobility of the SF-PTV and (DBAB)n block copolymer could be much smaller compared to the RR-C12-PTV. The high resistance of SFPTV is possibly due to the presence of the sulfone unit on thiophene ring which may negatively affect the electronic coupling or conjugation on the main chain. The high resistance of the (DBAB)n block copolymer is possibly due to not yet optimized chemical structures particularly the solid state packing or morphology. Of the 0.5-1% C12-PTV based diode cells, we do see some improvements of the photo currents of the C12-PTV/QD-CNT cells (~30 µA/cm^2, and 0.45 Volt) versus the C12-PTV/CNT cells without QDs (~25 µA/cm^2, and 0.37 Volt). We are still investigating detailed causes and alternatives and ways to improve these type of OE device performances.

We believe high efficiency organic or polymer based optoelectronic devices based on polymer/CNT materials systems could be achieved with following further optimizations: 1) Readily availability of pure semiconducting phase of CNTs including QD-CNTs; 2) Readily availability of a variety of energy gaped and side group derivatized conjugated polymers (Eg between 1.0-1.8eV) with chemical structures in such a way that they could be easily self assembled into highly ordered and desired morphology at nano scale for efficient exciton dissociation and charge transport. 3) The frontier orbitals of both polymers and the CNTs or QD-CNTs should also be optimized for efficient charge separation but inefficient charge recombination.

4. OTHER ACCOMPLISHMENTS (PROJECT TASK #4)

4.1 Students/Staff Training and Educational Activities

In addition to research accomplishments, at least five graduate students and over five undergraduate students at NSU were trained and/or benefited from this project award (though most students are supported by NSU or other sources), as all research students are part of the PI's research team and they contribute fully or partially to the project related research and training activities. Specifically, during the project period, at least three NSU graduate students in the research team successfully defended their M.S. thesis related to the project in the materials science MS program, and two of them have entered into NSU's Materials Science and Engineering (MSE) Ph.D. program. So far, three graduate students in the PI's research team already passed Ph.D. qualifying exams and two students already passed the Ph.D. research project proposal defenses, *i.e.*, both are in their final Ph.D. degree candidacy status. One new graduate student joined the NSU research team during spring 2010 and has been fully involved in the supported research activities during summer 2010. Most graduate students have been actively participating and presenting their research findings at national/international scientific meetings, and most of them co-authored refereed journal publication articles. During each semester or summer, between two to four NSU chemistry major undergraduate senior level students will participate our funded research projects, and their research are generally supervised or assisted directly by the graduate students. Almost all of the NSU chemistry major students continued working for advanced degrees or find jobs in science, technology, and engineering areas. Also during the project period, one research faculty in the NSU team has become a tenure-track faculty member in the chemistry department of the university. In Co-PI's team at UD, at least one Ph.D. student who participated this project obtained his Ph.D. degree in 2009.

4.2 Selected Publications

1. Nguyen, T.; Zhang, C.; Li, R.; Sun, S.; "A New Series of Sulfone-Derivatized Phenylenevinylene (SFPV) Based Conjugated Copolymers with Lower Energy Gaps", **2010**, a full article manuscript under review.
2. Zhang, C.; Matos, T.; Li, R.; Sun, S.; Lewis, J.; Zhang, J.; Jiang, X., "Poly(3-dodedyl-2,5-thienylenevinylene)s from the Stille coupling and the Horner–Emmons reaction", *Polym. Chem.*, **2010**, *1*, 663-669.
3. Zhang, C.; Sun, J.; Li, R.; Black, S.; Sun, S.; "Synthesis and Energy Gap Studies of A Series of Sulfone-Substituted Polyphenylenevinylenes (SF-PPVs)", *Syn. Met.*, **2010,** *160*, 16-21.
4. Nguyen, T.; Zhang, C.; Li, R.; Sun, S.; "A Series of New Vinylene Based Conjugated Polymers with Sulfone Phenylene and Different Donor Co-monomers for Energy Applications", *Poly. Mater. Sci. Eng.*, **2010**, *103*, 421.
5. Sun, S.; Zhang, C.; Nguyen, T., "ENERGY GAP AND FUNCTIONAL GROUP ENGINEERING OF C-POLYMER BLOCKS", *Poly. Prep.*, **2010**, *51(1)*, 707-708.
6. Zhang, C.; Nguyen, T.; Sun, J.; Li, R.; Black, S.; Bonner, C.; Sun, S.; "Design, Synthesis, Characterization, and Modeling of A Series of S,S-Dioxo-Thienylenevinylene-Based Conjugated Polymers with Evolving Frontier Orbitals", *Macromolecules*, **2009**, *42*, 663-670.

7. Zhang, C.; Annih, E.; Li, R.; Sun, S., **"**C12-PTV with controlled regioregularity for photovoltaic application**"**. *SPIE*, **2009**, *7213* (DOI:10.1117/12.808508).

8. Sun, S. and Dalton, L. eds, *Introduction to Organic Electronic and Optoelectronic Materials and Devices*, CRC Press/Taylor & Francis: Boca Raton, Florida, USA, May **2008** (ISBN-10**:** 0849392845; ISBN-13: 978-0849392849).

9. Sun, S., "Basic Electronic Structures and Charge Carrier Generation in Organic Optoelectronic Materials", in *Introduction to Organic Electronic and Optoelectronic Materials and Devices*, CRC Press/Taylor & Francis: Boca Raton, Florida, USA, **2008,** chapter 3, pp 47-86.

10. Qu, L; Dai, L; Sun, S., "Conjugated Polymers, Fullerene C_{60} and Carbon Nanotubes for Optoelectronic Devices", in *Introduction to Organic Electronic and Optoelectronic Materials and Devices*, CRC Press/Taylor & Francis: Boca Raton, Florida, USA, **2008,** chapter 8, pp 237-261.

11. Zhang, C and Sun, S., "Organic and Polymeric Photovoltaic Materials and Devices", in *Introduction to Organic Electronic and Optoelectronic Materials and Devices*, CRC Press/Taylor & Francis: Boca Raton, Florida, USA, **2008,** chapter 14, pp 401-420.

12. Sun, S. "Organic and Polymeric Solar Cells", an invited review article in *Handbook of Organic Electronics and Photonics*, edited by S. H. Nalwa, American Scientific Publishers, Los Angeles, California, **2008**, vol. 3, chapter 7, pp 313-350.

13. Nguyen, Thuong H.; Zhang, Cheng; Sun, Sam-Shajing. "Synthesis and characterization of a functional low energy gap poly(thienylenevinylene-S,S-dioxide-thienylene vinylene) for potential supramolecular optoelectronic applications". *Poly. Prepr.*, **2008**, *49(1)*, 381-382.

4.3   Selected Lectures/Presentations

1. Nguyen, T.; Zhang, C.; Li, R.; Sun, S.; "A Series of New Vinylene Based Conjugated Polymers with Sulfone Phenylene and Different Donor Co-monomers for Energy Applications", presentation at the American Chemical Society (ACS) national fall convention, Boston, MA, August, **2010**.

2. Sun, S.; Nguyen, T.; Zhang, C., "New terminal functionalizable conjugated polymer blocks with evolving energy levels and gaps", presentation at the Materials Research Society (MRS) spring convention, San Francisco, California, April, **2010.**

3. David, T.; Nguyen, T., Zhang, C. and Sun, S., "ENERGY GAP AND FUNCTIONAL GROUP ENGINEERING OF C-POLYMER BLOCKS", presentation at the American Chemical Society (ACS) national convention, San Francisco, California, March, **2010**.

4. Sun, S., *et al.*, "*POLYMERS FOR SOLAR ENERGY APPLICATIONS*", presentation at the 17TH International Conference on Composites or Nano Engineering, Honolulu, Hawaii, July 29, **2009.**

5. Sun, S. "*Principles of Organic/Polymeric Optoelectronics*", an invited lecture at Oak Ridge National Lab (US Department of Energy), Oak Ridge, Tennessee, July 16, **2009**.

6. Sun, S. "*Organic and Polymeric Photovoltaics: A Potential Renewable, Clean, and Cost Effective Energy Alternative*", an invited lecture at Central Michigan University, Mount Pleasant, MI, March 6, **2009**.

7. Sun, S., "*DEVELOPMENT OF SUPRAMOLECULAR BLOCK COPOLYMERS FOR PHOTOVOLTAICS*", presentation at the "SECURING OUR ENERGY FUTURE NEXT GENERATION PHOTOVOLTAICS AND SOLAR FUELS*"* conference, University of North Carolina, Chapel Hill, January 18, **2009.**

8. Sun, S. "*Organic and Polymeric Photovoltaics: A Potential Renewable, Clean, and Cost Effective Energy Alternative*", an invited lecture at University of Tennessee, Knoxville, Tennessee, August 8, **2008**.

9. Sun, S. "*Organic and Polymeric Photovoltaics: A Potential Renewable, Clean, and Cost Effective Energy Alternative*", an invited lecture at US Department of Energy, Oak Ridge National Lab, Oak Ridge, Tennessee, July 31, **2008**.

10. Sun, S., "Development of Conjugated Block Copolymers and Low E_g Polymers for Light Harvesting Applications", presentation at the US Air Force polymer projects review meeting *"2008 Polymer Chemistry",* Holiday Inn, College Park, Maryland, May 7, **2008.**

11. Sun, S. *et al*., "Synthetic Strategies and Properties of –DBAB- and –DBA- Type Light Harvesting Supramolecular Block Copolymers", presentation at the Materials Research Society (MRS) spring convention, San Francisco, California, April, **2008.**

12. Sun, S. *et al*., "Synthesis and Characterization of a Functional Low Energy Gap Poly(thienylenevinylene-S,S-dioxide-thienylene vinylene) for Potential Supramolecular Optoelectronic Applications", presentation at the 234th American Chemical Society (ACS) national convention, New Orleans, Louisiana, April, **2008**.

13. Sun, S. *et al*., "Improved Synthesis and Characterization of a Low Energy Gap and Mono-End Functional Poly-(3-dodecyl-2,5-thienylenevylene)", presentation at the 234th American Chemical Society (ACS) national convention, New Orleans, Louisiana, April, **2008**.

14. Sun, S., "Global Warming and Solar Energy", an invited panel presentation and discussion at a public forum *Global Warming Symposium: Challenges Facing the Next Generation,* Norfolk State University, Norfolk, Virginia, January 31, **2008.**